On the design of chemical processes with improved controllability characteristics

On the design of chemical processes with improved controllability characteristics

Proefschrift

ter verkrijging van de graad van doctor
aan de Technische Universiteit Delft
op gezag van de Rector Magnificus prof. dr. ir. J.T. Fokkema
voorzitter van het College voor Promoties,
in het openbaar te verdedigen op maandag 10 februari om 10:30

door

Frederik Michiel MEEUSE

scheikundig ingenieur
geboren te Voorburg

Dit proefschrift is goedgekeurd door de promotor:
Prof. ir J. Grievink

Samenstelling promotiecommissie:

Rector Magnificus, voorzitter	
Prof. ir J. Grievink	Technische Universiteit Delft, promotor
Prof. dr ir A.C.P.M. Backx	Technische Universiteit Eindhoven
Prof. ir O.H. Bosgra	Technische Universiteit Delft
Prof. ir G.J. Harmsen	Technische Universiteit Delft
Prof. dr P.D. Iedema	Universiteit van Amsterdam
Prof. dr F. Kapteijn	Technische Universiteit Delft
Prof. E.N. Pistikopoulos PhD	Imperial College, United Kingdom
Prof. dr ir P.J. Jansens	Technische Universiteit Delft, reserve lid

Published and distributed by: DUP Science
DUP Science is an imprint of
Delft University Press
P.O. Box 98
2600 MG Delft
The Netherlands
Telephone: +31 15 27 85 678
Telefax: +31 15 27 85 706
E-mail: info@library.tudelft.nl

ISBN 90-407-2376-1

Copyright (c) 2002 by F. Michiel Meeuse

All rights reserved. No part of the material protected by this copyright notice may be reproduced or utilized in any form or by any means, electronic or mechanical, including photocopying, recording or by any information storage and retrieval system without written permission from the publisher: Delft University Press

'My work consists of two parts: The one presented here plus all that I have not written. And it is precisely this second part that is the important one'.

Ludwig Wittgenstein

Contents

1 Introduction **1**

1.1 Chemical Processes . . . 2

1.2 Problem sketch . . . 3

1.3 Structure and main results of the Thesis . . . 4

2 Conceptual process design, a literature review **7**

2.1 Introduction . . . 8

2.2 Generic design principles . . . 11

2.3 Context of Conceptual Process Design . . . 13

2.3.1 Supply chain . . . 14

2.3.2 Process Life Span . . . 15

2.4 Conceptual Process Design practices . . . 17

2.4.1 Hierarchical decomposition . . . 18

2.4.2 Optimization-based conceptual design . . . 20

2.5 Concluding Remarks . . . 22

3 Integration of design and control, an assessment 25
3.1 Introduction 26
3.2 Inherent limitations on the closed-loop performance 28
3.3 Current approaches towards integration of Design and Control . . 31
  3.3.1 Anticipating sequential approaches 31
  3.3.2 Simultaneous approaches 35
3.4 Refined problem formulation 37

4 Controllability in the synthesis phase 39
4.1 Introduction 40
4.2 System Description 41
  4.2.1 General dynamic system model 41
  4.2.2 Inventory based system description 42
  4.2.3 Macroscopic system description 44
  4.2.4 Distributed systems 51
4.3 Process Design, an approach based on non-equilibrium thermodynamics 51
  4.3.1 Heat exchanger 54
  4.3.2 Distillation 55
4.4 Controllability, an approach based on non-equilibrium thermodynamics 56
  4.4.1 Irreversible thermodynamics and stability 57
  4.4.2 Non-equilibrium thermodynamics and control performance 58
4.5 Examples 60
4.6 Discussion and Conclusions 64

5 New Controllability analysis tools 67
5.1 Introduction 68
5.2 Closed-loop controllability 68
  5.2.1 Process and disturbance models 69
  5.2.2 Optimal closed-loop variance 71
  5.2.3 Robustness considerations 73
5.3 Closed-loop controllability and economics 76
  5.3.1 Multi objective optimization 77
  5.3.2 Closed-loop economic optimization 78
5.4 Example: binary distillation 81
  5.4.1 Multi-objective analysis 82

5.4.2 Robustness 84
5.4.3 Closed-loop validation 86
5.4.4 Closed-loop economic optimization results 89
5.5 Dynamic interaction of control loops 91
5.5.1 Review of dynamic RGA 92
5.5.2 Proposed Approach 94
5.5.3 Examples 98
5.5.4 Discussion 102
5.6 Conclusions 103

6 Application: Fischer Tropsch synthesis reactor 107
6.1 Introduction 108
6.2 The Fischer Tropsch synthesis 108
6.2.1 Background of the Process 108
6.2.2 FTS Process Characteristics 109
6.3 Reactor section designs 110
6.3.1 Basis of Design 110
6.3.2 Major design decisions 112
6.3.3 Conceptual design of reactor section 112
6.3.4 Reactor Model 112
6.3.5 Remaining design variables 117
6.4 Application of the TCA method 118
6.5 Controllability analysis 121
6.5.1 Setting up the problem 121
6.5.2 Computational Steps 123
6.5.3 Results 123
6.6 Conclusions 124

7 Integrated design of a periodic operating Fischer Tropsch synthesis process 127
7.1 Introduction 128
7.2 Periodic operation of Fischer Tropsch synthesis 129
7.3 Process Model 131
7.4 Problem formulation 133
7.5 Solution approach 135
7.6 Results 137
7.7 Conclusions 138

8 Outlook **141**

Appendix A Mixed Integer Dynamic Optimization **147**
A.1 Problem formulation 147
A.2 MIDO solution algorithm 148

Appendix B Design of the Internal Model Controller **151**

References **153**

Summary **163**

Samenvatting **167**

Dankwoord **171**

Curriculum Vitae **173**

1

Introduction

The effectiveness of a chemical plant is determined by the interplay between the process, the mode(s) of operation and the control system. The topic of this thesis is integration of process design and control system design. Once the mode of operation (usually steady-state continuous operation) has been established the other two design activities are usually carried out sequentially. But they are highly related and interactive. The central research question in this work is ”How do process design decisions influence the achievable control performance of the system in the conceptual phase of the design?” This problem is explored in three dimensions (1) improvements in the design process itself, (2) application to a novel process with high economic impact and (3) exploiting a wider set of operating modes. The improvements in the design process itself are mainly focussed on the synthesis and analysis phase. The newly developed methods and tools are applied on a novel reactor design for Fischer Tropsch synthesis. Then the economic potential of integrated design of the process and the operational policy for a periodically operated Fischer Tropsch synthesis process is demonstrated.

1.1 Chemical Processes

The products of the chemical industry can be found everywhere in our modern society. Besides typical products like transportation fuels, plastics and solvents, the chemical industry also produces products like medicine, food additives, paint and detergents.

The importance of the chemical industry for the dutch economy becomes clear from the following figures, taken from CBS (2001). In 1999, the turnover of the chemical industry (including the refined petroleum products and manufacture of rubber and plastic products) was 38 billion euro of which 67 % is exported, with a profit of 1.9 billion euro. The investments in the chemical industry in 2000 were about 2.1 billion euro, 25% of the total industrial investments. About 98.000 people are directly employed by the chemical industry.

The basic function of chemical processes is that feedstocks are converted into products that satisfy certain societal needs. This conversion can be just the seemingly simple process of mixing the ingredients of formulations. But it can also be a highly complex process containing multiple chemical reactions, recycles and separation stages. During the last decades chemical processes have become increasingly complex. Ogunnaike (1996) mentions the following three reasons that have led to this increasing complexity:

- the continuous drive for more consistent attainment of high product quality,
- more efficient use of energy,
- tighter safety and environmental regulations.

Moreover chemical processes are considered to be part of a supply chain (Backx et al., 1998) leading to increasing operational requirements. This increased complexity requires novel process design methodologies that can integrate external factors like controllability, safety and sustainability from the earliest design phases on.

These developments inspired the foundation of the Delft Interdisciplinary Research Center (DIOC) ”Mastering the Molecules in Manufacturing (M3)”. The objective of M3 is to develop a novel model based design methodology for complex industrial processes. An essential element in this approach is to consider all relevant phenomena ranging from the smallest molecular time and length scale to the large scales of complete plants and sites. In this thesis the results of the project on integration of process design and control system design are reported.

1.2 Problem sketch

The state of the art in conceptual process design is a three step approach.

- In the first step the operational policy is determined. Will the process be operated in steady-state, (semi-)batch or periodic? How many operating points will be considered?
- Then one designs the process by searching for the optimum process that satisfies all boundary conditions like safety and environment aspects. Optimum is generally defined in some economic sense, for instance the return on investment, based on steady state operation only.
- Only after this conceptual process design a control system is designed to compensate for disturbances.

A more thorough description of the state of the art in conceptual process design is presented in Chapter 2.

From an economic point of view it is desirable that the system can be controlled accurately. This is becoming more and more important because of the supply-chain environment in which the process is operating. Off-spec production can be very expensive because of waste of feedstock. In addition generating excessive amounts of wastes leads to financial costs. Therefore the quality of the control performance can contribute significantly to the overall economics of the system. The achievable control performance is determined by a combination of the operational policy, the process and the control system. An ill controllable process can have the small capital costs, but due to off-spec production, the operational costs can be large or the revenues can be small as well. However there is no straightforward relation between controllability and economics. The interaction between process and control system is certainly not a novel insight. Ziegler and Nichols (1943) already stated that:

> *"...it is important to realize that controller and process form a unit; credit or discredit for results obtained are attributable to one as much as the other."*

Note that the operational policy is usually not considered.

The ideal situation would be that the economic effects of the control performance could be assessed in the process design phase. A first step would be to have an solid understanding about how the design decisions made in the process design phase influence the achievable control performance. When this knowledge is available the design decisions can be made considering both the static economics based on nominal operation *and* the achievable control performance.

Based on this a preliminary problem definition is formulated:

> *How do process design decisions influence the achievable control performance of the system in the conceptual phase of the design?*

This problem will be explored in three dimensions:

- What improvements in the design process itself are needed?
- Are improvements applicable to realistic situations; i.e. to a novel process with high economic impact?
- Can dynamic modes of operation be included?

In Chapter 3 this problem definition will be refined based on a review of existing practices.

1.3 Structure and main results of the Thesis

In Chapter 2 the state of the art in process design is outlined. The context of the conceptual process design phase is sketched and an introduction is presented of currently available process design methodologies. Some generic design principles that can be found in different engineering design disciplines will be introduced and their application in chemical process design will be discussed. The generic design cycle will be presented. This model of the design process will used throughout this thesis to put the new contributions in place.[*]

Chapter 3 continues with a discussion of existing literature in the field of integration of process design and control system design. Alternative currently available methods will be identified. Their limitations will be discussed and a refined problem definition is presented. The refined research objectives are developments of a controllability method applicable for the synthesis phase, novel controllability analysis methods and testing on a novel design case study, as well the integrated design of the operational policy and the process for periodically operated processes.

---

[*] This Chapter is written jointly with Gijsbert Korevaar. In his upcoming PhD thesis he will show how sustainability issues can be integrated in the conceptual design phase.

In Chapter 4 a new Thermodynamic Controllability Assessment (TCA) approach is presented. This approach, based on non-equilibrium thermodynamics allows the designer to account for controllability in the synthesis phase.

In Chapter 5 a new controllability analysis indicator is developed that overcomes some of the limitations of existing indicators. This indicator is based on LQG control. It is also shown how this indicator can be used to make a tradeoff between controllability and economics. Moreover a novel analysis method is developed for dynamic interaction analysis of control loops. The major benefit of this method is that the interaction analysis is done in the time domain, without restrictive assumptions on the type of control being used.

Subsequently in Chapter 6 the methods that were developed in Chapter 4 and 5 are demonstrated in a case study: the Fischer Tropsch synthesis reactor section. The controllability characteristics of alternative designs of a novel Fischer Tropsch synthesis reactor will analysed.

All processes considered up to Chapter 6 have the same operational policy; it are steady-state continuous processes. In Chapter 7 we will show that an alternative operational policy can sometimes lead to significant economic benefits. We will present an integrated design of the operational policy and the process for a periodically operated Fischer Tropsch synthesis process. This integrated design of the system and the control reference signal leads to a dynamic optimization problem.

In Chapter 8 the results obtained in this thesis will be put into perspective and recommendations for future developments will be presented.

2

Conceptual process design, a literature review[†]

In this chapter the field of conceptual process design is investigated. First the relevance of conceptual process design research is identified. Then conceptual design is placed in a societal context. After a brief discussion of generic design principles, the currently standard approaches of conceptual process design are discussed. This description of conceptual process design can be used to put all developments made in the remainder of the thesis into general conceptual process design perspective.

[†] This Chapter has been written together with Gijsbert Korevaar

2.1 Introduction

The objective of chemical processes is to convert a specific feed stream into specified products. The design of the process begins with the desire to produce profitable products that satisfy societal needs (Seider et al., 1999). The products include petrochemicals, industrial gases, foods, pharmaceuticals, polymers and many other (bio-)chemical products, etc. A large number of steps are taken between the original idea and plant operation, of which conceptual process design is a specific step. Douglas (1988) defined conceptual process design as:

> *[...] to find the best process flowsheet (i.e., to select the process units and the interconnections among these units) and estimate the optimum design conditions.*

In the more recent textbooks on process design, Biegler et al. (1997) and Seider et al. (1999) give similar definitions. The importance of conceptual process design becomes clear when one realizes that, although a relatively small fraction of the total budget is spent during the conceptual design, the majority of investment costs is assigned in this phase. Figure 2.1 illustrates this schematically. Sirola (1997) estimates that decisions made in the conceptual design phase, which accounts for about two or three percent of the project costs, fix approximately eighty percent of the combined capital and operational costs of the final plant. So the success of a chemical plant is for a large part determined by the conceptual design.

Conceptual process design is a highly complex task. Therefore systematic methods for conceptual process design are required. The following characteristics of conceptual design contribute to this complexity:

- A large number of alternatives is possible.
- A large variety of requirements should be satisfied.
- Large differences in temporal and spatial scales are involved.

These characteristics will now be discussed in some more detail.

Number of alternatives Douglas (1988) estimates that for a typical design the number of alternatives that might accomplish the same goal can be over 1 billion. Out of these alternatives one wants to select the one that best suits the

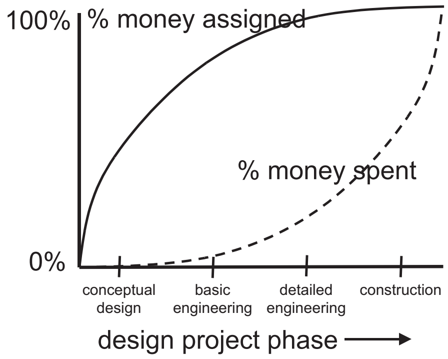

Figure 2.1: *Financial characteristic of conceptual process design.*

objectives, e.g. the design with the lowest financial costs that satisfies all other constraints. The main difficulty with this large number of alternatives is that the path from design decisions to the demands to be satisfied is complex and highly non-linear. This requires systematic methods to reduce the number of alternatives early in the design process.

Quality factors In process design, the designer has to cope with a large variety of requirements. Some of these are explicitly state in the Basis of Design, others not. Herder (1999) defined all requirements as quality factors. Based on group discussions with industrial experts, Herder (1999) identified a large list of quality factors that are relevant for chemical processes. These quality factors are arranged in two dimensions. On one dimension there are the following four classes:

functional what functions shall the system provide?

operational how shall the system be operated?

physical what are the physical conditions, the system shall endure?

economic what are the costs and budget limitations?

The other dimension concerns the system levels: plant level, site level and world level. Table 2.1 shows a representative list of external factors, classified according to these two dimensions, from a case study presented by Herder (1999).

Table 2.1: *Example of external and adjustable factors (Herder 1999)*

	Plant	Site	World
Functional	Battery Limits Process technology Process outputs Process inputs Heat integration Waste water treatment Solvent choice Unit to handle emission	Storage facilities Site selection Utilities Quality of raw material	Environment and safety Emission permits
Operational	Operation/Automation Steady operation Operability	Storage possibilities on site Restrictions induced by local plants	Fugitive emissions Company safety records
Physical	Material selection Plant layout Reactor choice	Location, lay-out Local weather	Climate
Economic	Optimization base Plant optimization Solvent availability Reactor flexibility Sensitivity for fouling Availability Strategic behaviour by designers	Site selection Raw material and product price Integration with local facilities	Integration options with local companies Competitors Political stability

All those factors are regarded nowadays as relevant, but it stays very hard to consider them during the decision-making in the conceptual phase of the chemical processes, especially since the different criteria play a role at different phases in the design. The problem is that the route from a design decision to the quality factor is quite complex, comprising many causal steps and being highly non-linear in its behaviour. So a challenge for conceptual process design is to know when which quality factors should be considered and how the design decisions made have an influence on these quality factors.

Multiple scales The performance of chemical processes is determined by phenomena operating at various temporal and spatial scales. On the one hand nano-scale phenomena are dominant at for instance catalyst surfaces with typical spatial scales of 10^{-9}m and typical temporal scale of 10^{-3}s. On the other hand phenomena on global scale influence the operational policies of chemical processes with typical spatial scales of 10^{6}m an typical temporal scales of 10^{6}s. Figure 2.2 shows the various scales schematic.

This Chapter is organized as follows. First some generic design principles will be discussed. These are principles found in other engineering disciplines, but also applicable in chemical process design. Then the context of conceptual process design is sketched. This context contains two dimensions; the supply chain and the process life span. In section 2.4 the conceptual process design practices, as found in the literature, are presented. The Chapter ends with some final remarks.

2.2 Generic design principles

Design is an activity that is carried out in a wide variety of application fields. Railway-tracks, a new engine for a Formula 1 car, a new chair and a CD player are all products that are designed (by engineers). The design of such products is often a multi-disciplinary activity. Despite this wide variety in design, there are several common factors.

Several authors describe the essential element of design as reasoning from *function* to *form* (e.g. Gero, 1990, Roozenburg and Eekels, 1995, Kroes, 2000). The design starts with the need for a product that fulfills a specific function. The designer should then determine the product that (optimally) satisfies the

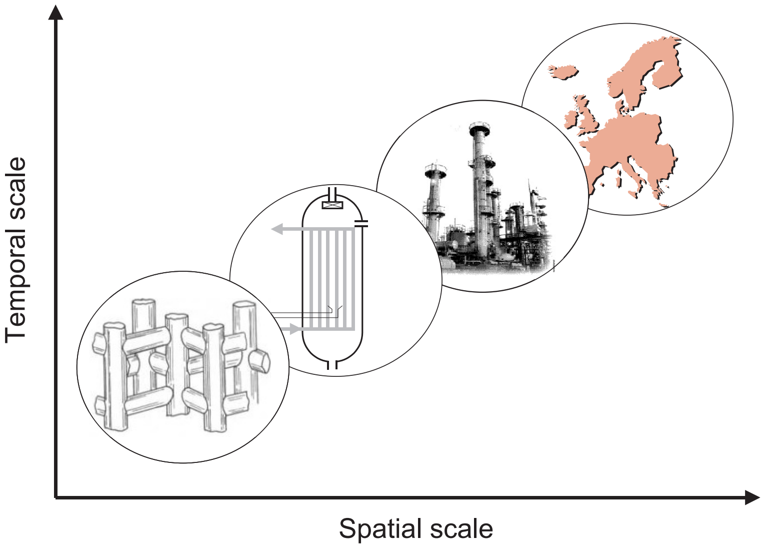

Figure 2.2: *Schematic representation of the relevant scales for chemical processes.*

required tasks. The form of the product consists of a description of both geometric properties and the physico-chemical properties. In chemical process design the function is generally described as *to convert a feed into products with specified properties.* (Douglas, 1988)

A model that describes the various activities carried out in the process of reasoning from function to form is the so-called *basis cycle of design* (Roozenburg and Eekels, 1995). This model is found in various alternative design fields, including industrial design engineering (Roozenburg and Eekels, 1995), chemical process design (Siirola, 1996) and mechanical engineering design (Cross, 1994). Figure 2.3 shows this cycle. The process starts with formulation of the design problem. In this stage the basis of design is defined. This includes specification of the external factors that needs to be considered, selection of the design space and of the building blocks to be used and identification of the required domain knowledge. Then, in the synthesis phase, alternatives are generated. The (physical) behaviour of the alternatives is determined in the analysis phase. In the evaluation phase the performance of the system is compared with the required

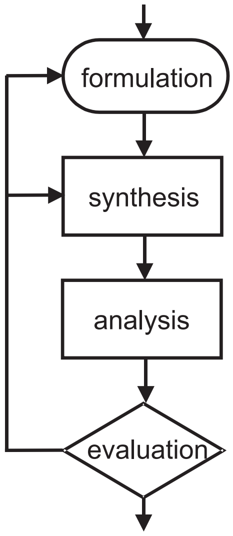

Figure 2.3: *Basis cycle of design.*

performance, as specified in the problem formulation phase. So this relates to the societal appreciation of the alternatives. If the performance is not acceptable, one should either reformulate the problem, or generate other alternatives in the synthesis phase. When the behaviour is acceptable, one can proceed with the design to the next level of detail.

2.3 Context of Conceptual Process Design

Every chemical process is designed for a given infrastructure within a certain environment, this implies that many interactions exist between the performance of the chemical plant and the world around. The context of the conceptual process design can be sketched in two dimensions (Grievink, 2002); the supply chain and the process life span. This is illustrated in Figure 2.4.

2.3.1 Supply chain

Traditionally chemical processes were studied separately from their environment. Because of the growing urge for industrial symbiosis (Konz and van den Thillart, 2002) and growing complexity of industrial product life cycles (Kleineidam 2000) this is no longer sufficient. This is the incentive for the emerging field of supply chain management (see for example, Applequist et al., 2000, Hall 2000, Zhou et al., 2000). The supply chain is defined, as the whole of processes that surrounds the process and that is required to bring the product to the customer. The supply chain is somewhat related to the product life cycle, which describes the life of a product from cradle to grave. The difference is that the viewpoint in the supply chain is the process whereas the viewpoint in the product life cycle is the product. The supply chain describes all factors influencing the operation of the process.

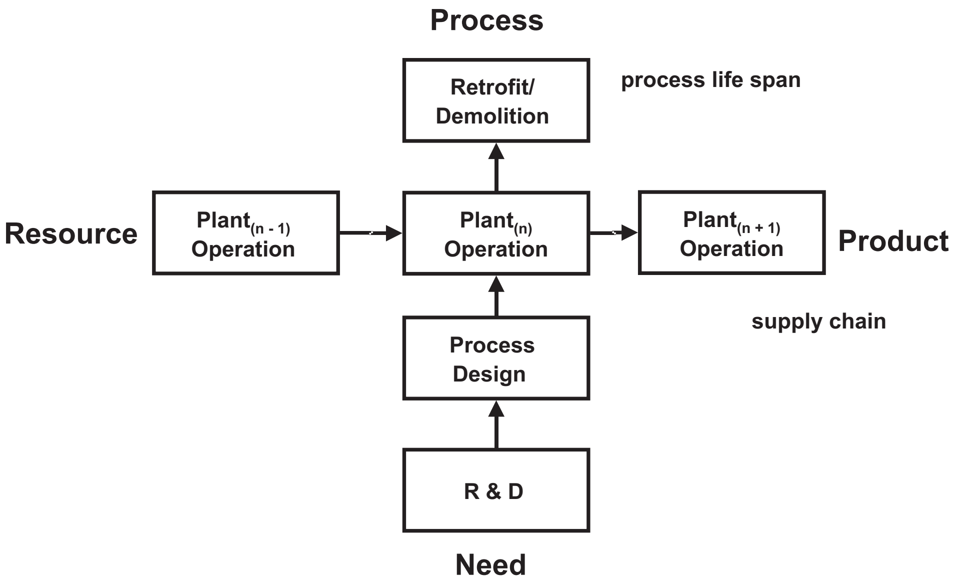
Process
Retrofit/ Demolition
process life span
Resource
Plant(n - 1) Operation
Plant(n) Operation
Plant(n + 1) Operation
Product
supply chain
Process Design
R & D
Need

Figure 2.4: *The context of conceptual process design.*

The supply chain starts with the exploration of resource materials and ends with the final product (Backx et al., 1998), the transportation and inventory steps in between are also taken into account. The chain does not only contain material flows, but also information flows, which determine the purchasing, planning and marketing. This kind of schemes (as presented in Figure 2.5), can be helpful in locating the process in its larger context by considering the input and output of the process as outcomes of the supply chain modelling (Backx et al., 1998).

The whole supply chain can be modelled (Garcia-Flores et al., 2000) and optimization tools can be used in supply chain management (Gupta et al., 2000). Supply chain considerations will influence some external factors in the Basis of Design. Typical examples are turn-down ratios and flexibility requirements with respect to product grades and associated qualities.

2.3.2 Process Life Span

The Conceptual Process Design is only a part of the process life span of chemical plants, as already indicated in Figure 2.4. Here we discuss a general description of the procedure to come to a chemical process taken from Siirola (1995), see Figure 2.6. According to the author, the building of a chemical plant is an organized multistage goal-directed process. This process leads from the identification of the customers' needs to a plant operation producing a material that fulfils the needs. The construction of a chemical plant is carried out in various ways, depending on the organization of the company or the nature of the chemical process, for example the development of a new facility requires more steps than the improvement of an existing plant. Figure 2.6 shows that the conceptual process design covers the stages basic chemistry to basic plant engineering. In the stage of basic chemistry fundamental reaction chemistry is selected. In the detailed chemistry stage chemical details of catalysis, solvents and reaction conditions are defined. The task identification identifies physical operations to prepare raw materials for reaction and isolate reaction products for sale. In the unit operations stage, chemical and physical operations that are defined previously are associated with actual pieces of equipment and basic plant engineering means the definition of supporting utilities and other facilities infrastructure. This sequence however is strongly focussed on petro-chemicals. For processes with micro-structured products the micro-structure should be considered explicitly early in the process.

The innovation process is not a linear process, in which each stage is visited once. On the contrary, the process is highly iterative and stages may be revisited

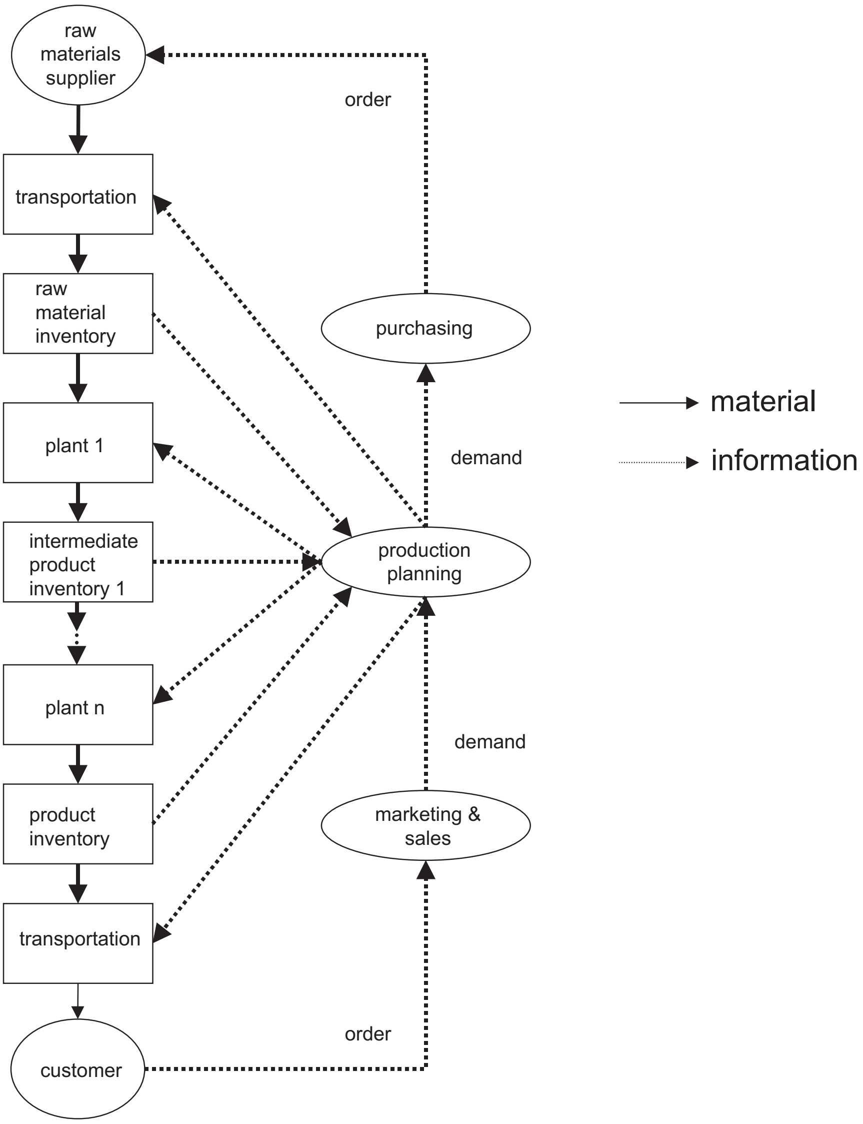
raw materials supplier
order
transportation
raw material inventory
purchasing
material
information
demand
plant 1
intermediate product inventory 1
production planning
plant n
demand
product inventory
marketing & sales
transportation
order
customer

Figure 2.5: *Schematic representation of a supply chain (Backx et al., 1998).*

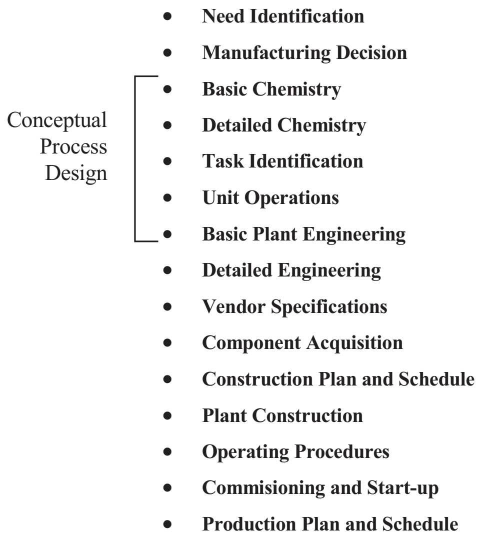
Conceptual Process Design
Need Identification
Manufacturing Decision
Basic Chemistry
Detailed Chemistry
Task Identification
Unit Operations
Basic Plant Engineering
Detailed Engineering
Vendor Specifications
Component Acquisition
Construction Plan and Schedule
Plant Construction
Operating Procedures
Commisioning and Start-up
Production Plan and Schedule

Figure 2.6: *General Innovation Cycle (Siirola).*

several times until an acceptable solution is reached. This implies that each visit to a stage can be conducted at different levels of detail.

Especially from the viewpoint of sustainable development, life span issues of the chemical plant are important during the development of chemical processes (Ishii 1997), which can be covered by incorporation of LCA-(Life Cycle Assessment)-tools in the process design stage (Azapagic 1999).

2.4 Conceptual Process Design practices

Traditionally conceptual process design was a kind of evolutionary activity. New plants were designed mainly based on existing plants. In the early seventies some progress was made towards a systematic approach for conceptual process design (Rudd et al., 1973). This was mainly inspired by the increasing demands both from an economic point of view and from an environmental and energy consumption point of view. But only in the last two decades of the 20th century the major advances in conceptual process design were made. The approaches can be classified into two groups: hierarchical decomposition and superstructure optimization (Douglas and Stephanopoulos, 1995, Daichendt and Grossman, 1998). Hierarchical decomposition and superstructure optimization are sometimes presented as two competing approaches. They should however, be considered as complementary rather then competing (Douglas and Stephanopoulos, 1995). In the earlier design stages the emphasis will be more on hierarchical decomposition, while optimization methods will be more important in the later design stages. In these stages the number of alternatives is reduced and usually models will be available. Therefore optimization methods will be more useful then in the earlier phases.

2.4.1 Hierarchical decomposition

The basic idea of hierarchical decomposition is that the design problem is too complex a problem to be solved at once. Therefore it is decomposed into several sub-problems with increasing amount of detail. Two different types of hierarchical decomposition are often encountered into the literature. The most often referred to approach is the one originally presented by Douglas (1985, 1988). This approach starts with considering only the input-output structure of the process. In the subsequent design levels, more details are added, finally ending with the complete flowsheet. The design decisions are mainly made using heuristics and short-cut models. The evaluation is done based on economics only. Table 2.2 shows the levels according to Douglas and Stephanopoulos (1995).

Table 2.2: *Design levels of Douglas hierarchical decomposition.*

Level 0	Input information
Level 1	Number of plants
Level 2	Input/output structure
Level 3	Recycle structure
Level 4	Separation structure
Level 5	Heat exchanger network

In all levels the decisions are made based on the total annualized costs. The method was originally developed for gas/liquid processes only, Douglas (1985, 1988). Extensions to solid processes (Rajagopal et al., 1992), polymer processes (Malone and McKenna, 1990, McKenna and Malone, 1990) and multi-step reaction plants (Douglas, 1990) have been presented afterwards.

The second direction into hierarchical decomposition is a task-driven method (Siirola, 1995, 1996). In this method the properties of the product and the feedstocks are compared. The raw materials are considered to be the initial state. The desired product is the goal state. When property differences exist between the initial state and goal state, tasks are required that eliminate these differences. According to Siirola (1995) a natural hierarchy among property differences (and hence tasks) exists: molecular identity, amount, composition, phase, temperature and pressure, form. This hierarchy arises because changing the properties lower in the hierarchy will generally not influence the properties higher in the hierarchy. Table 2.3 shows the hierarchy in property differences and some resolution methods. Once all required tasks have been identified, equipment should be designed to realize these tasks. In this step significant savings can be achieved when multiple tasks are integrated in one piece of equipment. The last item of the hierarchy, form, however seems not to fit in. Meeuse et al. (2000) showed that for products with in internal microstructure one should start with considering this structure, rather then end with it.

Table 2.3: *Property hierarchy and common difference elimination methods (Siirola, 1996).*

Property Difference	Resolution Method
Molecular Identity	Reaction Mixing
Amount	Splitting, Purchase
Composition	Mixing, Separation
Phase	Enthalpy Change
Temperature, Pressure	Enthalpy Change
Form	Various

The Delft Conceptual Design Matrix (Grievink 2002) is a combination of the task driven method, Douglas approach and the general design paradigm. This matrix is shown schematic in Figure 2.7. In this novel level framework one of the levels contains the task description. This also enables the designer to think into the more fundamental tasks then in terms of traditional unit operations. Meeuse et al. (2000) and Jadhav et al. (2002) have demonstrated the effectiveness of such an approach for structured products.

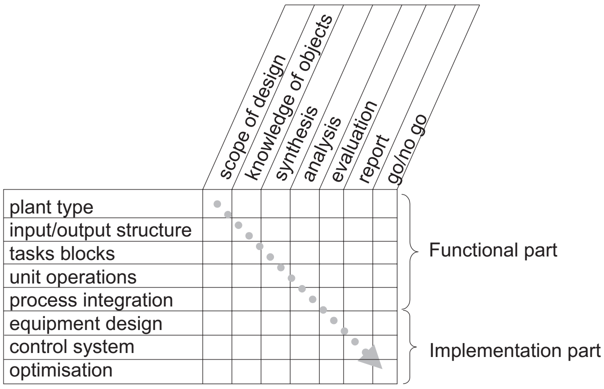
scope of design
knowledge of objects
synthesis
analysis
evaluation
report
go/no go
plant type
input/output structure
tasks blocks
unit operations
process integration
equipment design
control system
optimisation
Functional part
Implementation part

Figure 2.7: *Delft Conceptual Design matrix.*

2.4.2 Optimization-based conceptual design

The process design problem can also be formulated (and solved) as an optimization problem. A typical characteristic of such an optimization problem is that it consists of both continuous design variables, like sizes, temperatures, pressures and flowrates, and discrete design variables, indicating the structure of the process. These discrete design variables are associated with a so-called superstructure, which has embedded a large set of feasible process operations and interconnections that are candidates for an optimal process design. Figure 2.8 gives an example of such a superstructure. This structure contains a plug flow reactor, a CSTR and all combinations of these two reactors, as well as two different separation sequences. The number of trays and feed tray location are additional design variables.

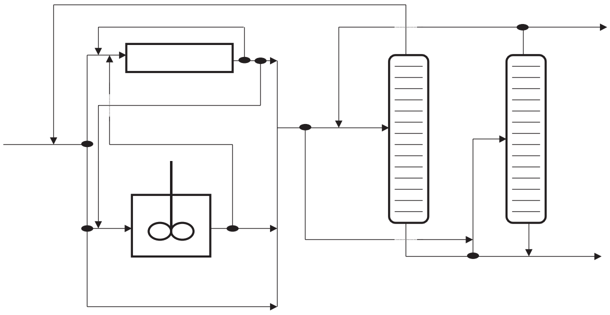

Figure 2.8: *Process superstructure.*

Mathematically the problem can be formulated as follows. Let a process systems be described by a set of Differential Algebraic Equations (DAE):

$$\begin{aligned} \dot{x} &= f(x, z, u, \delta, \sigma, \phi), \\ 0 &= g(x, z, u, \delta, \sigma, \phi), \end{aligned} \tag{2.1}$$

where $x \in \mathbb{R}^{n_x}$ are the state variables, $z \in \mathbb{R}^{n_z}$ are the algebraic variables, $u \in \mathbb{R}^{n_u}$ are the input variables, $\delta \in \mathbb{R}^{n_\delta}$ are the disturbance variables, $\sigma \in \mathbb{R}^{n_{\sigma_c}} \times [0,1]^{n_{\sigma_d}}$ are the design parameters, and $\phi \in \mathbb{R}^{n_\phi}$ are the uncertain parameters. The design variables contain real-valued, σ_c, and integer-valued numbers, σ_d. Real-valued design parameters are for example dimensions, pressures and temperatures. Integer-valued design parameters are related to structural design decisions e.g. the number of trays in a column or the type of reactor. In this chapter all uncertain variables are considered to have their nominal values, $\phi = \phi_0$ so that these can be omitted from the analysis. f are the differential equations and g are the algebraic equations. The domain of validity is described with the following inequality constraints:

$$0 \leq k(x, z, u, \delta, \sigma), \tag{2.2}$$

where k represent the inequality constraints.

The static process design problem can then be formulated as:

$$\begin{aligned} \min_{\sigma,u} \quad & J(x,z,u,\delta,\sigma), \\ s.t. \quad & 0 = f(x,z,u,\delta,\sigma), \\ & 0 = g(x,z,u,\delta,\sigma), \\ & 0 \leq k(x,z,u,\delta,\sigma), \end{aligned} \tag{2.3}$$

where J is an economic parameter like the return on investment or the total costs.

The numerical optimization techniques that can be employed to find the optimum design embedded in the superstructure can be either gradient based, mixed integer non linear programming techniques (MINLP) (Grossman, 1997, Floudas, 1995) or genetic algorithms (Emmerich et al., 2000).

Most applications are for subsystems rather then for complete flowsheets. Floudas (1995) presents an overview of several applications: heat exchanger networks, separation systems, reactor networks and reactor-separator-recycle systems. Papalexandri and Pistikopoulos (1996) present an alternative superstructure based on mass and heat transfer modules rather then on equipment. This approach is closely related to the task driven approach, allowing for the generation of novel type of processes. One of the difficulties in this approach is however to formulate an objective function since there is no direct relation with equipment sizes and hence with the capital costs.

The main benefit of the optimization-based approaches is that it can really find the optimum solution embedded within the problem statement. However the time required for this is substantial. Especially the formulation of the problem and the efforts required to get the converged solution from arbitrary initial conditions can be significant.

2.5 Concluding Remarks

In this Chapter we investigated the field of conceptual process design, one of the earliest phases of the design of chemical plants. The conceptual process design problem aims to find a flowsheet that converts a specified feedstock into a specified product and that fulfils the requirements of the assignment. In practice, an assignment is given to design a chemical plant for the production of a certain product or a set of products, within a given environment and with required specifications.

The focus of our work is to incorporate the quality factors controllability[†] and sustainability[‡] in conceptual process design. In the current design practices presented in this Chapter, these quality factors are not considered explicitly. Therefore, design methodologies need to be improved such that these issues can be incorporated. It is important that the design methodology helps to make decisions explicitly. The methodology has to improve the generation of alternatives and locate the analysis tools. During the generation of alternatives, heuristic-based tools are used, because a decision has to be made with lack of information. In the analysis and evaluation phase, it is necessary to define new tools, that can quantify the controllability or the sustainability.

Notation

Roman symbols

f	differential equations
g	algebraic equations
J	objective function
k	inequality constraints
u	inputs
x	state variables
z	algebraic variables

Greek symbols

δ	disturbances
σ	design variables
ϕ	uncertain parameters

Subscripts

0	nominal value

[†] This thesis

[‡] The upcoming thesis by Gijsbert Korevaar

c	continuous variables
d	discrete variables

3

Integration of design and control, an assessment

This chapter gives an overview of the literature on integration of process design and control system design. Available methods are classified into two classes: anticipating sequential design and simultaneous design. Both classes are discussed extensively. The limitations of the existing approaches are identified. One of the main limitations is that all available methods can only analyse the controllability of given process alternatives. No clues are given on how to generate alternatives with improved controllability. Based on this discussion a refined problem definition for further research is presented.

3.1 Introduction

In the previous chapter an overview of conceptual process design methodologies was presented. Once a process is operating, it will however always operate with a control system installed. During the last decades chemical processes have become increasingly complex. Ogunnaike (1996) mentions the following three reasons that have led to this increasing complexity:

- the continuous drive for more consistent attainment of high product quality,
- more efficient use of energy,
- tighter safety and environmental regulations.

Moreover chemical processes are considered to be part of a supply chain (Backx et al., 1998) leading to increasing operational requirements.

Traditionally there is a three step approach. First the operational policy is determined, then the process is designed. Finally the control system is designed as an add-on to the process. So the control system design only starts once the main features of the process have been established. When no control system with an acceptable performance can be designed for the process, the process design needs to be modified, leading to iterations between the process design and the control system design. Obviously these iterations are undesirable since they cost time and money. Especially since the need for modifications is sometimes only noticed after construction of the system, during start-up. Figure 3.1 shows this approach schematically. The disadvantages associated with this approach have led to the need to consider the inherent control limitations of the process from the earliest phases of the design process on.

Integration of design and control is certainly not a new topic. The first paper on this topic was published in 1943 (Ziegler and Nichols, 1943). There it is stated

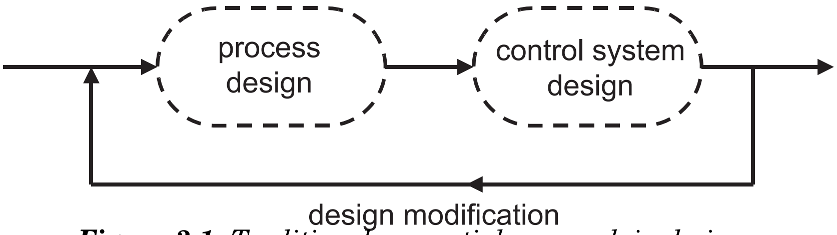

Figure 3.1: Traditional sequential approach in design .

that:

> *"...it is important to realize that controller and process form a unit; credit or discredit for results obtained are attributable to one as much as the other."*

They also give a definition of controllability:

> *[Controllability is] the ability of the process to achieve and maintain the desired equilibrium value.*

This definition is in line with the modern definition presented by Skogestad and Postlethwaite (1996):

> *(input-output) controllability is the ability to achieve acceptable control performance that is, to keep the outputs within specified bounds or displacements from their references, in spite of unknown but bounded variations, such as disturbances and plant changes, using available inputs and available measurements.*

One should note that this controllability concept is completely different from the state controllability concept introduced in the 1960s, and nowadays widely used in the systems theory. The difference between these two concepts is clearly illustrated by Skogestad and Postlethwaite (1996).

The first industrial problem related to controllability that appeared in the open literature is due to Anderson (1966). This problem deals with feed-effluent heat exchanger that was designed improperly. The energy recycle led to positive feedback that destabilized the system under certain operating conditions. A complete redesign was required to run the plant at its design capacity. Verwijs (2001) has presented some recent examples of industrial problems related with design and control. Unfortunately, the majority of problems in this field, faced by industry is not available in the open literature, mainly because of confidentiality. In the academic world integration of design and control is a very active research area. Van Schijndel and Pistikopoulos (2000) give over 500 references related to this topic. Perkins (1998) even called integration of design and control "*the holy grail of process systems engineering*".

An implicit assumption in the work on integration of design and control is that the operational policy has already be choosen; almost always continuous operated steady-state processes. In principle however also different operational modes are possible, e.g. (semi)-batch processes or periodic processes. Therefore ideally the following three aspects should be considered: the operational policy, the process and the control system. In this thesis the processes considered are, unless otherwise stated, steady-state continuous processes.

In this chapter an overview of the literature available related to the interaction between process design and process control will be presented. First some general background information will be presented. Then the fundamental limitations to the achievable closed-loop performance will be identified. This will be followed by a discussion on the available approaches towards integration of design and control. The chapter will end with a refined problem formulation.

3.2 Inherent limitations on the closed-loop performance

Despite the large research effort in integration of design and control, almost no effort has been put in identifying the fundamental reasons for controllability problems. In order to identify these problems, let us first present a generic model of a closed-loop system. It is assumed that the system is a square continuous time system without constraints. The closed-loop behaviour of any process system is determined by a combination of the process, the measurement system, the control system and the actuators. Figure 3.2 shows a typical representation of a generalized closed-loop system, containing all these elements. For a single input single output system, the closed-loop transfer function in the Laplace domain is then given by:

$$y(s) = \frac{G_p(s)G_a(s)G_c(s)}{1+G_p(s)G_a(s)G_c(s)G_m(s)} y_{sp}(s) + \frac{1}{1+G_p(s)G_a(s)G_c(s)G_m(s)} d(s), \quad (3.1)$$

where $G_p(s)$, $G_a(s)$, $G_c(s)$ and $G_m(s)$ are the process, actuator, controller and measurement transfer function respectively, $y(s)$ are the controlled variables, y_{sp} are the set-points and $d(s)$ are the disturbances.

An often made assumption is that the dynamics of the measurement system and the actuators are neglected. This leads to the simplified version of equation 3.1:

$$y(s) = \frac{G_p(s)G_c(s)}{1+G_p(s)G_c(s)} y_{sp}(s) + \frac{1}{1+G_p(s)G_c(s)} d(s). \quad (3.2)$$

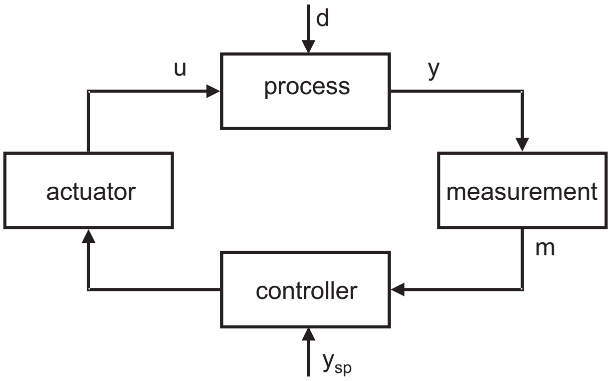

Figure 3.2: *Typical closed-loop process system.*

Note that this ignores the fact that especially composition measurements can have large time delays and sampling intervals .

Based on this closed-loop transfer model Morari (1983) identified the inherent limitations of the process on the closed-loop behaviour of the system. He introduces the concept of perfect control for this. The open-loop system can be represented by:

$$y(s) = G_p(s)u(s) + d(s). \tag{3.3}$$

where $u(s)$ are the manipulated variables. The system is perfectly controlled if:

$$y(s) = y_{sp}(s), \;\forall\;\; d(s), y_{sp}(s). \tag{3.4}$$

This requires that:

$$u(s) = G_p^{-1}(s)(y(s)_{sp} - d(s)). \tag{3.5}$$

Hence perfect control requires that the process transfer matrix can be inverted. In order to be implemented the inversion should also be realized in physical reality. All aspects limiting this inversion, or the realization of this inversion are inherently controllability limitations. Morari (1983) showed that the following aspects limitations for invertibility:

- time delays
- right half plane zeros

- manipulated variable constraints
- model uncertainty

Time delays If the elements of $G(s)$ contain time delays, the elements of $G^{-1}(s)$ will contain predictive elements. Obviously this cannot be realized. Hence time delays are inherent controllability limitations. A more detailed discussion of time delays (in multivariable systems) is given by Holt and Morari (1985b).

Right Half Plane zeros When the transfer function $G(s)$ is inverted the zeros of $G(s)$ become the poles of $G^{-1}(s)$ and the poles of $G(s)$ become the zeros of $G^{-1}(s)$. When $G(s)$ contains right half plane zeros, $G^{-1}(s)$ will contain right half plane poles. Hence G^{-1} will not be stable. Therefore right half plane zeros are an inherent limitation on the controllability. For multivariable systems one should however look at the RHP-transmission zeros (Holt and Morari 1985a)

Manipulated variable constraints The required values of the manipulated variables are given by equation 3.5. However these values could be well out of range. This then leads to saturation of the inputs. So this saturation of input variables is another controllability limitation.

Model uncertainty The expression for perfect control, equation 3.5 assumes that the system transfer function $G(s)$ is known. A mismatch between the real process and the transfer function $G(s)$ will lead to deviations from perfect control. This is also clearly illustrated with the concept of Internal Model Control (Garcia and Morari, 1982). Figure 3.3 shows the internal model controller for the plant G. The model of G is $\tilde{G}$. The system G_c is the invertible part of $\tilde{G}$. The closed-loop transfer function is then given by:

$$y(s) = G \cdot G_c(I + (G - \tilde{G})G_c)^{-1}(y_{sp} - d) + d. \tag{3.6}$$

So a condition for perfect control is that the plant model fully matches the plant:

$$G = \tilde{G}. \tag{3.7}$$

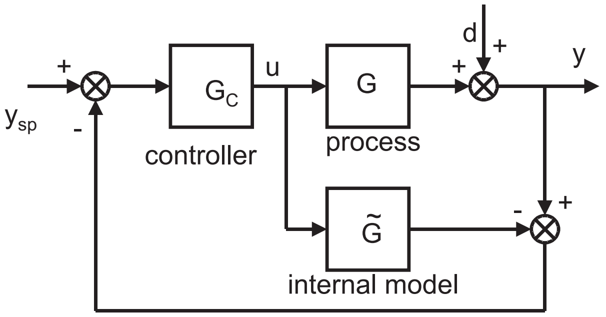

Figure 3.3: *Internal model controller.*

3.3 Current approaches towards integration of Design and Control

Various different approaches are available for the design of the process and the control system. Lewin (1999) classifies the different approaches in three classes:

- Sequential design of the process and the control system.
- Anticipating sequential design with screening of alternatives using controllability indices.
- Simultaneous design of the process and the control system.

The first class is the traditional sequential approach (Figure 3.1) of which the disadvantages have been already introduced. The other two classes will now be discussed.

3.3.1 Anticipating sequential approaches

The basic idea of the anticipating sequential approaches is that still a certain decomposition exists between process design and control system design. However, in the process design phase one already takes into account that the systems needs to be controlled later on. In the process design phase the control objectives are established and the manipulated variables are identified. In the next step the open-loop behaviour of alternative designs are analysed using controllability indices. These indices should reduce the iterations between the process design and the control system design, as shown in Figure 3.4. A large number of controllability indices is available in the literature. The majority of these indices is based on the static gain matrix. The static gain matrix is simply the transfer function $G(s)$ at steady-state, so $G(0)$. Some of the most often used indices are the Relative Gain Array, RGA (Bristol, 1966), the condition number, the minimum singular value, the closed-loop Disturbance Gain, CLDG (Skogestad and Postlethwaite, 1996) and the Relative Disturbance Gain, RDG (Marino-Galarraga et al., 1987). All these indices are only applicable on linear static systems.

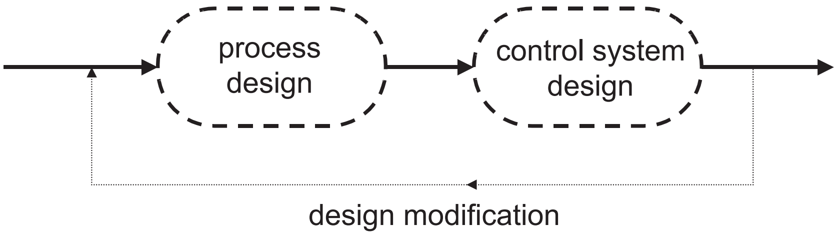

Figure 3.4: *Modified sequential design approach.*

There are however from a process design perspective a number of disadvantages associated with these indices. Morari and Perkins (1995) have stated that: *what is ultimately of interest is the closed-loop behaviour of the system once it is operating and subjected to disturbances.* However, the relation between these controllability indices and the closed-loop behaviour is often unclear. What does it mean that *"the minimum singular value of a (properly scaled system) equals 1?"* when a design is being made.

An additional limitation is that it might be impossible to compare process design alternatives of different dimensionality. Compare for instance a single CSTR or two CSTR reactors in series. As shown in Figure 3.5 the single CSTR has two manipulated variables and two controlled variables. The two CSTR in series have three controlled and manipulated variables. However, comparing the condition number of a 2*2 matrix and a 3*3 matrix is physically not relevant .

In addition it is not clear how the controllability inidices are related to the

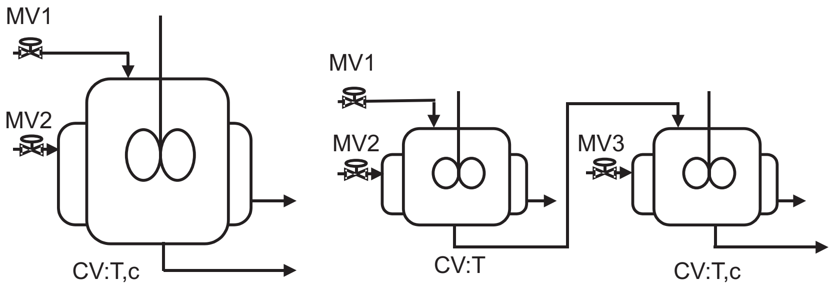

Figure 3.5: *Single CSTR and two CSTRs in series.*

overall process economics.

Some attempts have been made to extend these indices to the frequency domain. Then the indices can be calculated as a function of the frequency. This leads, however, to several difficulties:

1. The indices are sometimes no longer uniquely defined.
2. The frequency domain has limited applicability for chemical process design.
3. Some indices presume on unrealizable controllers.

These three arguments will now be discussed a in detail.

1. For the frequency dependent controllability indices the process transfer matrix $G(s)$ is used with $s = j\omega$. For some of the indices this leads to indices containing complex elements. In order to interpret the indices some 'tricks' are used to obtain indices with real values. Take for instance the Relative Gain Array. The frequency depended RGA is defined by:

   $$RGA(j\omega) = G(j\omega) \bigotimes G(j\omega)^{-1^T} \tag{3.8}$$

   where $\otimes$ indicates element by element multiplication. The resulting RGA matrix contains complex elements. Several alternative ways have been proposed to convert these for interpretation purposes to real elements. Seider et al. (1999) for example, propose to take the magnitude of one element and then use the property that the sum of elements in a row or column is 1, to find the other elements in the matrix. This might work for a 2*2 system, but the results now depend strongly on the selected element from which the magnitude is taken. In Chapter 5 an alternative method is introduced.

2. The frequency domain stems from the systems and control community. It has however never been embraced by chemical engineers, especially not by those working outside academia. The key limitation of the frequency domain is the linear additivity of such transformations, while chemical processes have non-linear features.
3. Indices that require the inversion of the transfer matrices assume perfect control. In section 3.2, the limitations for perfect control were already presented.

An alternative method more tuned to the needs of chemical process designers has been presented by Seferlis and Grievink (1999). This method can easily cope with non-square systems, non-linear systems and constraints. Their approach essentially involves the following:
Given:

- a static process model,
- a set of controlled variables,
- set points for the controlled variables, y_{sp},
- a set of manipulated variables,
- nominal values of the manipulated variables, u_0,
- process constraints,
- a static disturbance, d,

such that the setpoints and nominal values for the manipulated variables satisfy the process model for zero valued static disturbances,
Find:

- the minimum combined deviation of the nominal values of the manipulated variables and the set point violation of the controlled variables.

This minimum combined deviation can then be used as controllability index. Mathematically this can be formulated as:

$$\begin{aligned} \min_{u} \quad & \theta = (y - y_{sp})^T W_y (y - y_{sp}) + (u - u_0)^T W_u (u - u_0) \\ st: 0 &= f(x, z, u, \delta, \sigma) \\ 0 &= g(x, z, u, \delta, \sigma) \\ y &= h(x, z) \\ 0 &\leq k(x, z, u, \delta, \sigma) \end{aligned} \tag{3.9}$$

where u are the manipulated variables, y are the controlled variables, x are the state variables, z are the algebraic variables, δ are the disturbance variables, σ are the design variables, W_u and W_y are weighting matrices allowing a trade-off between set-point deviation and manipulated variable action, f are the differential equations, g are the algebraic equations, h are the output equations, and k are the inequality constraints.

Compared with the static gain matrix based indices this approach has several advantages. The most important advantage is that the physical meaning of this index is clear and relevant for some control purposes. In addition, the sensitivity of the index θ with respect to the model constraints are obtained when solving the optimization problem from the Kuhn-Tucker multipliers. Moreover this index can be applied to a large set of alternative process models, without tight requirements with respect to the dimensionality of the alternatives. This method however, only gives information about the static disturbance sensitivity. Extensions that included dynamics would be desirable.

3.3.2 Simultaneous approaches

In chapter 2 a mathematical formulation was given for the design of a process system. This formulation can be extended to a formulation including the control system design and the relevant disturbance scenarios. This is the basis of the approaches for the simultaneous design of the process and control system. Figure 3.1 is now updated to Figure 3.6. Mohideen et al. (1996) and Bansal (2000) formulate the problem as follows:

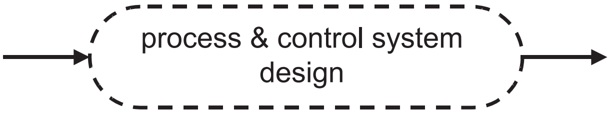

Figure 3.6: *Simultaneous design of the process and the control system.*

Problem $\mathcal{P}1$:

Given:

- a process model,
- a set of constraints for feasible plant operation,
- a disturbance scenario,
- a model describing the uncertainty in the system,
- a superstructure describing the potential unit operations and their connectivity,
- a superstructure describing the potential control configurations.
- a set of control objectives and types of controllers,
- cost data for the equipment, operating costs and controller costs and
- a finite time horizon,

Find:

- the process design and control scheme with minimum annualized cost while ensuring feasible operation over the entire time horizon under the specified uncertainty.

In Appendix A a mathematically formulation of this problem is given, together with an outline of an algorithm for solving this problem. A strong point of the simultaneous approach is that it takes economics and dynamics into account in the overall objective function. The practical limitations are threefold:

- The definition of a suitable superstructure requires strong fundamental insights in both process design and control.

- It requires rather detailed dynamic process models that might not be available at the beginning of the design process or are anyway too expensive to be made;
- The ensuing mixed integer, non-linear dynamic optimization problem (MIDO) can be computationally extremely demanding.

Given the current state-of-the art in computing and modelling this method is believed to be excellent for improvement of critical sections or units in a process design once some design options have been established. It seems less suitable for the initial stages of design.

There are two differences when problem $\mathcal{P}1$ is compared to the superstructure optimization presented in chapter 2. Firstly this optimization problem is a dynamic optimization problem whereas the problem defined by equation 2.3 is a static optimization problem. Secondly the extended superstructure in this problem also contains the controller superstructure. Therefore this problem is much more difficult to solve than the problem defined by equation 2.3.

3.4 Refined problem formulation

For the remainder of this thesis we will focus, unless otherwise stated, on the anticipating sequential design of the process and the control system. When we look back at the basis cycle of design, introduced in Chapter 2, we see that all current approaches for integration of design and control are aimed at the analysis phase. Contributions for the synthesis and evaluation phase are lacking. So, the first objective of this work is:

> *Investigate how the controllability can be included in the synthesis phase, exploiting physical principles and models.*

Although a large number of controllability indices is available, there does not seem to be a clear and consistent method for controllability analysis. The second objective for this work is:

> *Develop a consistent approach for the controllability analysis from a chemical process design perspective. A clear relation with the physical phenomena and economics should be established*

The third objecitive is:

> *Test the newly developed synthesis and analysis tools on a relevant innovative process*

As briefly mentioned before, ideally the operational policy is also explicitly in the integrated design problem. The final objective is a first step towards this full integration:

> *Integrate the designs of the operational policy and the process for a periodically operated continuous process.*

Notation

Roman symbols

d	disturbances
f	differential equations
g	algebraic equations
G	transfer function
h	output equations
k	inequality constraints
u	manipulated variables
s	Laplace variable
W	weighting
x	state variables
y	controlled variables
z	algebraic variables

Subscripts

0	nominal value
a	actuator
c	controller
m	measurement
p	process
sp	set-point
u	manipulated variables
y	controlled variables

4

Controllability in the synthesis phase

All currently available controllability tools are aimed at analysis of controllability of given process alternatives. In this chapter a new approach is developed: Thermodynamic Controllability Assessment (TCA). One specific part of controllability, disturbance sensitivity, is included in the synthesis phase. The microscopic theory of non-equilbrium thermodynamics is extended to a macroscopic description, leading to an explicit appearence of design variables. Using the passivity concept this leads to design guidelines from a controllability point of view. The approach is still limited to systems with a single dominant flow and force. The TCA approach will be demonstrated using heat exchanger systems and distillation systems as examples.

4.1 Introduction

In this chapter one of the aspects of controllability, *disturbance sensitivity*, will be included into the synthesis phase. In order to include the controllability in the synthesis phase, one needs to have insight in how the internal structure of a non-equilibrium process affects the controllability. The inner working of a process is determined by a set of interacting rate processes associated with ongoing physico-chemical phenomena. The framework of irreversible thermodynamics is the fundamental theory describing these rate processes in terms of rates, driving forces and geometric parameters such as volumes and surfaces. Therefore this theory is an appropriate fundamental starting point for dealing with controllability.

Recently some work has been done on the connection between process control and irreversible thermodynamics. Ydstie and coworkers have focused on the stability of process systems, e.g. Ydstie and Viswanath (1994) and Farschman et al. (1998). They use a storage function, related to the exergy function for their analysis. Tyreus (1999) has used thermodynamics to select control variables for partial control strategies. However we are not aware of any work in the field of process design for controllability using irreversible thermodynamics.

In this work aspects of three different scientific fields will be combined: process design, non-equilibrium thermodynamics and systems theory. The resulting theory is called Thermodynamic Controllability Assessment, TCA. Figure 4.1 shows how these are combined. The presentation of the TCA in this Chapter follows this structure. In section 4.2 the modelling framework based on irreversible thermodynamics will be presented. Section 4.3 will show how this framework can be used for process design, enabling a formal link between process design and non-equilibrium thermodynamics. Section 4.4 elaborates on the work of Ydstie and coworkers on passivity of process systems. It will be shown how the passivity is related to non-equilibrium thermodynamics. Their stability results will be extended to disturbance sensitivity. It will then be shown how these results can be used during the synthesis phase of the process design procedure to end up with processes that have improved controllability characteristics. Throughout the chapter two examples will be used to illustrate the ideas: a heat exchanger and a distillation column. An application to the design of chemical reactors for the Fischer Tropsch synthesis is covered in Chapter 6.

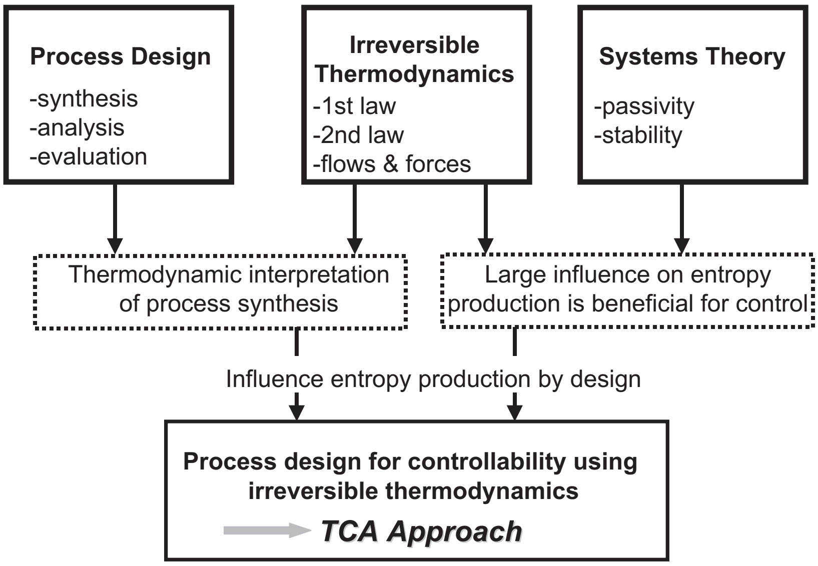
Process Design
-synthesis
-analysis
-evaluation
Irreversible Thermodynamics
-1st law
-2nd law
-flows & forces
Systems Theory
-passivity
-stability
Thermodynamic interpretation of process synthesis
Large influence on entropy production is beneficial for control
Influence entropy production by design
Process design for controllability using irreversible thermodynamics
TCA Approach

Figure 4.1: *Relation between the different competence fields.*

4.2 System Description

4.2.1 General dynamic system model

Dynamic systems can be represented as a network of lumped parameter systems. We consider systems of which the dynamic behaviour can be described in terms of the following Differential Algebraic Equation (DAE) model:

$$\begin{aligned} \dot{x} &= f(x, z, u, \delta, \sigma, \phi), \\ 0 &= g(x, z, u, \delta, \sigma, \phi), \end{aligned} \tag{2.1}$$

with x the states, z the algebraic variables, u the inputs, δ, the disturbances, σ the design variables, ϕ the uncertain parameters, f the differential equations, g the algebraic equations. The design variables include both discrete and continuous design variables. In this Chapter it will be assumed that value of the uncertain parameters equals their nominal value. Hence these parameters can be excluded from our analysis. It is assumed that all functions f and g are continuous with respect to each argument, except the discrete design variables. Extension to

Partial Differential Algebraic Equation (PDAE) models is straightforward, but for clarity this is not considered.

A large class of alternative systems can be represented with the model formulation of (2.1). However this formal model structure does not reveal the inner working of the system. For the synthesis phase the internal physical structure must be exploited. Therefore we will now zoom in to a smaller class of systems: process systems (Ydstie and Alonso, 1997).

4.2.2 Inventory based system description

A more specific description of these systems will be derived based on thermodynamics that is in line with the one proposed by Farschman (1998), using inventories. An inventory, $\mathcal{V}$, for system $\mathcal{S}$, is a nonnegative function of the state, such that if s_1 is the state of system $\mathcal{S}_1$ and s_2 is the state of system $\mathcal{S}_2$, the inventory of the combined system $\mathcal{S}$ is given by:

$$\mathcal{V}(s) = \mathcal{V}(s_1) + \mathcal{V}(s_2). \tag{4.1}$$

Equation (4.1) defines inventories to be extensive variables. Typical inventories are energy, exergy, total mass and molar amounts. For the densities of the inventories, v, the general (micro)balance for a (homogeneous) element with a fixed position in space is given by:

$$\frac{\partial v(s)}{\partial t} = p(s) + J(s, u, d, y), \tag{4.2}$$

with v the density of the inventories, p the production of an inventory per unit volume and J the net flux of the inventory. The convention that $J > 0$ implies flow into the system will be used. The flux term can further be divided into a convection term, J_{cv}, a conduction term, J_{cd} and for energy balances a radiation term, J_{rd}. However this radiation term can generally be neglected, leading to the generic form:

$$\frac{\partial v(s)}{\partial t} = p(s) + \nabla J_{cv} + \nabla J_{cd} \tag{4.3}$$

Now expressions for the terms in equation (4.3) will be derived.

In the theory of non-equilibrium thermodynamics (De Groot and Mazur, 1969) all physico-chemical processes can be described by a combination of driving forces, X, and fluxes, J. Table 4.1 gives an overview of the typical driving forces occurring in chemical processes. Note that there is a difference between the heat conduction, diffusion and electrical conduction on the one hand and chemical reaction on the other. This latter is a scalar quantity whereas the others are vectorial quantities.

Sufficiently close to thermodynamic equilibrium the relation between the fluxes and forces can be described by linear relations with phenomenological constants, L:

$$\begin{array}{lcl} J_1 & = & L_{11}X_1 + L_{12}X_2 + \ldots + L_{1n}X_n \\ J_2 & = & L_{21}X_1 + L_{22}X_2 + \ldots + L_{2n}X_n \\ \vdots & & \qquad \vdots \\ J_n & = & L_{n1}X_1 + L_{n2}X_2 + \ldots + L_{nn}X_n \end{array} \tag{4.4}$$

The off-diagonal elements in 4.4 imply that a driving force for one state variable can lead to a flux of another state variable. All the individual phenomenological constants can be put into the phenomenological constant matrix, $\mathcal{L}$. Onsager (1931) proved that this matrix is positive semi-definite and that the following condition holds:

$$\mathcal{L} = \mathcal{L}^T \tag{4.5}$$

The cross-effects, described by the off-diagonal elements, are especially important for systems in which multi-component mass transfer takes place. Cross effects between scalar and vectorial effects are impossible. The entropy production in the system is given as a function of the fluxes and driving forces:

$$p_S = \sum_i J_i X_i. \tag{4.6}$$

Table 4.1: *Physico-chemical processes and their flows and forces.*

Process	**Flow**	**Force**
Heat conduction	Energy flow	$\nabla \frac{1}{T}$
Diffusion	Mass flow	$-\nabla \frac{\mu_i}{T}$
Chemical reaction	Rate of reaction	$\frac{\mathcal{A}}{T}$
Electrical conduction	Electrical current	$-\nabla \frac{\varphi}{T}$

We now have a set of equations describing the inner structure of a process system. The state variables x of equation 2.1, are chosen to be the inventories v, including the component hold-ups, the energy hold-up and the entropy hold-up. The driving forces, X, the flows, F and the production terms are part of the algebraic variables, z.

4.2.3 Macroscopic system description

Up till now only a microscopic system description was considered. It will now be shown how this can be extended to a macroscopic description in order to be directly applicable for typical process systems. For clarity, macroscopic driving forces will be indicated by $\bar{X}$.

Equation 4.3 is integrated over the system volume, V, that is time indifferent:

$$\iiint\limits_V \frac{\partial v}{\partial t} dV = \iiint\limits_V p dV + \iiint\limits_V \nabla J_{cd} dV + \iiint\limits_V \nabla J_{cv} dV \tag{4.7}$$

Application of both the Gauss theorem and the Leibniz theorem leads to:

$$\frac{\partial}{\partial t} \iiint\limits_V v dV = \iiint\limits_V p dV + \iint\limits_A J_{cd} dA + \iint\limits_A J_{cv} dA, \tag{4.8}$$

where A is the area of the surface surrounding the system. The parts of this area through which convective fluxes and conductive fluxes flow are called respectively A_{cv} and A_{cd}. The total hold-up, $\mathcal{V}$, is defined as:

$$\mathcal{V} = \iiint\limits_V v dV, \tag{4.9}$$

and the total production, $\mathcal{P}$, as:

$$\mathcal{P} = \iiint\limits_V p dV \tag{4.10}$$

When it is assumed that the fluxes are uniform over the respective surfaces, equation (4.8) can be reduced to:

$$\frac{d\mathcal{V}}{dt} = \mathcal{P} + \sum A_{cd} J_{cd} + \sum A_{cv} J_{cv} \tag{4.11}$$

where $\mathcal{P}$ is the total production in the system. The summation is carried out over all conductive and convective surfaces.

A net conductive (vectorial) flow to the system is now given by:

$$F_{cd} = A_{cd} J_{cd} = A_{cd} L \bar{X} \tag{4.12}$$

Besides these vectorial flows, scalar flows also contribute to the entropy production. For scalar flows A_{cd} should be interpreted as a volume. The most relevant scalar flow is the production of a chemical species. The flowrate is the reaction rate, driven by the chemical affinity.

At this point it is pertinent to note that with the introduction of geometric variables, the necessary degrees of freedom in process design are appearing. For the remainder it is convenient to introduce a new variable, K, which is the product of the phenomenological constant L and the relevant geometric variable. So for vectorial processes K is defined as:

$$K = L A_{cd} \tag{4.13}$$

and for scalar processes K is defined as:

$$K = LV. \tag{4.14}$$

This variable is called the *thermodynamic design factor*. The reason for this will become clear in section 4.3. This leads to the following linear relation between the driving force and the flow:

$$F_{cd} = K \bar{X} \tag{4.15}$$

Now a macroscopic expression of the entropy production as a function of the macroscopic flows and forces is derived form equations 4.6 and 4.10. First a distinction is made between the vectorial and the scalar processes contributing to the entropy production:

$$p_S = \sum_{vectorial} J_{cd,i} X_i + \sum_{scalar} J_{r,j} X_j. \tag{4.16}$$

So equation 4.10 can be rewritten as:

$$\mathcal{P} = \iiint\limits_V \sum_{vectorial} J_{cd,i} X_i + \iiint\limits_V \sum_{scalar} J_{r,j} X_j. \tag{4.17}$$

For the vectorial processes X_i can be rewritten as ∇Y_i leading to:

$$\sum_{vectorial} J_{cd,i} \nabla Y_i = \sum_{vectorial} \nabla \left(J_{cd,i} Y_i \right) - Y_i \nabla J_{cd,i} \tag{4.18}$$

The second term on the right hand side of equation 4.18 can be neglected as a second order effect. Application of Gauss theorem leads to:

$$\iiint_V \sum_{vectorial} \nabla \left(J_{cd,i} Y_i \right) dv = \iint_A \sum_{vectorial} J_{cd,i} Y_i da \tag{4.19}$$

For a homogeneous system the following holds:

$$\iint_A \sum_{vectorial} J_{cd,i} Y_i da = \sum_{vectorial} J_{cd,i} \Delta Y_i A \tag{4.20}$$

where ΔY_i is the macroscopic driving force, also written as $\bar{X}_i$

For the scalar processes the expression $\sum_{scalar} J_{r,j} X_j$ can directly be integrated. For a homogeneous system this leads to:

$$\iiint_V \sum_{scalar} J_{r,j} X_j = \sum_{scalar} V J_{r,j} X_j . \tag{4.21}$$

So the entropy production in the system is directly related to the flows and forces according to:

$$\mathcal{P}_S = \sum_{vectorial,scalar} F_i \bar{X}_i . \tag{4.22}$$

The driving forces defined in Table 4.1 are based on a microscopic description. This should be extended to a macroscopic description in order to be directly applicable for typical process systems. This will be done for the two examples that will be used throughout this chapter; a heat exchanger and a binary distillation column.

Heat exchanger Consider the system shown in Figure 4.2. The system is a heat-exchanger with two streams. The system consists of three phases, two fluid phases and a solid wall where the heat transfer occurs. The fluid phases are assumed to be ideal mixed, Moreover it is assumed that only the heat conduction contributes to the entropy production and that the phenomenological coefficient for heat transfer is independent of the temperature in the temperature range considered. The temperature of the solid wall is distributed in the l-direction only, as shown in Figure 4.2. Now an expression for the heat transfer between the two fluid phases, through the solid phase will be developed. Through the surfaces A1.1, A1.2, A2.1 and A2.2, convection dominates, through the surfaces A1.3 and A2.3 conduction dominates. So the heat between the two fluid phases is transferred through conduction only. The (steady-state) energy balance for the fluid phases are given by:

$$0 = A_{1.3} J_{cd} + A_{1.1} J_{cv1,in} - A_{1.2} J_{cv1,out}, \tag{4.23}$$

$$0 = A_{2.3} J_{cd} + A_{2.1} J_{cv2,in} - A_{2.2} J_{cv2,out}. \tag{4.24}$$

For the solid phase, a steady-state energy balance is constructed for a slice in the m-direction, parallel to the areas $A_{1.3}$ and $A_{2.3}$:

$$0 = A_{cd} L_{thermal} \nabla \frac{1}{T}\bigg|_{m=m} - A_{cd} L_{thermal} \nabla \frac{1}{T}\bigg|_{m=m+dm} \tag{4.25}$$

where A_{cd} is the conduction area. The corresponding boundary conditions are:

$$T\big|_{m=0} = T_{1,out}, \tag{4.26}$$

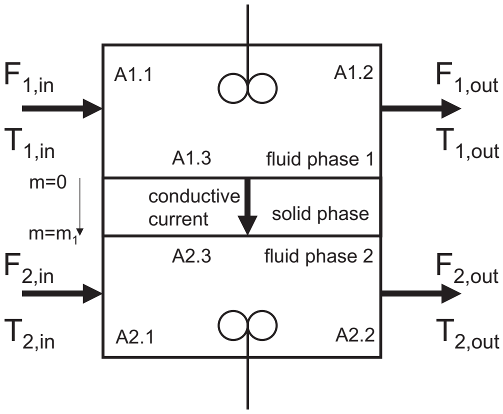
F1,in
T1,in
m=0
m=m1
F2,in
T2,in
A1.1
A1.2
A1.3
fluid phase 1
conductive current
solid phase
A2.3
fluid phase 2
A2.1
A2.2
F1,out
T1,out
F2,out
T2,out

Figure 4.2: *Schematic representation of the heat exchange system.*

and

$$T\Big|_{m=m_1} = T_{2,out}. \tag{4.27}$$

Integration of equation (4.25) with the boundary conditions leads to:

$$F = A_{cd}\frac{L_{thermal}}{m_1}\left(\frac{1}{T_{2,out}} - \frac{1}{T_{1,out}}\right) = A_{1.3}J_{cd} = A_{2.3}J_{cd}. \tag{4.28}$$

So the macroscopic driving force for heat transfer is:

$$\bar{X}_{thermal} = \Delta\frac{1}{T}, \tag{4.29}$$

where $\Delta\frac{1}{T}$ indicates the difference of inverse temperatures between the two phases. For this system the thermodynamic design factor, K, the flow and the total entropy production are given by:

$$K = A_{cd}\frac{L_{thermal}}{m_1}, \tag{4.30}$$

$$F = K\Delta\left(\frac{1}{T}\right), \tag{4.31}$$

and

$$\mathcal{P}_S = K\left(\Delta\frac{1}{T}\right)^2. \tag{4.32}$$

We now showed how a heat exchanger can fully be represented in a macroscopic non-equilibrium thermodynamic framework. This example will be used later in this Chapter to demonstrate the application of non-equilibrium thermodynamics based disturbance rejection in process synthesis.

Distillation In Figure 4.3 a schematic representation of a distillation column and a single tray is shown. The single tray consists of two fluid phases; a liquid phase and a vapour phase. Both phases have three interfaces. Through the surfaces A1.1, A1.2, A2.1 and A2.2, convection dominates, through the surfaces A1.3 and A2.3 conduction dominates. The conductive mass flow originates from the molar driving force. In this example the mass exchange will be considered to be the key contribution to the entropy production. All other contributions are ignored. The steady-state mass balances for the vapour and liquid phase are

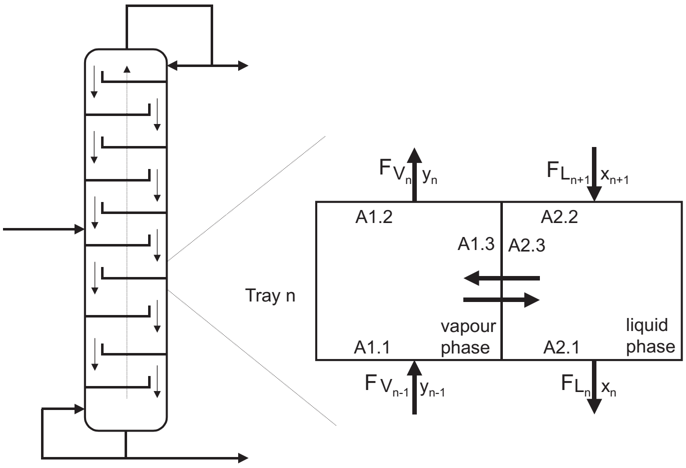

Figure 4.3: *Schematic representation of the distillation system.*

given by:

$$0 = \int\limits_{A_{1.3}} J_{cd} ds + F_{L,n+1} x_{n+1} - F_{L,n} x_n, \tag{4.33}$$

$$0 = \int\limits_{A_{2.3}} -J_{cd} ds + F_{V,n-1} y_{n+1} - F_{V,n} y_n, \tag{4.34}$$

where F_L and F_V are the liquid and vapour flows on the trays, and x and y are the liquid and vapour mole fractions. The microscopic driving force for the conductive flow is given by:

$$X_{diffusion} = \nabla \frac{\mu}{T}. \tag{4.35}$$

In order to determine the conductive flow between the two phases, detailed information is required about the flow pattern on the trays. De Koeijer et al. (1999) proposed to determine the molar driving force on a tray as the average between the forces at the inlets and the outlets of the tray. This would imply that the molar driving force on tray n is given by:

$$\bar{X}_{molar,n} = \frac{\frac{1}{2}\left(\mu_{l,n+1} + \mu_{l,n}\right) - \frac{1}{2}\left(\mu_{v,n-1} + \mu_{v,n}\right)}{T_n} \tag{4.36}$$

The outlet vapour and liquid flow are assumed to be in thermodynamic equilibrium, $\mu_{l,n} = \mu_{v,n}$. So the average driving force on the tray is only a function of the chemical potential of the incoming vapour and liquid chemical potential:

$$\bar{X}_{molar,n} = \frac{(\mu_{l,n+1} - \mu_{v,n-1})}{2T_n} \tag{4.37}$$

Summation of the driving forces over all trays from the bottom tray to the top tray leads to the expression:

$$\sum \bar{X}_{molar,n} = \frac{\mu_{l,top} + \mu_{l,top-1}}{T_{top}} - \frac{\mu_{v,bottom} + \mu_{v,reboiler}}{T_{bottom}} \tag{4.38}$$

where $\mu_{l,top}$ is equal to the chemical potential of the top product in the liquid phase, $\mu_{l,top-1}$ is equal to the chemical potential of the top product in the vapour phase, $\mu_{v,bottom}$ is equal to the chemical potential of the bottom product in the liquid phase and $\mu_{v,reboiler}$ is equal to the chemical potential of the bottom product in the vapour phase. Hence the overall driving force is a function of the top and bottom composition only.

The conductive flow on a tray is given by:

$$F_n = \int\limits_{A_{1.3}} LX ds = A_{1.3} L\bar{X}. \tag{4.39}$$

The surface is proportional to the reflux rate in the column:

$$A = A_{min}\frac{R}{R_{min}} \tag{4.40}$$

with A_{min} the surface for a column operating at minimum reflux, R the reflux rate and R_{min} the minimum reflux rate. So the total convective flow is:

$$F = K\left(\frac{\mu_{top}}{T_{top}} - \frac{\mu_{bottom}}{T_{bottom}}\right) \tag{4.41}$$

The thermodynamic design factor and entropy production are now given by:

$$K = A_{min}\frac{R}{R_{min}}L \tag{4.42}$$

and

$$\mathcal{P}_S = K\left(\frac{\mu_{top}}{T_{top}} - \frac{\mu_{bottom}}{T_{bottom}}\right)^2 \tag{4.43}$$

We now showed how a distillation system can fully be represented in a macroscopic non-equilibrium thermodynamic framework.

4.2.4 Distributed systems

Up till now only ideal mixed systems were considered. However a large number of process systems are distributed systems, e.g. tubular reactors, heat exchangers and packed distillation and absorption beds. It will be shown how the local driving force can be integrated to obtain an average driving force. These average driving forces can then be used in the analyses. Let us consider again a heat transfer process. Figure 4.4 shows again a heat exchanger, but now with a temperature gradient in both fluid phases in the n-direction. The flux at position n is given by:

$$J|_n = L\bar{X}|_n \tag{4.44}$$

The flow increment at this point is given by the product of the flux and the area:

$$dF|_n = J|_m adn, \tag{4.45}$$

where a is the exchange area per unit length. The total flow can be found by integrating the local heat flow over the n-direction:

$$F_{total} = \int_{n0}^{n1} F|_n dn \tag{4.46}$$

The average driving force, $\bar{X}$, is defined as:

$$\bar{X} = \frac{1}{n1 - n0} \int_{n0}^{n1} X dn \tag{4.47}$$

So the total flow in the system is given by:

$$F_{total} = K\bar{X} \tag{4.48}$$

So for a distributed system equation (4.15) should be replaced by equation (4.48).

4.3 Process Design, an approach based on non-equilibrium thermodynamics

In Chapter 2 the difference between the synthesis step and the analysis step was already briefly discussed. In the synthesis step all input parameters and

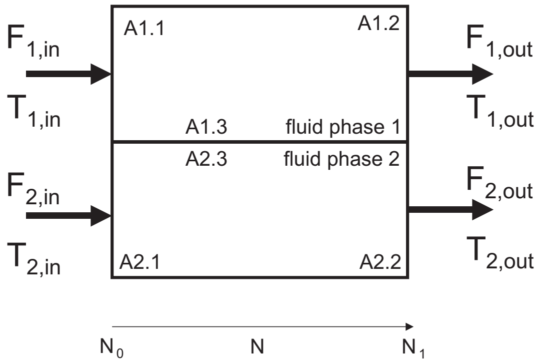
$F_{1,in}$
$T_{1,in}$
$F_{2,in}$
$T_{2,in}$
A1.1
A1.2
A1.3
fluid phase 1
A2.3
fluid phase 2
A2.1
A2.2
$F_{1,out}$
$T_{1,out}$
$F_{2,out}$
$T_{2,out}$
N_0
N
N_1

Figure 4.4: *Schematic representation of the distributed heat exchange system.*

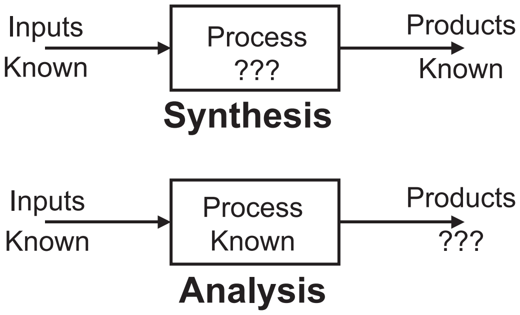
Inputs
Known
Process
???
Products
Known
Synthesis
Inputs
Known
Process
Known
Products
???
Analysis

Figure 4.5: *Difference between synthesis and analysis, taken from Doherty and Malone (2001).*

the desired performance at the output side are given. The unit for the desired transformation needs to be determined. In the analysis step all input parameters and the unit model are given and the behaviour of the system can be analysed. A combination of the physico-chemical conditions and the geometric properties of the system determine this behaviour. The difference between synthesis and analysis is also illustrated by Figure 4.5, taken from Doherty and Malone (2001). In this section it will shown how the non-equilibrium thermodynamic framework can be used in the synthesis phase of conceptual process design.

Intermezzo, Degrees of Freedom

A central concept in the synthesis phase is the concept of degrees of freedom (Sinnott, 1993). The degrees of freedom, DoF, are given by:

$$DoF = \#\text{variables} - \#\text{(independent) equations}$$

Besides the behaviour equations some variables are given as fixed inputs variables. These fixed inputs describe inlet conditions of streams entering the system. Another class of variables are the design targets. Examples are the outlet temperature of a stream leaving a heat exchanger and the composition leaving a reactor system. The design degrees of freedom, $DDof$, are now defined as:

$$\begin{aligned} DDof = \#\text{variables} - \#\text{(independent) equations} \\ - \#\text{fixed inputs} - \#\text{design targets} \end{aligned}$$

Three different situations can now be discriminated:

- $DDof = 0$, there is usually one, unique solution (more if the model allows for multiplicity) to the problem. Hence the problem is not a true design problem.
- $DDof < 0$, the problem is over defined. There is either one, trivial solution, or the problem is inconsistent.
- $DDof > 0$, there is an infinite number of alternative solutions. This represents real design problems.

So the essence of design problems is that there are design degrees of freedom left such that design choices can be made

4.3.1 Heat exchanger

Let us consider again the heat exchanger shown in Figure 4.2. The energy balances for the two fluid phases are given by:

$$0 = -F_{cv} + (F_{cd}\rho c_p T)_{1,in} - (F_{cd}\rho c_p T)_{1,out}\,, \tag{4.49}$$

$$0 = F_{cv} + (F_{cd}\rho c_p T)_{2,in} - (F_{cd}\rho c_p T)_{2,out}\,. \tag{4.50}$$

with:

$$F_{cv} = A_{1.3} L_{thermal} \left(\frac{1}{T_{1,out}} - \frac{1}{T_{2,out}} \right) \tag{4.51}$$

The mass balances for the two fluid phases are given by:

$$0 = F_{cd1,in} - F_{cd1,out} \tag{4.52}$$

$$0 = F_{cd2,in} - F_{cd2,out} \tag{4.53}$$

A degree of freedom analysis will now be performed. For simplicity the density, the heat capacities and the phenomenological coefficients are assumed to be independent of the temperature. The system contains the following ten variables:

- 4 temperatures,
- 1 conductive flow,
- 4 convective flows,
- 1 area.

The system contains the following five equations:

- 2 energy balances, eqn (4.49) and (4.50)
- 2 mass balances, eqn (4.52) and (4.53)
- 1 relation for the convective flow

In addition there are three fixed inputs:

- 2 inlet temperature specifications: $T_{1,in}$, $T_{2,in}$,
- 1 inlet flow specifications: $F_{cd1,in}$,

and one design target:

- 1 design target: $T_{1,out}$.

So the $DDof$ is given by:

$$DDof = 10 - 5 - 3 - 1 = 1 \tag{4.54}$$

This remaining degree of freedom can be removed by either fixing $T_{2,out}$, or the area. This choice defines the thermal driving force. Alternative designs of a heat exchange system will have different values of $T_{2,out}$ and will hence have a different thermal driving forces in the system. However the total heat flow in the system (=heat duty) is the same for all designs.

4.3.2 Distillation

We now go back to the distillation column, shown in Figure 4.5. Also for this system a degree of freedom analysis will be performed. The assumptions for this degree of freedom analysis are that there are only two components, and that there is constant molar overflow (so the energy balance is neglected). The system then contains the following 7n+1 variables, where n is the number of trays:

- n molar hold-ups
- 2n liquid mole fractions
- 2(n-1) vapour mole fractions
- n-2 liquid flows: F_L
- n-2 vapour flow: F_V
- 1 reflux rate
- 1 vapour boil-up rate
- 2 product flow rates
- 2 feed properties: flowrate and composition
- 1 number of trays

The system contains the following 7n-4 equations:

- 2n component balances

- n-1 VLE-relationships
- n-1 liquid flow relationships
- n-1 vapour flow relationships
- 2n-1 normalization conditions for the molar fractions

In addition there are two fixed inputs:

- 2 feed specifications: flowrate and feed composition

and two design targets:

- 2 product specifications

So the $DDof$ is given by:

$$DDof = 7n + 1 - 5n - 4 - 2 - 2 = 1 \tag{4.55}$$

Specification of these compositions is equivalant to setting the specifications of the chemical potentials at top and bottom and hence, to the driving force over the column. Some mathematical manipulations will reveal that either the number of trays, or the reflux rate still needs to be specified. Looking back at equations (4.38) and (4.41) one sees all alternative designs will have the same overall driving force in the systems since this only depends on the two product specifications. The total flow in the system will be different for different designs. It is related to the design degree of freedom left. Hence distillation is a so-called force- specified process.

4.4 Controllability, an approach based on non-equilibrium thermodynamics

It was shown that process design can be described in the non-equilibrium thermodynamic framework. In Chapter 3 the need for considering controllability issues from the earliest phases of conceptual process design on was emphasized. Now it will be shown how this can be done in this framework. First the results obtained by Ydstie and coworkers on non-equilibrium thermodynamics and stability will be presented. Then these results will be extended to controllability and the relation with conceptual process design will be established.

4.4.1 Irreversible thermodynamics and stability

First the concept of *Lyapunov functions* will be introduced. A Lyapunov function, $Y(x(t))$, is a positive scalar that depends on the system's state. By definition, the time derivative of a Lyapunov function is non-positive. Mathematically these conditions can be described by:

- $Y(x(t)) \geq 0$
- $\dot{Y}(x(t)) \leq 0$

If it is possible to find a Lyapunov function for a dynamic system operating around a state x^*, x^* is a stable state that is approached asymptotically.

The second concept is the *supply rate*. The supply rate, w, is a real-valued function of the system inputs and outputs. It is assumed that $w(u, y)$ satisfies:

$$\int_t^{t+\tau} |w(u, y)| dt < \infty \tag{4.56}$$

The system $\mathcal{S}$ is now said to be dissipative if there exists a nonnegative function S of the states, called the *storage function*, such that for all $u \in \mathcal{U}$, $x \in X$, $t \geq 0$ (Willems, 1974):

$$S(x(t+\tau)) - S(x(t)) \leq \int_t^{t+\tau} w(u, y) dt, \tag{4.57}$$

When energy is taken as the storage function, equation 4.57 should be interpreted as follows: the rate of energy increase in the system is not bigger then the input power. Sepulchre et al. (1997) give the example of a potato in a microwave. As long as the potato is not allowed to burn, the energy increase of the potato is always less or equal to the energy supplied by the microwave.

It can easily be verified that for an unforced ($w(u, y) = 0$) dissipative system, the storage function satisfies the conditions for a Lyapunov function:

- $S(x(t)) \geq 0$, this is satisfied by the definition of S,
- $\dot{S}(x(t)) \leq 0$, this is satisfied since $w(u, y) = 0$ for an unforced system.

Hence the unforced system is asymptotically stable.

In order to study forced systems the concept of *passivity* is introduced. A passive system is a dissipative system where the net supply of stored quantity is a function of the measured outputs and manipulated inputs only (Luyben et al., 1999). The concept *passivity* originates from electronic circuit theory, where passive components are e.g. resistors and capacitors.

Passive systems can be proven to be asymptotically stable because the dissipative storage function is a Lyapunov function. So if an arbitrary dynamic system can be made passive, the system can be stabilized. Ydstie and Alonso (1997) have proven that for process systems a storage function exists that leads to a passive system. We call this storage function the Ydstie function. This Ydstie function is constructed from variables already available in the thermodynamic description. It is given by:

$$\mathcal{V}_A(x) = \mathcal{V}_E(x) - T_0\mathcal{V}_S(x) + \mathcal{V}_{A_0} \tag{4.58}$$

where $\mathcal{V}_A(x)$ is the Ydstie function, $\mathcal{V}_E(x)$ is the energy and $\mathcal{V}_{A_0}(x)$ an constant. An appropriate selection of $\mathcal{V}_{A_0}$ will guarantee that $\mathcal{V}_A(x) \geq 0$. In the notation it is indicated that $\mathcal{V}_A(x)$, $\mathcal{V}_E(x)$ and $\mathcal{V}_S(x)$ are functions of the state, x, of the system. Note that the Ydstie function does not equal to the exergy function since the exergy function is defined as:

$$\mathcal{V}_B(x) = \mathcal{V}_H(x) - T_0\mathcal{S}(x) \tag{4.59}$$

where $B(x)$ is the exergy and $H(x)$ the enthalpy.

The general inventory balance (4.2) for $\mathcal{V}_A(x)$ is given by:

$$\frac{d\mathcal{V}_A(x)}{dt} = \phi_A + \mathcal{P}_E(x) - T_0\mathcal{P}_S(x) \tag{4.60}$$

where ϕ_A is the net flow of the quantity $\mathcal{V}_A$ and T_0 is the reference temperature. Since the energy is conservative, $\mathcal{P}_E(x)$ is always zero, leading to:

$$\frac{d\mathcal{V}_A(x)}{dt} = \phi_A(x) - T_0\mathcal{P}_S(x) \tag{4.61}$$

The effectiveness of using this storage function in distillation control has been demonstrated by Coffey et al. (2000).

4.4.2 Non-equilibrium thermodynamics and control performance

When the system is in a steady-state, equation 4.61 reduces to:

$$0 = \phi_A - T_o\mathcal{P}_S(x). \tag{4.62}$$

Now the system is exposed to a step change perturbation in ϕ_A, $\Delta\phi_A$. So the system will move away from it's original steady-state. The entropy production, $\mathcal{P}_S$, is a function of the state of the system. Hence $\mathcal{P}_S$ will change since the perturbation in ϕ_A leads to a change of the state of the system. The stability results presented above teach us that eventually the system will go to a new steady-state. Obviously also in this state equation 4.62 holds. When these two steady-states are compared, we can define the difference in $\mathcal{V}_A(x)$ as $\Delta\mathcal{V}_A(x)$ and the difference in $\mathcal{P}_S(x)$ as $\Delta\mathcal{P}_S(x)$. Analogous to Luyben et al. (1999) a response time, τ, is defined:

$$\tau = \frac{\Delta\mathcal{V}_A(x)}{T_0\Delta\mathcal{P}_S(x)} \tag{4.63}$$

From a controllability point of view it is now desirable that the response time is small. The only factor in equation 4.63 that can be influenced by the design of the system is $\Delta\mathcal{P}_S(x)$. Since the response time decreases with increasing $\Delta\mathcal{P}_S(x)$, the design objective is to have a large influence on the entropy production rate. In order to see how the design decisions influence the entropy production we go back to the entropy production as described by equation 4.22. Let us consider a system operating in steady-state. A departure from the steady-state will lead to a change of entropy production. For small departures from steady-state the following approximation holds:

$$\Delta\mathcal{P}_S = \sum X\Delta F + \sum \Delta X F \tag{4.64}$$

Since the flux and force are related as described by equation (4.4), this can be rewritten to:

$$\Delta\mathcal{P}_S = \sum 2KX\Delta X. \tag{4.65}$$

Now one has to discriminate between the two types of systems earlier introduced: flow-specified systems and force-specified system.

Let us first consider the flow-specified system. For these systems all alternative designs will have the same value of KX. Hence the difference in $\Delta\mathcal{P}_S$ between the alternatives is determined completely by the difference in ΔX. The selection of either a large X or a small X depends on the relation between ϕ_A and X. For a design with a small nominal driving force, the disturbance, $\Delta\phi_A$, will have a much larger effect on the driving force then for a system with a bigger nominal driving force. This can be illustrated with the heat transfer example. Two alternatives will be compared. Both designs have a hot side temperature of 350K. One design has a cold side outlet temperature of 340K, leading to a thermal gradient of $8.4.10^{-5}K^{-1}$, the other design has a cold side outlet temperatures 300K, leading to a thermal gradient of $4.8.10^{-4}K^{-1}$. Now the temperature of the hot side increases due to the disturbance in $\Delta\phi_A$. When this temperature increase is 1K, the thermal gradient of the first design will increase with 9.7%. The thermal gradient of the second design will increase with only 1.7%. So the design with the small driving force has a larger difference in the driving force, and hence a larger effect on the entropy production. Hence for flow-specified processes, a small driving force is desirable from a controllability point of view.

For a force-specified process all alternative designs will have the same value for the driving force, X. The alternatives differ in K and ΔX. However analogous to the flow specified situation, we can conclude that the cange in X for the alternative designs is relatively small since they all have the same nominal value of X. Hence the difference in $\Delta\mathcal{P}_S$ between the alternatives is mainly by the difference in K. Alternatives with a large value of K will have a large effect on the entropy production since K acts like a multiplier in equation 4.65. Hence from a controllability point of view large flows are desirable for force-specified processes. For the previously introduced distillation example this has the following implications. Alternatives with a large reflux have a large value of K. Hence these design alternatives will be more controllable then alternatives with a small K. So for force specified processes a large flow is desirable form a controllability point of view.

The analysis was based on a linear relation between the flow and the force. Far from equilibrium this linear relation will not be accurate anymore. However extension to this range will be possible using a first order Taylor series expansion for the relation between the flow and the force.

4.5 Examples

Now two examples will be presented to demonstrate the application of the developed approaches. The first example is a flux-specified system: a heat exchanger. Alternatives with different heat transfer areas will be compared. The second example is a force-specified process: distillation. Alternatives with a different number of trays will be compared.

In order to test the conclusions of the previous section, the results should be compared with a traditional approach to analyse the controllability of given designs. A large set of alternative controllability indicators are available, including the Relative Gain Array, singular value decomposition based methods. When selecting the appropriate index, one should keep in mind that one wants to analyse the disturbance sensitivity. Ideally the closed-loop regulating performance of alternative designs is compared. Obviously the RGA and singular value decomposition based indices are not suited for this. The disturbance sensitivity approach of Seferlis and Grievink (1999) is proposed to be used. They analyse the steady-state disturbance sensitivity within an optimization framework. For a specified disturbance δ the following optimization problem is formulated. Given the process model, the nominal steady-state value of the inputs (u_0) and the controlled variables (y_0):

$$\begin{array}{rcl} \min\limits_{u} & & \theta = (y - y_{sp})^T W_y (y - y_{sp}) + (u - u_0)^T W_u (u - u_0) \\ st : 0 & = & f(x, z, u, \delta, \sigma) \\ 0 & = & g(x, z, u, \delta, \sigma) \\ y & = & h(x, z) \\ 0 & \leq & k(x, z, u, \delta, \sigma) \end{array} \tag{3.9}$$

where θ is the objective function and W_u and W_y are weighting matrices. Note that the objective function of equation (3.9) is closely related to the LQG objective function.

Heat transfer Four different designs of a heat exchanger are considered, two co-current and two counter-current designs. All designs have the same duty. Table 4.2 shows the design parameters of the different designs and the logarithmic mean temperature differences. The driving force profiles are shown in Figure

Table 4.2: *Alternative heat exchanger designs.*

Design	**Flow mode**	$\mathbf{T_{h,in}}$	$\mathbf{T_{h,out}}$	$\mathbf{T_{c,in}}$	$\mathbf{T_{c,out}}$	$\mathbf{\Delta T_{ln}}$
A	counter-current	50	40	20	27	21.5
B	counter-current	50	40	20	32	19.0
C	co current	50	40	20	27	20.3
D	co-current	50	40	20	32	16.6

4.6. Based on the theory presented above, a smaller driving force should have a positive effect on the controllability. This would imply that the 'best controllable' design is D, followed by B, C and finally A. The output and manipulated variables were scaled for the disturbance sensitivity index, θ, such that a difference of 1°C in the hot stream output temperature is penalized equally as a 20 % difference in manipulated variable action. A disturbance of 1°C in the cold temperature inlet was considered. Table 4.5 shows for the various designs the disturbance sensitivity index and the average driving force. This Table shows that the controllability is closely correlated with the average driving force. An

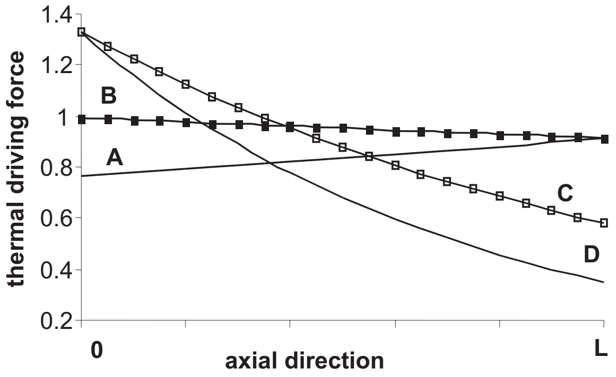

Figure 4.6: *Thermal driving force profiles.*

Table 4.3: *Controllability results for distributed heat exchanger .*

Design	**Average driving force**	θ
A	1.00	0.109
B	0.88	0.091
C	0.94	0.106
D	0.77	0.079

interesting observation is that this is independent of the flow configuration.

Distillation The distillation column example is based on the well known column A, introduced by Skogestad (1997). All alternatives are designed to have a bottom composition of 0.01 and a top composition of 0.99. The feed stream is a saturated liquid stream with a composition of 0.50. The phase equilibrium is modelled with a constant relative volatility of 1.5. Alternative designs vary in the number of stages but have the same sum of driving forces. For all alternatives the feed stage is located in the middle of the column. Table 4.5 shows some of the typical values belonging to the some alternative designs. Now the effect is calculated of a disturbance in feed composition. Figure 4.5 shows θ divided by θ for the base case design (41 stages) for a feed composition of 0.45. The input and output variable deviations are scaled with their nominal value. The three different graphs represent three different sets of weighting matrices. Respectively $W_u = I, W_y = I$, $W_u = I, W_y = 0.2I$ and $W_u = I, W_y = 5I$. The controlled variables are the top and bottom composition. The manipulated variables are the reflux rate and the vapour boil-up rate. Figure 4.5 clearly shows that a small number of trays is beneficial from a controllability point of view. This is in line with the prediction made in Section 4.4 that for a force-specified process large flows are desirable from a control point of view. It also shows that the result is insensitive for the weighting matrices.

Table 4.4: *Alternative designs for Column A.*

design	1	2	3	4	5
number of stages	29	35	41	47	53
feed stage	15	18	21	24	27
reflux ratio	12.26	6.96	5.41	4.72	4.37
sum of molar flows	13.13	7.88	6.35	5.67	5.31

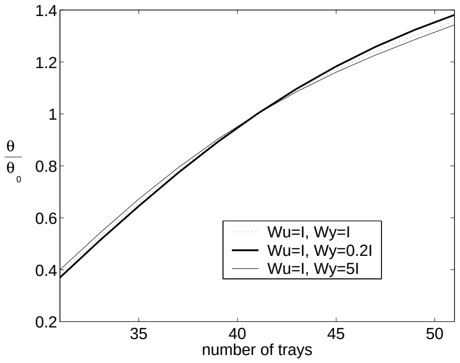

Figure 4.7: *Results for distillation example.*

4.6 Discussion and Conclusions

All existing approaches for integration of design and control are especially aimed at analysing the controllability of a given set of alternatives. This work is a first attempt to included controllability in the synthesis phase of conceptual process design. Fundamental physical properties, as described by the theory of irreversible thermodynamics, are exploited, rather than an observation of the input-output behaviour of the system. One of the attractive aspects of this method is that it allows a controllability study in the earliest phase of the conceptual design.

It was shown that from a controllability point of view the thermodynamic design factors should be large. For flow-specified processes this implies small driving forces. For force-specified processes this implies large flows. In this work the method is verified on relatively simple systems only; single units. In order to be more general applicable the following two developments are required: studies of systems containing multiple units and integrated units like reactive separations.

Notation

Roman symbols

A	area
$\mathcal{A}$	chemical affinity
cp	heat capacity
$\mathcal{D}$	disturbance space
f	differential equations
F	flow
g	algebraic equations
h	output variable equations
J	flux
k	inequality constraints
K	thermodynamic design factor
l	spatial coordinate
L	phenomenological constants
$\mathcal{L}$	phenomenological constant matrix
m	spatial coordinate
p	production per unit volume
$\mathcal{P}$	total production in the system
R	reflux rate
s	state of a system
S	storage function
$\mathcal{S}$	system
t	time
T	temperature
u	inputs
$\mathcal{U}$	input space
v	density of the inventories
V	volume
$\mathcal{V}$	inventory
w	supply rate
W	weighting matrix
X	driving force
$\mathcal{X}$	state space
x	liquid mole fraction

x	state variables
y	outputs
Y	Lyapunov function
$\mathscr{y}$	vapour composition
$\mathcal{Y}$	output space
z	algebraic variables

Greek symbols

δ	disturbances
λ	spatial coordinates
μ	chemical potential
ϕ	net flow
ρ	density
θ	design variables
Θ	design space
φ	electrical potential

Subscripts

0	nominal value
A	storage function as defined by Ydstie and Alonso (1997)
cd	conduction
cv	convection
E	energy
L	liquid
min	minimum
rd	radiation
S	entropy
sp	setpoint
u	inputs
V	vapour
y	outputs

5

New Controllability analysis tools[†]

In this chapter two new controllability analysis tools will are developed; closed-loop controllability index and dynamic interaction analysis. The closed-loop controllability index is based on LQG control. It allows one to assess the optimum closed-loop variance of a system exposed to a stochastic disturbance scenario. Issues like robustness and a trade-off with economics are also discussed. The dynamic interaction analysis is an dynamic extension of the RGA in the time domain. It allows one to determine the dynamic interaction between control loops without unrealistic assumptions on the controller.

[†] Parts of this Chapter have been published by Meeuse and Tousain (2002), Meeuse et al. (2002) and Meeuse and Huesman (2002)

5.1 Introduction

In chapter 3 the currently available controllability analysis tools were reviewed. It was shown that most controllability indicators suffer from several disadvantages:

- the physical interpretation of the is indices unclear,
- the indices are based on steady-state or assume perfect control,
- design alternatives of different dimensionality might be impossible to compare.

In this chapter two new methods that partly overcome these limitations will be introduced.

The first method is closed-loop controllability analysis. This method gives clear disturbance sensitivity information, just like the method presented by Seferlis and Grievink (1999), but now based on dynamic models and stochastic disturbances. Moreover robustness issues will be included in this method. It is based on the approach presented by Tousain et al. (2000) for the optimal sensor selection in a High Density Polyethylene reactor.

The second method is a closed-loop interaction analysis of the control loops, based on the Relative Gain Array. This tool can be used to analyse whether control with multiple Single Input-Single Output (SISO) loops is sufficient. Compared to existing dynamic analysis the main benefit is that the analysis is done in the time domain, and does not assume perfect control.

This chapter is organized as follows. The next section presents the closed-loop controllability approach. Obviously there will be a trade-off between the steady-state economics and the closed-loop performance. Two alternative approaches to tackle this trade-off will be presented: multi-objective optimization and closed-loop economic optimization. Both approaches will be demonstrated for the design of a distillation column as a case study in section 5.4. The novel dynamic interaction analysis method will be presented in section 5.5. Finally some conclusions will be drawn.

5.2 Closed-loop controllability

As already mentioned before, what is ultimately important from an operational point of view, is the closed-loop performance of the process. Figure 3.2 showed that this is determined by a combination of the process, the control system, the measurement system and the actuators. The dynamics of the measurement system and the actuators are generally neglected. So the closed-loop performance analysis should be based on the combination of the process and the control system.

The majority of controllability analysis is either based on perfect control, or on specific choices of the control structure and algorithm. The first option, perfect control, is not realizable in reality so the practical value of the results is not clear. Schweiger and Floudas (1997) and Bansal (2000) give examples of the second option. The closed-loop performance of alternative designs is compared, but the control system is based on decentralized PI controllers only. In this case there is a possibility that different, more advanced, controllers would lead to different optimal designs.

In this section a new concept will be introduced, closed-loop controllability. The essential idea is that the controllability analysis is done based on the *optimal achievable* closed-loop performance. First the process and disturbance models are introduced, followed by a derivation of the closed-loop controllability analysis. Then it will be shown how robustness criteria can be included in the closed-loop controllability analysis.

5.2.1 Process and disturbance models

The process model In this section processes of which the behaviour can be described by a system of Differential Algebraic Equations (DAE) will be considered:

$$\begin{aligned} \dot{x} &= f(x, z, u, \delta, \sigma, \phi), \\ 0 &= g(x, z, u, \delta, \sigma, \phi), \end{aligned} \tag{2.1}$$

where $x \in \mathbb{R}^{n_x}$ are the state variables, $z \in \mathbb{R}^{n_z}$ are the algebraic variables, $u \in \mathbb{R}^{n_u}$ are the input variables and $\delta \in \mathbb{R}^{n_\delta}$ are disturbance variables. $\sigma \in \Sigma$ are the n_σ design parameters. $\phi \in \mathbb{R}^{n_\phi}$ are the uncertain parameters. First all uncertain variables will have their nominal values, $\phi = \phi_0$ so that these can be omitted from the analysis. f are the differential equations and g are the algebraic equations. The equations f and g are assumed to be continuous in all variables except the integer design variables, and at least once differentiable. Selected output variables, y are given by:

$$y = h(x, z, \delta, \sigma) \tag{5.1}$$

The operation of the plant is subject to operating constraints given by:

$$y_l \leq y \leq y_u, \tag{5.2}$$

and

$$u_l \leq u \leq u_u, \tag{5.3}$$

where the bounds are chosen appropriately.

Linearized models can describe the behaviour of the plant in or close to its steady-state operating point(s). For these models the standard state-space notation is used:

$$\begin{aligned} \Delta\dot{x} &= A_p(\sigma)\Delta x + B_p(\sigma)\Delta u + \delta, \\ \Delta y &= C_p(\sigma)\Delta x, \end{aligned} \tag{5.4}$$

where Δx, Δu and Δy_m are respectively the deviations of the states, the inputs and the outputs from their steady-state values, and the system matrices $[A_p, B_p, C_p]$ are obtained through linearization of equations 2.1 and 5.1. They are functions of σ only because each choice of σ uniquely defines a steady-state. In the remainder the dependence of σ will be omitted from the notation.

Process disturbances and measurement noise Often, some a priori knowledge on the sources and characteristics of disturbances and measurement noise will be available. To assess their effect on the process operation (and more important: how process design influences this!) one should include this knowledge in the design stage. Disturbances and noise are dealt with in a stochastic framework. This is in contrast to e.g. Seferlis and Grievink (1999) where only static disturbances are considered. It is assumed that the disturbances can be described by coloured noise. The following disturbance model will produce coloured noise from a white noise input signal. The matrices A_f, B_f, C_f can be tuned to obtain the required coloured noise profile:

$$\begin{aligned} \dot{x_f} &= A_f x_f + B_f w_d, \\ \delta &= C_f x_f. \end{aligned} \tag{5.5}$$

where w_d is the Gaussian white noise disturbance with covariance matrix R_d, and x_f are the states of the disturbance model. The plant model can now be augmented with this disturbance model and the measurement noise, leading to:

$$\begin{aligned} \begin{bmatrix} \dot{x}_p \\ \dot{x}_d \end{bmatrix} &= \begin{bmatrix} A_p & B_f C_f \\ 0 & A_f \end{bmatrix} \begin{bmatrix} x_f \\ x_f \end{bmatrix} + \begin{bmatrix} B_p \\ 0 \end{bmatrix} u + \begin{bmatrix} 0 \\ B_f \end{bmatrix} w_d, \\ y_m &= C_p x_p + w_m, \end{aligned} \tag{5.6}$$

where w_m is Gaussian white noise measurement noise with respectively covariance matrix R_m and y_m are the measurements. So in the standard state-space notation the system matrices $[A, B_U/B_D, C]$ are given by:

$$A = \begin{bmatrix} A_p & B_f C_f \\ 0 & A_f \end{bmatrix} \tag{5.7}$$

$$B_U = \begin{bmatrix} B_p \\ 0 \end{bmatrix} \tag{5.8}$$

$$B_D = \begin{bmatrix} 0 \\ B_f \end{bmatrix} \tag{5.9}$$

$$C = C_p \tag{5.10}$$

5.2.2 Optimal closed-loop variance

The general idea of all design methods which take process control into consideration is that *the plant should be designed such that, using some kind of control, one can achieve or optimize some kind of operating performance*. The two main problems are (i) what are the assumptions for the controller, and (ii) how is the operating performance quantified? To circumvent these problems we base our analysis on *optimal control*. The big advantage of optimal control is that, given a model of the plant and the control objective function, the controller itself is unambiguously defined, so there is no need for restrictive assumptions with respect to the controller design. Further, using optimal control guarantees that an upper limit of the practically achievable control performance is attained.

Because we want to account for the effect of stochastic disturbances and measurement noise on the closed-loop behaviour of the process, the controllability indicator proposed in this work is the weighted (*closed-loop*) variance of the process outputs and inputs:

$$CLC = \min E \left\{ \lim_{T\to\infty} \frac{1}{T} \int_t^T (\Delta y^T Q_y \Delta y + \Delta u^T Q_u \Delta u) dt \right\}, \tag{5.11}$$

where CLC is the closed-loop controllability indicator, E denotes expectation, and Q_y and Q_u are square weighting matrices of appropriate dimensions. How this closed-loop variance can be determined becomes clear from the theory of Linear Quadratic Gaussian (LQG) Control.

Linear Quadratic Gaussian Control In the LQG control problem one seeks the control $u(t)$ which should be applied to system (5.6) to minimize the following performance measure:

$$J = E\left\{\lim_{T\to\infty}\frac{1}{T}\int_t^T(\Delta x^TQ_x\Delta x + \Delta u^TQ_u\Delta u)dt\right\}, \tag{5.12}$$

Note the this equation is equal to equation 5.11 when Q_x is selected as:

$$Q_x = C^TQ_yC \tag{5.13}$$

The solution of this LQG control problem is very elegant. The optimal controller is found by combining the optimal state observer (Kalman filter) with the optimal state feedback controller for the deterministic Linear Quadratic Regulator problem (with weighting matrices Q_x and Q_u). The resulting closed-loop system is show in Figure 5.1. For the details one is refer to Kwakernaak and Sivan (1972). The Kalman filter gain is given by:

$$L = PC^TR_m^{-1}, \tag{5.14}$$

where P is the solution of the estimator Algebraic Riccati Equation (ARE):

$$0 = AP + PA - PC^TR_m^{-1}CP + B_D^TR_dB_D. \tag{5.15}$$

The control law is a simple state feedback law:

$$u(t) = -G\hat{x}(t) \tag{5.16}$$

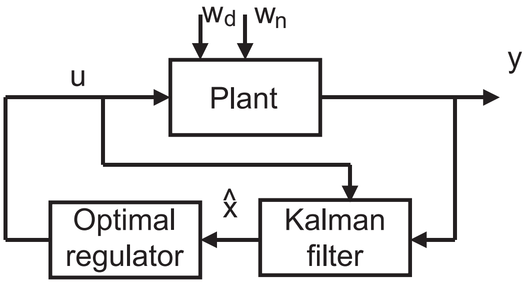

__Figure 5.1:__ Structure of the LQG controller.

where G is the feedback gain and $\hat{x}$ is the Kalman estimation of the states. The optimal state feedback gain is given by:

$$G = Q_u^{-1} B_U^T M \tag{5.17}$$

where M is the solution of the regulator ARE:

$$0 = MA + A^T M - MB_U R^{-1} B_U^T M + Q_x. \tag{5.18}$$

The optimal closed-loop controllability then ensues as follows

$$CLC = \text{tr}\left\{B_D R_d B_D^T M + G^T Q_u G P\right\}. \tag{5.19}$$

Obviously the results depend on the specific choice of the matrices Q_x and Q_u.

The controllability index CLC given by equation 5.11 is closely related related to the controllability index presented by Seferlis and Grievink (1999), equation 3.9. Both methods use the same objective function, minimization of the sum of manipulated variable action and controlled variable set-point deviations. The method presented by Seferlis and Grievink (1999) is based on a static model with static disturbances whereas our method is based on a dynamic model with stochastic disturbances.

A limitation of this index as it is defined right now is that it is not robust. Doyle (1978) showed by example that there exist LQG controllers with arbitrarily small gain margins. In the next section it will shown how robustness issues can be included in this formulation.

5.2.3 Robustness considerations

The controller designed in the previous section achieves optimal performance when the real plant equals the model. In general there will always be plant model mismatch. Take for instance only the fact the controller with optimal performance was based on a linearized model. Therefore any controller that will be implemented must also meet the design specifications despite the uncertainty in the system. This is called robustness. The LQG controller used in the CLC analysis has however no robustness properties. Two types of uncertainties are considered: parametric uncertainties and coprime factor uncertainties.

Parametric uncertainty In the beginning of this section it was assumed that the parameters ϕ have their nominal values, ϕ_0. Now the effect of uncertainty in these parameters on the closed-loop controllability indicator will be considered. The parameters ϕ are bounded by:

$$\phi_l \leq \phi \leq \phi_u, \tag{5.20}$$

where ϕ_l and ϕ_u are the lower and upper bound. The worst case, close loop minimum variance for a given design is then given by:

$$\begin{array}{rcl} CLC_{parametric} & = & \min \max\limits_{\phi} E\left\{ \lim\limits_{T\to\infty} \frac{1}{T} \int\limits_0^T \left(\Delta y^T Q \Delta y + \Delta u^T R \Delta u\right) dt \right\}, \\ st: & & \phi_l \leq \phi \leq \phi_u \\ & & LQGcontrol. \end{array} \tag{5.21}$$

where $CLC_{parametric}$ is the robust closed-loop controllability indicator for parametric uncertainty. Since the nominal values of ϕ are within the bounds, the following property always holds:

$$CLC_{parametric} \geq CLC. \tag{5.22}$$

Coprime factor uncertainty In the field of robust control one generally considers uncertainties on the elements of the transfer function, $\mathcal{G}$. This is modelled as perturbations on the plant transfer function. Let us denote the perturbed plant as $\mathcal{G}_\Delta$. Several different types of perturbations can now distinguished. A perturbation, Δ is additative if:

$$\mathcal{G}_\Delta = \mathcal{G} + \Delta. \tag{5.23}$$

A perturbation is multiplicative if:

$$\mathcal{G}_\Delta = (I + \Delta)\mathcal{G} \tag{5.24}$$

An alternative uncertainty description, often used in the area of robust control is coprime factor uncertainty. Assume that the process transfer function, $\mathcal{G}(s)$, has a normalized left coprime factorization (McFarlane and Glover, 1989):

$$\mathcal{G}(s) = M_l^{-1}(s) N_l(s), \tag{5.25}$$

where both $Ml(s)$ and $Nl(s)$ are stable. The perturbed plant can then be written as:

$$\mathcal{G}_\Delta = \left(M_l + \Delta_M\right)^{-1} \left(N_l + \Delta_N\right). \tag{5.26}$$

Figure 5.2 shows these three uncertainty models schematic. The coprime factor uncertainty model is very general. The robust stability margin is the maximum perturbation for which the closed-loop system is stable. McFarlane and Glover (1989) have shown that for this uncertainty model there exists an exact solution for the controller that maximizes this stability margin. This controller is also based on the state feedback law, equation 5.16. The stability margin, ϵ, for a controller K is given by:

$$\frac{1}{\varepsilon} = \left\| \begin{bmatrix} K \\ I \end{bmatrix} (I - \mathcal{G}K)^{-1} M_l^{-1} \right\|_{\infty}, \tag{5.27}$$

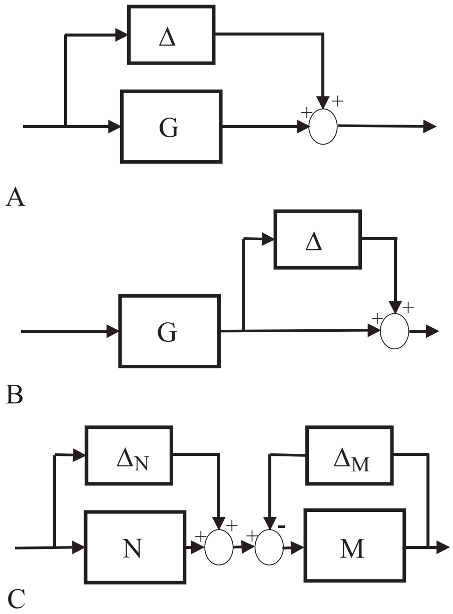

Figure 5.2: *Uncertainty models: A: additive uncertainty, B: multiplicative uncertainty, C: coprime factor uncertainty.*

In case of coprime factor uncertainty the robust closed-loop controllability is defined as:

$$\begin{aligned} CLC_{coprime} &= E\left\{\lim_{T\to\infty}\frac{1}{T}\int\limits_0^T\left(\Delta y^T Q_y \Delta y + \Delta u^T Q_u \Delta u\right)dt\right\}, \\ st: \quad & \frac{1}{\varepsilon} = \left\|\begin{bmatrix} K \\ I \end{bmatrix}(I-\mathcal{G}K)^{-1}M_l^{-1}\right\|_\infty, \\ & \varepsilon \geq \varepsilon_{\min}. \end{aligned} \tag{5.28}$$

If the stability margin for the nominal design is within the bounds, the optimum design based on the CLC is also the optimum based on $CLC_{coprime}$, hence:

$$CLC_{coprime} \geq CLC. \tag{5.29}$$

Balas et al. (1998) state that values of $\epsilon > 0.2 - 0.3$ are generally satisfactory.

We now have a novel controllability indicator with the main advantages that there exists a clear physical interpretation relating to the disturbance sensitivity and that it is based on realistic, but optimal controllers. We have also showed how robustness issues can be incorporated in this approach. Next it will be shown how this can be combined with economics.

5.3 Closed-loop controllability and economics

Just like all the other controllability indicators, the newly introduced closed-loop controllability indicator ignores the process economics. Two alternative ways to combine this closed-loop variance with the steady-state economics will be presented. The first, a multi-objective optimization approach, treats the closed-loop variance and the steady-state economics as separate objective functions. The second, a closed-loop economic optimization approach, includes the closed-loop variance in the constraints.

5.3.1 Multi objective optimization

When the closed-loop variance and the steady-state economics are both seen as objective functions, the design problem can be formulated as:

$$\begin{array}{ll} \min\limits_{p\in\mathcal{P}} & (J_{economic}, J_{clvar}) \\ s.t. & 0 = f(x,z,u,\delta,\sigma,\phi) \\ & 0 = g((x,z,u,\delta,\sigma,\phi), \\ & LQGdesign \\ & y_l \leq y \leq y_u. \end{array} \tag{5.30}$$

In general each objective function itself can be minimized, but it is not possible to simultaneously minimize both objective functions. Figure 5.3 shows a typical feasible solution set. The Pareto solution set consists of those designs where one objective can only be improved at the expense of the other objective function. For the designs that do not lay on the Pareto curve, always at least one objective can be improved, without resulting a negative effect on the other objectives. The solution of the design problem 5.30 is the Pareto set. A decision maker needs to select a single design afterwards by making a trade-off between the various objectives.

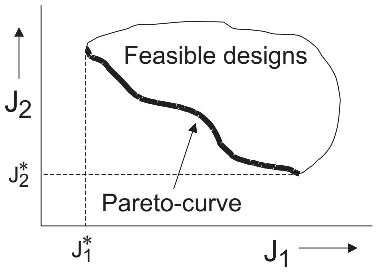

Figure 5.3: *Pareto curve for two objectives.*

Several alternative methods exist to generate the Pareto set (Clark and Westerberg, 1983). The first approach is to introduce a new objective function that is a weighted sum of the individual objective functions:

$$J_{new} = \sum \omega_i J_i \tag{5.31}$$

where w_i are the weights related to the various individual objectives. In this way the multi objective optimization problem is transformed in a single objective optimization problem. The difficulty in this approach is to assign the weights for the individual objectives. For our specific problem: how to weight the static economics compared to the closed-loop controllability.

When there are two objective functions, J_1 and J_2 a new objective function can be generated:

$$J_{multi} = \alpha J_1 + (1-\alpha) J_2, \tag{5.32}$$

with $0 \leq \alpha \leq 1$. A Pareto set can be generated by solving the optimization problem with the new objective function for different values of α.

Alternatively one can optimize one objective function while a constraint is added on the other objective function(s):

$$\begin{array}{ll} \min & J_{economic} \\ s.t. & J_{clvar} \leq \mathcal{J}, \end{array} \tag{5.33}$$

where $\mathcal{J}$ is the constraint value of the other objective function. By varying this constraint on can generate the Pareto curve.

For strictly integer design spaces the Pareto set can also be found by gridding of the design parameters.

The main advantage of the multi objective optimization approach is that clear insight in the trade-off between different objectives is obtained, however the “solution“ of (5.30) is a set of solutions rather than a single solution. Next, an alternative approach is presented with a single solution.

5.3.2 Closed-loop economic optimization

In the approach described above, all designs constraints (equations 5.2) are related to the expectations of y. This gives no information about the distribution of y around the expectation. Different design alternatives will have the same expectation, but can have completely different distributions. A more realistic approach would be to put constraints on the expectation value plus the variance. For instance specify the value the variables should have for e.g. 90% of the production time. A smaller variance can then lead to a design closer to the constraint. In general this will be economically attractive. It is also the basic concept of Taguchi techniques (Ross, 1988).

An example in distillation is to replace the constraint that the expectation of the the top purity is 99% by a constraints specifying that top purity should be above 99% for 95% of the time. A reduction of the variance gives the possibility to set the mean value closer to the constraints. This is shown schematically in Figure 5.4. Line A is the first design. A constraint violation is allowed for 10% of the production time. Line B has the same mean value, but a reduced variance. Since a much smaller part is below the constraint, the mean can be shifted closer to the constraint, line C, with still of constraint violation of 10% of the production time. This will generally be cost efficient. The dashed areas in the figure indicate the 90% region. A time domain visualization is presented in Figure 5.5. The constraint formulation (5.2) is now modified into:

$$\begin{aligned} y_l \leq \quad & y - \gamma\varsigma(y) & \\ & y + \gamma\varsigma(y) & \leq y_u, \end{aligned} \tag{5.34}$$

where ς indicates the standard deviation. The variable γ indicate the degree of constraint violation. For a normal distribution and $\gamma = 1$ allows the variable to violate the constraint for about 16% of the production time, $\gamma = 3$ allows the variable to violate the constraint for about 0.1% of the production time.

The standard deviation of the outputs is given by the square root of the diagonal elements of the closed-loop co-variance matrix. This co-variance matrix is given by:

$$E(yy^T) = \begin{bmatrix} C \\ 0 \end{bmatrix} Y \begin{bmatrix} C^T & 0 \end{bmatrix}, \tag{5.35}$$

where Y is state covariance matrix. This matrix is the solution of the Lyapunov

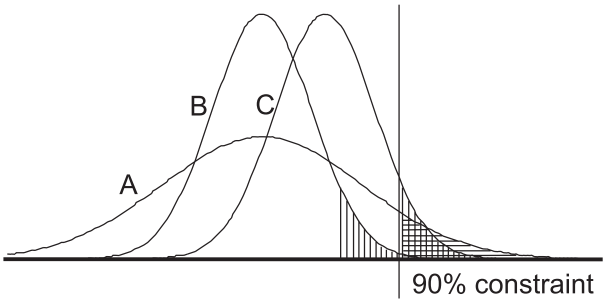

Figure 5.4: *A reduced variance allows to move closer to the constraints.*

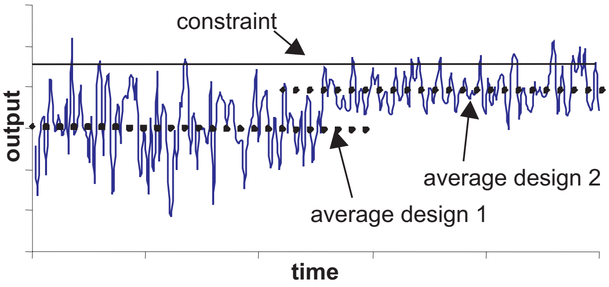

Figure 5.5: *Time domain interpretation of Figure 5.4.*

equation:

$$\begin{bmatrix} A-BG & -BG \\ 0 & A-LC \end{bmatrix} Y + Y \begin{bmatrix} A-BG & -BG \\ 0 & A-LC \end{bmatrix}^T + R_d = 0. \tag{5.36}$$

The design problem is then reformulated to:

$$\begin{array}{ll} \min\limits_{\sigma\in\Sigma,u} & J_{economic} \\ s.t. & 0 = f(x,z,u,\delta,\sigma), \\ & 0 = g(x,z,u,\delta,\sigma), \\ & LQGdesign \\ & 0 = \begin{bmatrix} A-BG & -BG \\ 0 & A-LC \end{bmatrix} Y + Y \begin{bmatrix} A-BG & -BG \\ 0 & A-LC \end{bmatrix}^T + R_d \\ & \sigma(y) = \left(diag(\begin{bmatrix} C \\ 0 \end{bmatrix} Y \begin{bmatrix} C^T & 0 \end{bmatrix}) \right)^{\frac{1}{2}}, \\ & y_l \le y - \gamma_y \sigma(y), \\ & y + \gamma_y \sigma(y) \le y_u. \end{array} \tag{5.37}$$

The solution of this optimization problem is more computationally demanding than the solution of the multi objective optimization problem because of the large dimension of the search space.

5.4 Example: binary distillation

The approach is now illustrate with a binary distillation column as case study.

System description The process model is based on the well known Column A, introduced by Skogestad (1997). The feed and product specifications for all alternative designs were based on those described by Skogestad (1997). The following modifications were made to the model:

- the feed is introduced above the feed stage instead of on the feed stage,
- perfect control instead of PI control is applied to the reboiler and condenser hold-up,
- the nominal hold-up on the stages is modelled proportional to the liquid flow to take the effect of the diameter of the column into account.

The design parameters that are varied are the number of stages and the feed stage location. The number of stages was varied from 31 to 51. The feed stage location was varied from the center stage minus 5 stages to the center stage plus 5 stages. The base case design has 41 trays and the feed tray is in the center (tray 21). This is a traditional design with the reflux ratio chosen 1.35 times the minimum reflux ratio. The feed is saturated liquid. The controlled variables are the top and bottom composition. The manipulated variables are the vapour boilup and liquid reflux stream, corresponding to the well known LV configuration. Other control configurations are not considered. For the calculation of the total annual costs the economic model provided Luyben and Floudas (1994) is used. This model takes the capital as well as the operational costs into account. All cost data are taken equal to those provided by Luyben and Floudas (1994).

Simultaneous disturbances in the feed flow rate and feed composition were considered with a variance of 0.044 and 0.011 respectively. The shaping filters for both disturbances were chosen low-pass second order such the inverse of the cut-off frequency is one fourth of the dominant time constant in the system (cut-off frequency 0.016 Hz). The measurement noise on the composition measurements was assumed to be white noise with a variance of 0.0001.

5.4.1 Multi-objective analysis

In this example all design parameters are integer variables. Therefore an alternative approach is used to generate the Pareto set. First generate the entire feasible area by gridding the parameter space. For all grid points both objectives are calculated. The grid points that form the Pareto optimum can then easily be selected. This leads to the following steps:

step 1 choose N grid points $\sigma_i \in \Sigma$, $i = 1, \ldots, N$ to discretize the search space,

step 2 for every grid point σ_i,

- determine a steady-state,
- compute the economic costs ($J_{economic}$) associated with the static design,
- compute a linearization $[A, B, C]$,
- solve the estimation and control Riccati equations and compute the closed-loop variance (CLC).

The weighted closed-loop variance of all designs is given in Figure 5.6. Figure 5.7 shows the total annual costs of the designs, as a function of the design parameters. All designs were generated with the specification of the nominal top and bottom composition as given above. The weighting matrices Q_y and Q_u were both identity matrices. The optimum from a economic point of view lies around the base-case design. The absolute values of the weighted closed-loop variance depends on the units used for the manipulated and controlled variables and the weighting matrices. Figure 5.6 clearly shows that the optimum design from a closed-loop controllability point of view has less stages than the nominal design. Alternative sets of weighting matrices ($Q_y = 10 * I, Q_u = I$ and $Q_y = I, Q_u = 10 * I$) gave the same trends. Note that this is in line with the results presented in Chapter 4. This result is in contrast with the statement made by Skogestad (1997) that for composition control increasing the number of stages would probably be beneficial. However it can be explained physically when one realizes that the total inventory in the column with 31 trays is larger than the total inventory in the column with 51 trays. Although the number of trays is smaller, the hold-up per tray is larger because of the higher reflux. For the specific type of disturbances, zero mean stochastic disturbances, this leads to lower disturbance sensitivity. Figure 5.8 shows the multi-objective results with

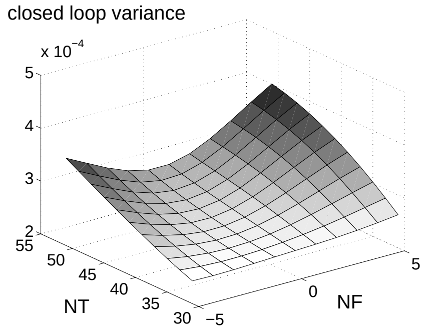

Figure 5.6: *Closed-loop variance as a function of design parameters.*

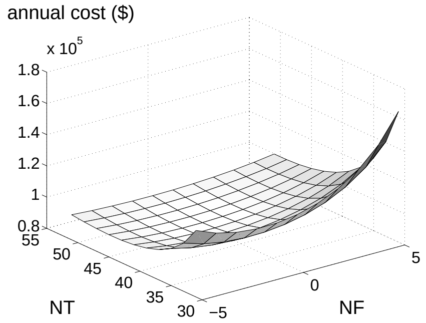

Figure 5.7: *Total annual costs as a function of design parameters.*

the closed-loop variance objective function plotted against the total annual costs objective function. Apparently the designs with a feed stage around the center lie very close to the Pareto curve. One can hence conclude that the feed stage position that is optimal with respect to both steady-state economics *and* closed-loop variance is in the center of the column. The trade-off between steady-state economics and closed-loop variance hence remains to be made by a choice of the number of stages only.

The results presented above did not take any robustness measures into account. Next it will be shown how the results differ when robustness is considered.

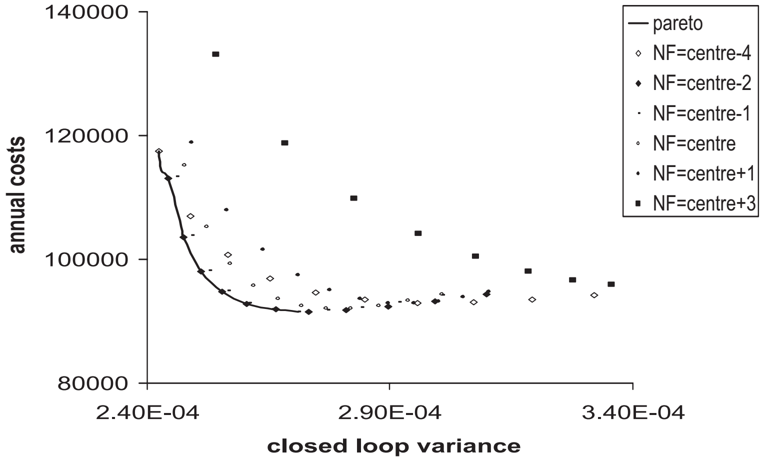

Figure 5.8: *Total annual costs versus the closed-loop variance.*

5.4.2 Robustness

Parametric uncertainty The uncertain parameters considered are the feed rate and the feed composition:

$$\theta = \left\{ \begin{array}{c|c} F & 0.9 \leq F \leq 1.1 \\ x_F & 0.45 \leq x_F \leq 0.55 \end{array} \right\} \tag{5.38}$$

Figure 5.9 shows the robust CLC results as defined by equation (5.21). It can clearly be seen that the robust CLC results give the same trends as the nominal results. The optimal design parameters using $CLC_{parametric}$ are not altered, compared with the optimal design parameters using CLC. Obviously the values of $CLC_{parametric}$ are higher then the nominal values since the values of maximized over the uncertainty domain.

Coprime factor uncertainty Figure 5.10 presents the stability margins for the various designs related to the coprime factor uncertainty. When this stability margin is added as a constraint to the optimization problem, the feasible area is reduced. In line with Balas et al. (1998) constraint that $\epsilon > 0.2$ is added. The resulting feasible area is indicated in Figure 5.10. The values of CLCR2 in the

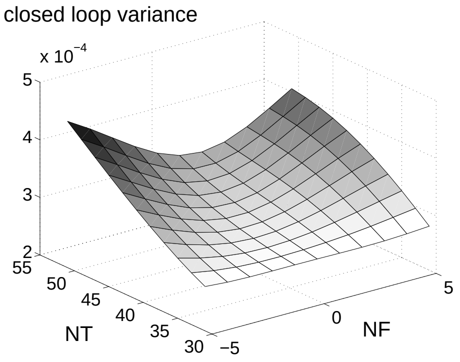

Figure 5.9: *Parametric closed-loop controllability.*

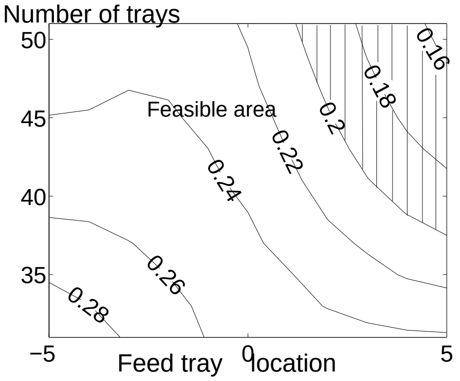

Figure 5.10: *Co prime factor uncertainty stability margin.*

feasible area are the same as the values of the CLC. Hence the optimum design parameters in case of coprime factor uncertainty have not changed, compared with the nominal design.

5.4.3 Closed-loop validation

Govtsmark and Skogestad (2002) disputed that the controllability analysis based on LQG control are of practical interest. They state that the results presented above are only valid when there is no model uncertainty and no delays. Based on μ-optimal control and RGA analysis they conclude that a large number of trays is beneficial for control. As stated before, the ultimate goal is the final closed-loop performance. Hence the controllability analysis should be inline with realistic closed-loop simulations. Therefore closed-loop simulations are carried out for columns with different number of trays: 31, 41 and 51, with PI control on the composition control loops. All columns are designed as presented before, with the feed stage in the middle. The full non-linear models were used for these simulations. For the inventory control in the reboiler and condenser P controllers are used, with gains as suggested by Skogestad. In the composition control loops a time delay of 1 minute was added to simulate measurement delays. Auto Tuning Variation was applied to determine the ultimate gain and the period of oscillation (Åström and Hägglund, 1988), required for the controller tuning. Tyreus-Luyben settings were used for the PI controllers (Tyreus and Luyben, 1992). Table 5.1 shows the ultimate gain and period of oscillation, together with the Tyreus-Luyben tuning parameters for the three designs. The three different col-

Table 5.1: *Physico-chemical processes and their flows and forces.*

	NT=31	**NT=41**	**NT=51**
top loop			
K_c	334	264	218
P_u	4.8	4.7	5
K_{TL}	104	83	68
$\tau_{i,TL}$	10.6	10.3	11
bottom loop			
K_c	-215	-177	-159
P_u	3.6	3.6	3.7
K_{TL}	-67	-55	-50
$\tau_{i,TL}$	7.9	7.9	8.1

umn designs were exposed to stochastic disturbances in the feed rate and feed composition, according to the disturbance scenario as defined before. The disturbance profiles are shown in Figure 5.11. The closed-loop responses of the top and bottom compositions are shown in Figure 5.12 and Figure 5.13. The (normalized) integral squared errors (ISE) are shown in Table 5.2. These results clearly show that form a disturbance sensitivity point of view, a column with a small number of trays is considerably better then for a column with a large number of trays.

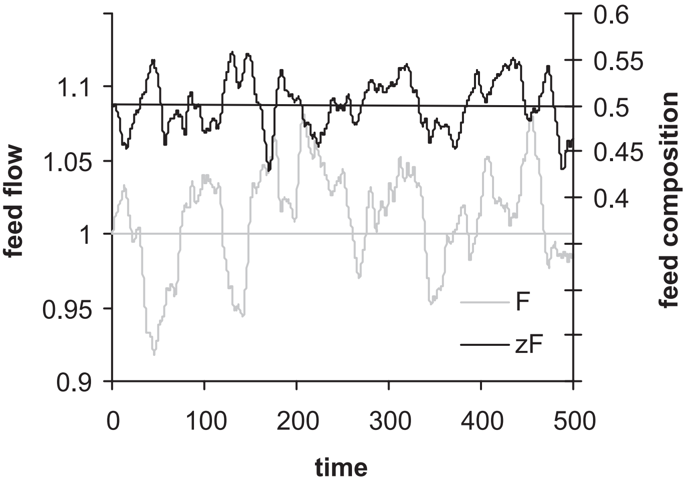

Figure 5.11: *Profiles of the disturbances in the feed flow (left axis) and feed composition (right axis).*

Table 5.2: *Integral Squared Errors for top and bottom composition under stochastic disturbance scenario, normalized with NT=31.*

	NT=31	**NT=41**	**NT=51**
ISE top	1.0	2.1	3.3
ISE bottom	1.0	2.0	2.6

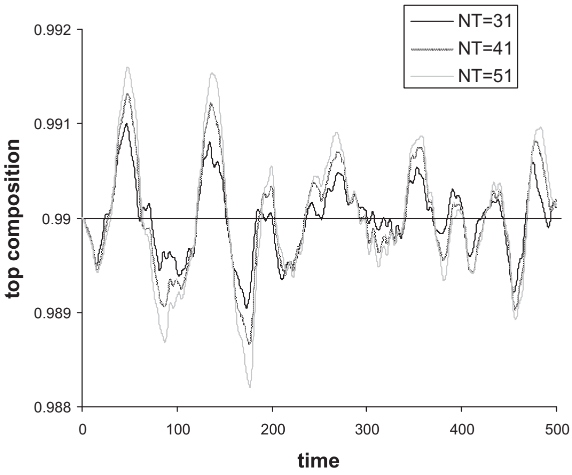

Figure 5.12: *Closed-loop response of the top compositions to the stochastic disturbance profile.*

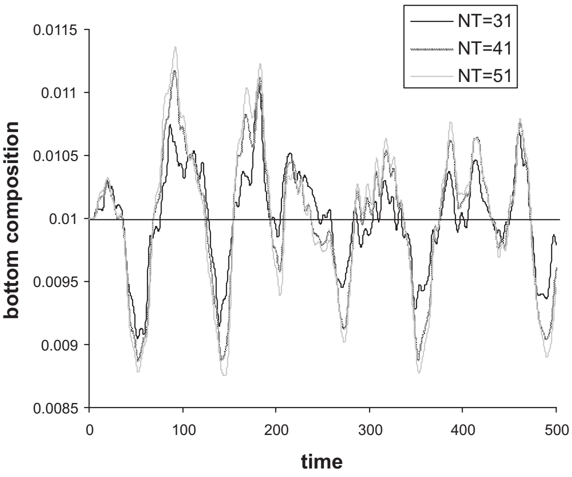

Figure 5.13: *Closed-loop response of the bottom compositions to the stochastic disturbance profile.*

5.4.4 Closed-loop economic optimization results

The closed-loop economic optimization problem (eq. 5.37) was also applied to this case. Instead of specifying the nominal values of the top and bottom composition, the mean value plus once the standard deviation is specified:

$$\mu(x_{top}) - \varsigma(x_{top}) \geq 0.99, \tag{5.39}$$

and

$$\mu(x_{bottom}) + \varsigma(x_{bottom}) \leq 0.01. \tag{5.40}$$

Figure 5.14 shows the total annual costs for the designs as a function of the design parameters for this problem statement. Figures 5.15 and 5.16 show respectively the mean top and bottom composition as a function of the design parameters. The designs with this approach are, for the same design parameters P, up to 12 % more expensive than the designs generated based on the nominal compositions due to back-off from the constraints. It can also be seen that the optimal choice of design parameters is almost equal to the design parameters for the steady-state optimal economic (41 trays and the feed tray in the center).

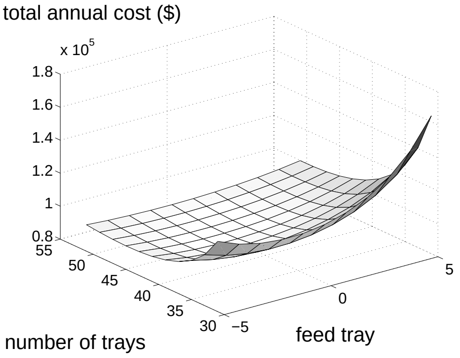

Figure 5.14: *Total annual costs for closed-loop economic optimization.*

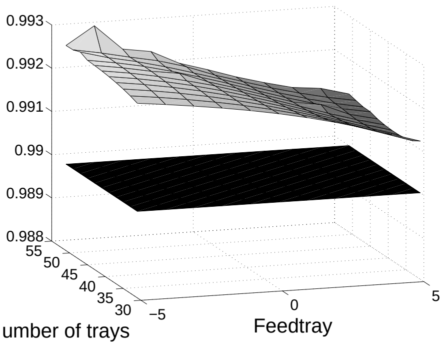

Figure 5.15: *Mean value of the top composition.*

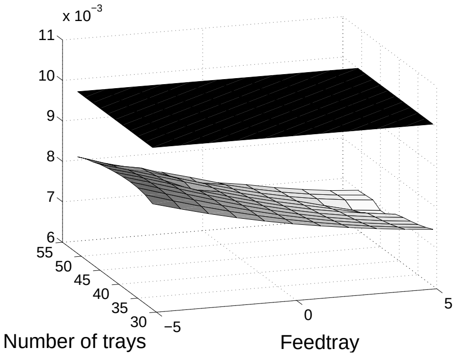

Figure 5.16: *Mean value of the bottom compositions.*

5.5 Dynamic interaction of control loops

Almost all chemical processes are multivariable by nature. Despite the fast developments in multivariable control, most control systems are still based on single input single output (SISO) control. This generally leads to a set of potentially interacting SISO control loops. Bristol (1966) introduced the well known Relative Gain Array (RGA) to quantify steady-state interaction. For a system with n manipulated and n controlled variables, the RGA is a nxn matrix whose entries consist of the ratios of the corresponding open-loop gain and closed-loop gains. The RGA can be used to determine which pairing of manipulated and controlled variables should be used in order to minimize interaction. For an overview of the RGA the reader is referred to textbooks like Stephanopoulos (1984) and Skogestad and Postlethwaite (1996).

The RGA is based on static gains, in other words the process dynamics are neglected. Especially for systems containing time delays, right half plane zeros or large differences in time constants an analysis of the dynamic interaction can be very important. Based on the steady-state analysis one would prefer a certain pairing, whereas the inclusion of the dynamics would lead to a different pairing. It should be noted however, that an acceptable static RGA remains a necessary condition. Therefore a dynamic analysis is only required for systems with an acceptable static RGA. Another motivation for a dynamic interaction analysis is that sometimes no preference for the pairing can be determined based on steady-state analysis only (e.g. a 2x2 system with all RGA elements close to 0.5). Dynamic analysis might reveal which pairing should be preferred.

Witcher and McAvoy (1977) proposed to extend the RGA to the frequency domain. Gagnepain and Seborg (1982) modified the dynamic approach of Witcher and McAvoy (1977) by averaging the frequency dependent RGA over the desired frequency range. The application of this is of rather limited use because now all dynamic effects are averaged. Tung and Edgar (1981) calculate the dynamic RGA out of a state-space description of the process. However their method is not essentially different from the method proposed by Witcher and McAvoy (1977). The methods discussed above are all based on perfect control. In the steady-state this might be realizable, but dynamic perfect control is in general not possible. Huang et al. (1994) define a Generalized Dynamic Relative Gain (GDRG) using more realistic control based on the Internal Model Control (IMC) principle. However the GDRG is also based on averaging the dynamic response over the frequency domain so the applicability is limited.

A new method for the analysis of dynamic interaction is now presented. The objective of this method is to do a meaningful analysis of dynamic interaction. This means that it is not based on the perfect control assumption. Moreover the analysis is done in the time domain because of the large advantages it offers for the interpretation.

First a review will be given of the dynamic RGA. Then our new approach will be presented, followed by a number of examples. Finally some conclusions will be drawn about the applicability of this new approach.

5.5.1 Review of dynamic RGA

Consider a square system with n manipulated variables u and n controlled variables y. The RGA element λ_{ij} that is the result of pairing the controlled variable y_i with the manipulated variable u_j is defined as:

$$\lambda_{ij} = \frac{\left(\frac{\partial y_i}{\partial u_j}\right)_{u_{l \neq j}\ constant}}{\left(\frac{\partial y_i}{\partial u_j}\right)_{y_{k \neq i}\ constant}} \tag{5.41}$$

The numerator in expression 5.41 is the gain of the loop ij, with all other manipulated variables kept constant (open-loop gain). The denominator is the gain of the same loop, but now with control applied on all other loops keeping all other controlled variables constant (closed-loop gain).

The complete RGA matrix Λ can be computed from the transfer function matrix $\mathcal{G}$:

$$\Lambda(s) = \mathcal{G}(s) \bigotimes \mathcal{G}(s)^{-1^T} \tag{5.42}$$

Where $\bigotimes$ denotes element by element multiplication and s the laplace variable.

When $s = 0$ is inserted into equation 5.42, the static gains are obtained and hence the original RGA as proposed by Bristol (1966). Witcher and McAvoy (1977) were the first to extend this to the frequency domain. The frequency dependent RGA is simply calculated by inserting $s = j\omega$ in equation 5.42. There are however some arguments against the use of this frequency dependent RGA:

- The physical interpretation is much less transparent than the steady-state interpretation.
- It makes use of not realizable controllers.

- Chemical engineers are less used to working in the frequency domain.

All these arguments will be discussed below.

Firstly, calculation of the frequency dependent RGA according equation 5.42 will lead to a matrix with complex elements. These complex elements can be represented by a magnitude and a phase. The interpretation of these complex elements is not very transparent. Witcher and McAvoy (1977) claim that: *"the magnitude can be interpreted in exactly the same way as the standard relative gain array."* However the standard RGA can have negative elements while the magnitude is always non-negative. Moreover the property that the sum of elements in a row or column equals one does not hold for the magnitudes. Seider et al. (1999) try to get around this by using a slightly modified expression for the dynamic RGA elements. For one element (lets suppose the 1,1-element) the following expression is used:

$$\lambda_{11} = sign\left(\lambda_{11}(0)\right) \cdot \left|\lambda_{11}(j\omega)\right| \tag{5.43}$$

Then the 1,2-element is calculated with:

$$\lambda_{12} = 1 - \lambda_{11}. \tag{5.44}$$

However different results will be obtained when the 1,2-element is used in equation 5.43, rather then the 1,1-element. So this frequency dependent RGA is not uniquely defined.

Secondly, the calculation of the dynamics of any closed-loop response relies on the selected controller. When the RGA is calculated according to equation 5.42, the implicit assumption is made that the controller is the inverse of the process. However this will lead to non-proper controllers that can also be unstable when right half plane zeros are present or unrealizable when time delays are present, Morari (1983).

Thirdly, the frequency domain seems to be not the most appropriate domain of analysis for chemical processes. The frequency domain stems from the systems and control community. It has however never been embraced by chemical engineers, especially not by those working outside academia. It is also our personal experience that in the industrial process control practice the frequency domain is completely omitted. One of the reasons for this could be that the frequency domain is very informative for sine shaped signals. For step responses however, the time domain is much more attractive to work in. In chemical processes, disturbances and set-point can in general much better be described by step responses then by sinuses.

5.5.2 Proposed Approach

The basic idea of our approach is to compare two step responses of the system after a manipulated variable action under different control conditions. The first step response is the open-loop response to a manipulated variable action, so all other manipulated variables are kept constant. The second is the closed-loop response, so all other control loops are put on automatic. Both responses will be calculated in the Laplace domain and then transformed to the time domain. A general square system will be considered as described by:

$$y = \mathcal{G} \cdot u, \tag{5.45}$$

with y the vector of outputs, u the vector of inputs and $\mathcal{G}$ the transfer matrix.

Open-loop response The open-loop step response of y_i to a change in u_j is then given by:

$$y_{ij,ol}(t) = \mathcal{L}^{-1}\left[\mathcal{G}_{ij}\frac{1}{s}\right], \tag{5.46}$$

where $\mathcal{L}$ denotes the Laplace transform.

Closed-loop response For the closed-loop response a controller needs to be designed for all other control-loops. Obviously this response depends on the selected control algorithm. Our approach uses Internal Model Control (IMC) as presented by Garcia and Morari (1985). Figure 5.17 shows the structure of IMC. The details of the IMC design used to construct Q can be found in Appendix B.

It should be noted that while calculating λ_{ij} the plant $\mathcal{P}$ equals $\mathcal{G}$ without the i-th row and the j-th column. Figure 5.18 shows the complete signal diagram for the closed-loop system. From this figure it can easily be seen that the closed-loop step response of y_i to a change in u_j is given by:

$$y_{ij,cl}(t) = \mathcal{L}^{-1}\left[\left(\mathcal{G}_{ij} - \mathcal{G}_{i,l\neq j}\mathcal{Q}\mathcal{G}_{k\neq i,j}\right)\frac{1}{s}\right] \tag{5.47}$$

Dynamic RGA In the traditional RGA the open-loop is divided by closed-loop gain. A seemingly logical extension would be to divide the open-loop time response by the closed-loop time response. However in case of time delays this might lead to division by zero. It is proposed to present the data as a parametric representation. That is for every time instant a point is plotted with the

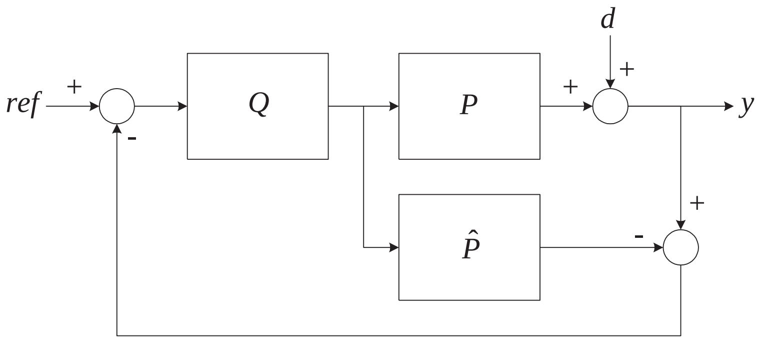

Figure 5.17: *The structure of IMC. The plant is indicated by $\mathcal{P}$, $\hat{\mathcal{P}}$ is a plant model and $\mathcal{Q}$ an approximation of the inverse of $\hat{\mathcal{P}}$.*

closed-loop step response as x-coordinate and the open-loop step response as y-coordinate. It should be clear that if the parametric representation coincides with the line $y = x$ both responses are the same.

Suppose that the open-loop and closed-loop response are given by:

$$y_{ol}(t) = \mathcal{L}^{-1}\left[\left(\frac{1}{s+1}\right)\frac{1}{s}\right] \tag{5.48}$$

$$y_{cl}(t) = \mathcal{L}^{-1}\left[\left(\frac{1}{s+1} + \frac{1}{s^2+3s+1}\right)\frac{1}{s}\right] \tag{5.49}$$

Then figure 5.19 shows the graph. The graph runs from the point $t = 0$ till $t = \infty$. All graphs are placed in an array, so for a 2x2 system the result would be four graphs placed in an array of two rows and two columns. In the rest of this article this array of graphs will be referred to as the dynamic RGA.

Properties of the dynamic RGA Now some properties of the dynamic RGA will be presented.

- *The graph always starts ($t = 0$) in the origin.*

The point of the graph corresponding with $t = 0$ is $(y_{cl}(0), y_{ol}(0))$. For smooth systems $y_{cl}(0) = y_{ol}(0) = 0$ and hence the starting point of the graph is the origin.

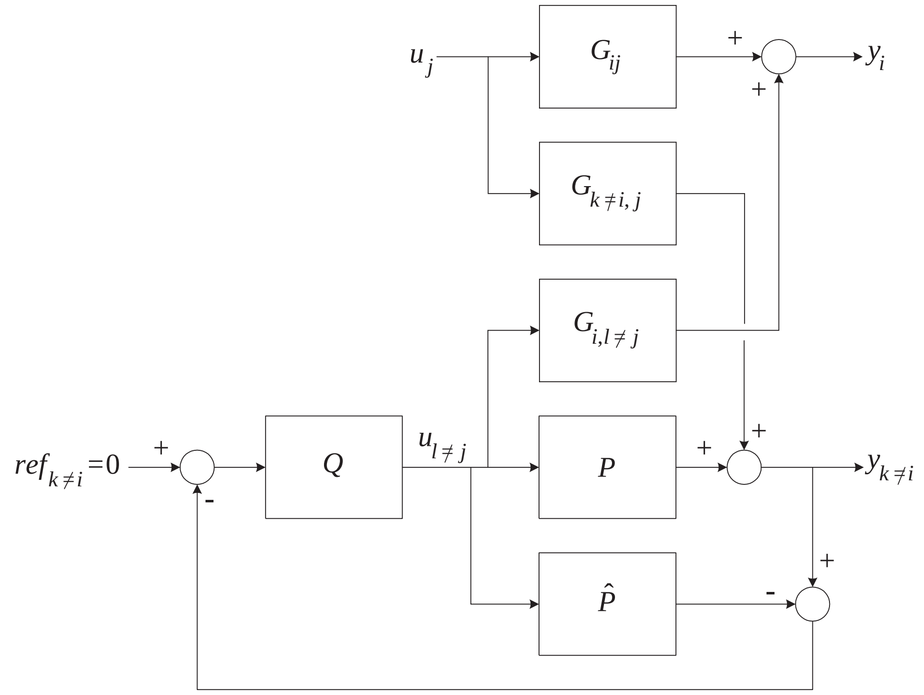

Figure 5.18: *Closed-loop structure containing the internal model controller.*

• *The static RGA values are given by dividing the final value of the open-loop step response by the final value of the closed-loop step response.*
The endpoint of the graph, corresponding with $t \to \infty$ is $(y_{cl}(\infty), y_{ol}(\infty))$. These are the open and closed-loop gain respectively and they do not depend on the applied control algorithm. So the static RGA is simply the open-loop gain divided by the closed-loop gain.
• *For stable systems the graph is finite.*
This is an obvious result from the previous property.
• *The property that the sum of the elements in a row or column equals one is lost.*
Given a matrix M containing only real elements. Then for the matrix M, given by:

$$M = K \bigotimes K^{-1^T}, \tag{5.50}$$

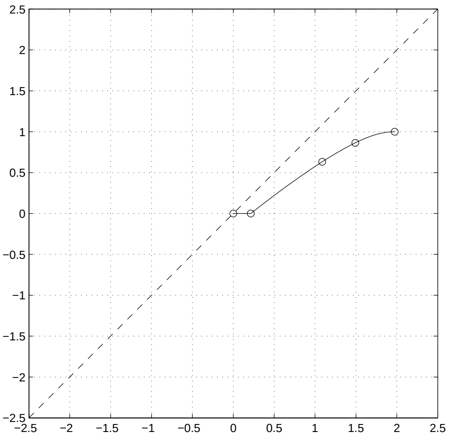

Figure 5.19: *A typical graph, the open-loop and closed-loop response are given by equations 5.48 and 5.49. Starting at the origin the circles indicate t = 0, 1, 2, 3 and 10 time units.*

the sum of elements in a row or column equals one. Equation 5.50 is the basis of the traditional RGA and of the frequency dependent RGA approaches. So for those approaches the sum of elements in a row or column equals one. Note however that in the frequency dependent approaches often the magnitude of the elements is selected. The property does not apply for the magnitude of the elements. In our dynamic RGA the calculation described by equation 5.50 is not performed, hence this property is lost.

• *For a completely decoupled system the graph coincides with the line $y = x$.*

For a completely decoupled system $y_{cl}(t) = y_{ol}(t) \forall t \in \mathbb{R}^+$. So the parametric representation coincides with the line $y = x$.

• *If the graph intersects the line $y = ax$, the RGA at that time instant has the value a.*

This results from the fact that at any time instant the x-coordinate of graph is the closed-loop response and the y-coordinate the open-loop response.

Interpretation of the graphs As already hinted before the most desirable situation, from an interaction point of view, is a completely decoupled system. This means that the graph coincides with the line $y = x$. Deviations from this line are a measure for the amount of interaction. As a matter a fact it is possible to "enclose" a graph by two lines through the origin. For example in figure 5.19 the graph can be enclosed by the lines $y = 0$ and $y = 0.6x$. So the dynamic RGA covers the interval [0, 0.6]. This interval should be compared with the "ideal" value of 1.

If the graph initially moves over the x-axis it implies that the closed-loop and open-loop response have different time delays. This represents an unfavourable pairing since opening other loops might result in a stability problem. Something similar happens when the graph moves into the second or forth quadrant. This means that the open-loop and closed-loop response have a different sign. So again this represents an unfavourable pairing because of a potential stability problem.

5.5.3 Examples

As explained before there are two reasons for extending the static RGA to a dynamic RGA:

- In some cases the static RGA prefers a pairing different from the best dynamic pairing.
- In other cases the static RGA does not prefer any pairing (when all elements have more or less the same value).

In this chapter two examples are given. In the first example the static RGA does not prefer any pairing and in the second example the static RGA prefers the wrong pairing.

Example 1 The plant P1 is given by:

$$P1(s) = \begin{pmatrix} \frac{e^{-s}}{s+1} & \frac{1}{s+1} \\ \frac{-1}{s+1} & \frac{e^{-2s}}{s+1} \end{pmatrix} \tag{5.51}$$

The static RGA can be calculated with equation 5.42:

$$\Lambda_{P1} = \begin{pmatrix} 0.5 & 0.5 \\ 0.5 & 0.5 \end{pmatrix} \tag{5.52}$$

So the static RGA does not prefer any pairing. The proposed dynamic RGA can be developed as follows. Equation 5.51 gives the various open-loop responses, for example the open-loop response of the 1,1-element is given by:

$$y_{11,ol}(t) = \mathcal{L}^{-1}\left[\left(\frac{e^{-s}}{s+1}\right)\frac{1}{s}\right] \tag{5.53}$$

The closed-loop step response of the same element can be derived by substituting the correct transfer functions in equation 5.47:

$$y_{11,cl}(t) = \mathcal{L}^{-1}\left[\left(\underbrace{\frac{e^{-s}}{s+1}}_{\mathcal{G}_{11}} - \underbrace{\frac{1}{s+1}}_{\mathcal{G}_{12}}\underbrace{\frac{s+1}{1}\frac{1}{0.1s+1}}_{\mathcal{Q}}\underbrace{\frac{-1}{s+1}}_{\mathcal{G}_{21}}\right)\frac{1}{s}\right] \tag{5.54}$$

Note that $\mathcal{Q}$ is calculated according to the procedure presented in Appendix B. Some rearrangements gives:

$$y_{11,cl}(t) = \mathcal{L}^{-1}\left[\left(\frac{e^{-s}}{s+1} + \frac{10}{s^2+11s+10}\right)\frac{1}{s}\right] \tag{5.55}$$

Repeating the same exercise for the other elements gives:

$$y_{12,cl}(t) = \mathcal{L}^{-1}\left[\left(\frac{1}{s+1} + \frac{10e^{-3s}}{s^2+11s+10}\right)\frac{1}{s}\right] \tag{5.56}$$

$$y_{21,cl}(t) = \mathcal{L}^{-1}\left[\left(\frac{-1}{s+1} - \frac{10e^{-3s}}{s^2+11s+10}\right)\frac{1}{s}\right] \tag{5.57}$$

$$y_{22,cl}(t) = \mathcal{L}^{-1}\left[\left(\frac{e^{-2s}}{s+1} + \frac{10}{s^2+11s+10}\right)\frac{1}{s}\right] \tag{5.58}$$

Equations 5.51, 5.55, 5.56, 5.57 and 5.58 are used to construct figure 5.20. Figure 5.20 confirms that the static RGA does not prefer any pairing. All graphs except the one of the 2,1-element end at (2,1). So the static RGA values of these elements is $\frac{1}{2} = 0.5$. The graph of the 2,1-element ends at (-2,-1), so the static RGA value of this element also equals $\frac{-1}{-2} = 0.5$. However figure 5.20 reveals that the diagonal elements approach this static RGA value quite differently than the off-diagonal elements. The graphs of the diagonal elements can be enclosed by the lines $y = 0$ and $y = 0.5x$, so the dynamic RGA of the diagonal elements covers the interval [0, 0.5]. The dynamic RGA of the off-diagonal elements move over the interval

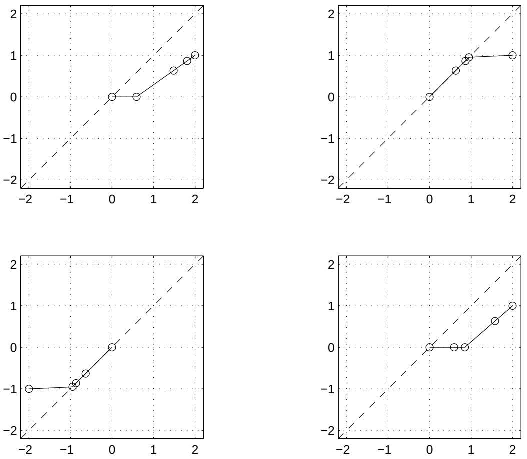

Figure 5.20: *The dynamic RGA of plant P1. Starting at the origin the circles indicate t = 0, 1, 2, 3 and 10 time units.*

[0.5, 1.0]. Note that the interval of the diagonal elements is further from the ideal value 1.0 than the interval covered by the off-diagonal elements. Another observation is that the diagonal elements move away from $y = x$ *right from the start over the line* $y = 0$. The off-diagonal elements also move away from $y = x$, but this happens *only after three time units*. So the open and closed-loop responses have different time delays. In other words the static RGA does not prefer any pairing but the dynamic RGA clearly prefers the off-diagonal pairing.

Example 2 Plant P2 is taken from Seider et al. (1999):

$$P2(s) = \begin{pmatrix} \frac{2.5e^{-5s}}{(15s+1)(2s+1)} & \frac{5}{4s+1} \\ \frac{1}{3s+1} & \frac{-4e^{-5s}}{20s+1} \end{pmatrix} \tag{5.59}$$

The static RGA can be calculated with equation 5.42:

$$\Lambda_{P2} = \begin{pmatrix} 0.667 & 0.333 \\ 0.333 & 0.667 \end{pmatrix} \tag{5.60}$$

So the static RGA prefers diagonal pairing (Seider et al., 1999). Substitution of the correct transfer functions in equation 5.47 gives:

$$y_{11,cl}(t) = \mathcal{L}^{-1}\left[\left(\frac{2.5e^{-5s}}{(15s+1)(2s+1)} + \frac{250s+12.5}{12s^3+127s^2+71s+10}\right)\frac{1}{s}\right] \tag{5.61}$$

$$y_{12,cl}(t) = \mathcal{L}^{-1}\left[\left(\frac{5}{4s+1} + \frac{(300s+100)e^{-10s}}{600s^4+6370s^3+3737s^2+371s+10}\right)\frac{1}{s}\right] \tag{5.62}$$

$$y_{21,cl}(t) = \mathcal{L}^{-1}\left[\left(\frac{1}{3s+1} + \frac{(80s+20)e^{-10s}}{600s^4+6370s^3+3737s^2+371s+10}\right)\frac{1}{s}\right] \tag{5.63}$$

$$y_{22,cl}(t) = \mathcal{L}^{-1}\left[\left(\frac{-4e^{-5s}}{20s+1} - \frac{6000s^2+3400s+200}{12s^4+247s^3+1341s^2+720s+100}\right)\frac{1}{s}\right] \tag{5.64}$$

Equations 5.59, 5.61, 5.62, 5.63 and 5.64 are used to construct figure 5.21. The RGA value of the diagonal elements moves over the interval [0, 0.667], while the RGA value of the off-diagonal elements covers the interval [0.333, 1.0]. Figure 5.21 also shows that the diagonal elements move away from $y = x$ over the line

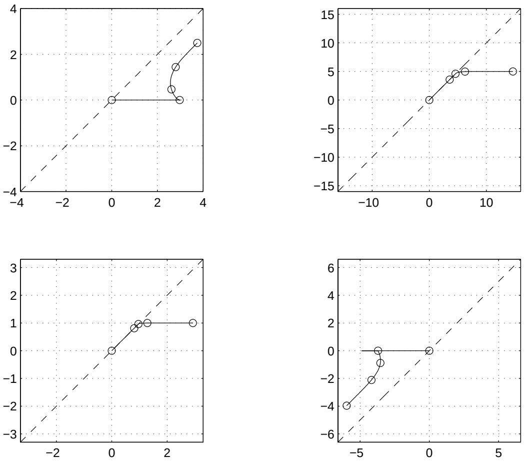

Figure 5.21: *The dynamic RGA of plant P2. Starting at the origin the circles indicate t = 0, 5, 10, 20 and 100 time units.*

$y = 0$ *during the first five time units*. The off-diagonal elements only move away from $y = x$ *after ten time units*. So the static RGA prefers diagonal pairing but the dynamic RGA clearly prefers off-diagonal pairing.

5.5.4 Discussion

In this section the RGA is seen as a structured way to compare open and closed-loop responses for different pairings. The static RGA was extended to include the dynamics of the plant based on the assumptions that:

- A unit step response is sufficient to characterize the dynamics.
- The closed-loop response should approach perfect control in a realistic way. This is achieved by IMC.

Rather than taking the quotient of the open and closed-loop responses, as done in the static RGA, the open and closed-loop responses are compared by means of a graph. In such a graph every time instant is a point with the closed-loop step response being the x-coordinate and the open-loop step response being the y-coordinate. For each possible pairing a graph is produced and placed in an array. This dynamic array is completely consistent with the static RGA (each value of the static RGA agrees with one point in each graph of the dynamic RGA).

From the two examples in this article it is clear that the approach described above works. The dynamic RGA provides extra and useful information in case that:

- The static RGA prefers the wrong pairing (for systems containing time delays, right half plane zeros or large differences in time constants).
- The static RGA does not prefer any pairing (when all elements have more or less the same value).

For 2x2 systems the approach is straightforward in the sense that the calculations (the IMC design) can be done manually. However for larger systems it is advisable to do the calculations by dedicated software (e.g. Matlab). Since the dynamic RGA is an extension of the static RGA an acceptable static RGA remains a necessary condition for an acceptable degree of interaction. So in other words it is a good idea to check the static RGA first.

5.6 Conclusions

Two new methods have been presented that can be used in the analysis phase to help designing more controllable processes:

- closed-loop controllability,
- dynamic interaction analysis.

The most important features of closed-loop controllability are that it can deal with stochastic disturbances and that the analysis is based on the optimal *closed-loop* behaviour of the system. Two alternative methods for considering the economics are presented. In the multi-objective optimization method clear insight in the trade-off between closed-loop variance and economics is gained. However the solution is not a single solution but a set of solutions. The alternative, closed-loop economic optimization, will give only a single solution, but considerable more computation effort is required.

Once one decides that the control system should be based on decentralized controllers, control loop interaction becomes an issue. A novel method has been presented that analysis this interaction in a dynamic way.

Both methods allow an analysis based on the dynamic performance, without unrealistic assumptions on the controllers.

Notation

Roman symbols

A	system matrix
B	system matrix
C	system matrix
CLC	closed-loop controllability
E	expectation
f	differential equations
F	feed rate
g	algebraic equations
G	optimal state feedback gain
$\mathcal{G}$	transfer function
h	output equations

I	identity matrix
J	objective function
$\mathcal{J}$	objective function constraint
K	controller gain
L	Kalman filter gain
$\mathcal{L}$	Laplace operator
M	solution of the regulator Algebraic Riccati Equation
M_l	left coprime factor
N_l	left coprime factor
P	solution of the estimator Algebraic Riccati Equation
$\mathcal{P}$	plant
Q	weighting matrix
R	covariance matrix
s	Laplace variable
t	time
T	total time
tr	trace
u	inputs
w	Gaussian white noise
x	state variables
y	output variables
Y	solution of Lyapunov equation
z	algebraic variables

Greek symbols

δ	disturbances
Δ	plant perturbation
ϵ	stability margin
γ	degree of constraint violation
λ	RGA element
ω	weighting coefficient
ϕ	uncertain parameters
σ	design variables
ς	standard deviation

Subscripts

0	nominal value
cl	closed-loop
d	disturbances
l	lower bound
m	measurement
ol	open-loop
p	process
u	inputs
u	upper bound
x	states

Superscripts

$\hat{}$	model
-1	inverse
T	transpose

6

Application: Fischer Tropsch synthesis reactor

In the previous chapters two complementary approaches have been developed for the design of processes with improved controllability. These approaches can be applied to the successive synthesis and analysis phases of the design process. In this chapter the applicability of these approaches will be demonstrated using Fischer Tropsch synthesis as case study. The controllability implications of a novel reactor type will be investigated: a monolithic reactor. Both methods consistently suggest that a large reactor, with a high single pass conversion, is desirable for a disturbance sensitivity point of view

6.1 Introduction

In the previous chapters two complementary approaches have been developed for the design of chemical processes with improved controllability characteristics. In chapter 4 a new method has been presented for considering disturbance sensitivity in the synthesis phase. The design alternatives are generated using the design guidelines developed with the Thermodynamic Controllability Assessment method (TCA). In chapter 5 novel methods for controllability analysis have been presented: (robust) closed-loop controllability and dynamic interaction analysis. In this chapter these approaches will be applied to a case study: the design of the reaction system for Fischer Tropsch synthesis. First an introduction on Fischer Tropsch synthesis is presented. Then alternative designs will be presented, all based on a novel reactor concept: a monolithic Fischer Tropsch synthesis reactor (De Deugd et al., 2002a). Since this is a new, unproven, reactor concept for Fischer Tropsch synthesis, no knowledge exists on the operational behaviour of the system. Therefore a controllability study can assist significantly in the development of the reactor system. In section 6.4 the driving forces and flows in the alternative designs are analysed and the controllability implications will be presented. In section 6.5 the novel controllability analysis tools will be applied to the alternative designs.

6.2 The Fischer Tropsch synthesis

6.2.1 Background of the Process

The conversion of natural gas to hydrocarbons is one of the most promising technologies in the energy industry today. Natural gas can be converted into high quality transportation fuels, specialty chemicals and waxes. The Fischer Tropsch synthesis (FTS) is a process that converts synthesis gas, a mixture of H_2 and CO, into straight chain hydrocarbons. The synthesis gas can be produced out of natural gas, coal or biomass. The Fischer Tropsch synthesis process has originally been developed in the early 1900s. Nowadays the process has regained industrial interest. The main reasons for this are:

- the products of the Fischer Tropsch synthesis are sulphur free
- the process enables one to utilize associated gas from oil fields and remote gas sources via gas to liquid technology

- it provides the possibility to use natural gas, coal and biomass for transportation fuels.

Knott (1997) gives on overview of commercial Fischer Tropsch synthesis activities and sketches some interesting future commercial developments.

6.2.2 FTS Process Characteristics

The Fischer Tropsch synthesis (FTS) is a highly exothermic reaction which produces mainly straight-chain paraffines. The reaction mechanism can be seen as a stepwise addition of one carbon segment to the chain. It is generally assumed that the ratio between chain growth probability and termination probability is independent of the chain length. This mechanism, shown in Figure 6.1, leads to a product distribution that can be described with the Anderson-Flory-Schulz (ASF) distribution (Sie, 1998):

$$M_n = \alpha^{n-1}(1-\alpha) \tag{6.1}$$

where M_n is the molar fraction in the product with a chain length of n, n is the chain length and α is the chain growth probability that is independent of the chain length. For modern Fischer Tropsch synthesis processes α is in the range 0.92 - 0.98.

The overall stoichiometry of the reactions in the Fischer Tropsch synthesis process can be represented by:

$$2\mathrm{H}_2 + \mathrm{CO} \rightarrow (1-\alpha)\mathrm{CH}_4 + (1-\alpha)\alpha\mathrm{C}_2\mathrm{H}_6 + (1-\alpha)\alpha^2\mathrm{C}_3\mathrm{H}_8 + \ldots + \mathrm{H}_2\mathrm{O}\,. \tag{6.2}$$

The reaction enthalpy for this overall reaction is 170 KJ/mol syngas. Typical process conditions are a temperature of 200°C - 240 °C and a pressure of 20 bara - 35 bara.

Reactor Concepts for Fischer Tropsch synthesis Commercial gas to liquid technology involve three main sections: synthesis gas production, Fischer Tropsch synthesis and product up-grade. The syngas production technologies and the hydrocracking technology for FT product grade-up are well established technologies. The bottleneck for making the entire GTL process profitable is the FT reactor technology. Many of the known reactor types have been exploited for the FT synthesis, with according to Krishna and Sie (2000) the most promising being

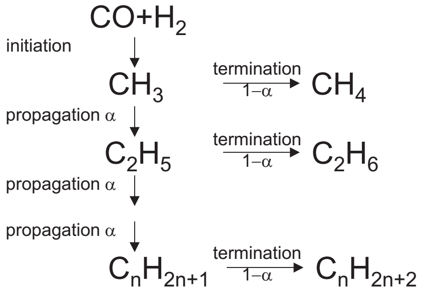

Figure 6.1: *Simplified reaction mechanism for Fischer Tropsch synthesis*

the multitubular trickle bed reactor and the slurry bubble column reactor. Alternative reactor concepts that were not part of the survey are gaslift loop reactors (Ghotage et al., 2002) and monolithic reactors (DeDeugd et al.,2002a,b). Especially the monolithic reactor seems to be attractive for Fischer Tropsch synthesis. In this chapter the controllability of this reactor concept will be studied.

6.3 Reactor section designs

In this section some alternative designs of reactor sections based on monolithic reactor technologies will be presented. In the subsequent sections these designs will be analysed from a controllability point of view using the methodologies developed in the previous chapters.

6.3.1 Basis of Design

Capacity The plant capacity should be 2 million tonnes per annum (MTPA) [69.4 kg/s] of middle distillates (kerosene, diesel and naphtha). Van Asperen et al. (1999) calculated that ultimately 92% of the carbon ends up in the product. This implies that for a required capacity of 2 MTPA product, the reactor section needs to be designed for 2.2 MTPA. According to Van Asperen et al. (1999) the mass yield of the total process is 38.1%. This implies that 5.7 MTPA synthesis gas is required. Assuming 8000 stream hours a year this corresponds with a syngas consumption of 18.6 kmol syngas/s with a H_2/CO ratio of 2.0.

Battery limits The battery limits of the reaction section designed are shown clearly in the block diagram (Figure 6.2). The only stream entering the battery limits is the fresh synthesis gas. This stream is to be delivered at a pressure 30 bara with a temperature of 240°C . The nominal value of the H_2/CO ratio is 2. Three streams leave the battery limits: product stream containing middle distillates, the water product and the purge. The product stream and the water stream should be delivered as liquids at a pressure of 25 bara and a temperature of 35°C . The purge stream should be delivered as a gas at a pressure of 25 bara and a temperature of 25°C .

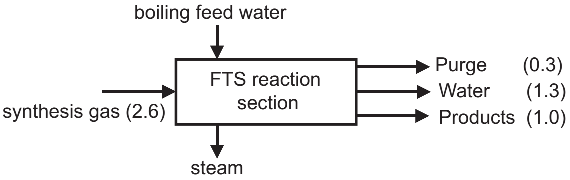

Figure 6.2: *Input-output diagram of the reaction section, values between brackets are flows in tn/tn product.*

Catalyst For the catalyst there are two major options: an iron based or a cobalt base catalyst (Sie, 1998). In this design a cobalt based catalyst is used. The product distribution of the selected catalyst can be described by the ASF distribution with $\alpha = 0.95$.

Control objectives The two main variables to be controlled are the temperature and the conversion at the outlet of the reactor. In our analysis we will use the gas phase hydrogen concentration as indicator for the conversion. This leads to the following controlled variables: the hydrogen conversion and the temperature at the end of the reactor. The throughput is considered to be determined by an upstream unit.

Disturbance variables The disturbance variables considered are the inlet gas temperature and the inlet synthesis gas inlet composition. The disturbance in the inlet gas composition is modelled as a disturbance in the inlet H_2 fraction. The disturbances are scaled such that a temperature deviation of 1°C counts equally as a disturbance in the inlet H_2 fraction of 3%.

6.3.2 Major design decisions

As already stated before, the selected reactor type is a monolithic reactor. A monolith is an example of a structured catalyst. The main advantages of this reactor type are the plugflow behaviour, the low pressure drop and the efficient mass transfer. Moreover no solid-liquid separation is required to separate the catalyst particles from the liquid product.

The monolithic reactor will operate adiabatically. Therefore a liquid recycle is required that can serve as a heat sink, preventing extreme temperature rises. An external heat exchanger should be installed in the liquid recycle to remove the heat produced.

The desired flow regime in the monolithic channels is Taylor flow (Kapteijn et al., 1999). Gas bubbles and liquid slugs flow co-current through the channels. Only a thin liquid film separates the gas from the catalyst leading to fast gas/solid mass transfer. The liquid slugs show internal recirculation during the transport through the channels. This flow regime is shown schematic in Figure 6.3.

6.3.3 Conceptual design of reactor section

The basic process flowsheet for a reactor system with a monolithic reactor is shown in Figure 6.4. Part of the liquid effluent of reactor R1 is cooled in E1 and then recycled back to the reactor feed, such that the right flow-regime is maintained in the reactor. The gas-liquid reactor effluent is cooled and partially condensed in E2 and feed to a gas/liquid/liquid separator, V2. Part of the gasflow out of the separator is recycled back to the reactor. The remaining part is purged.

6.3.4 Reactor Model

For the monolithic reactor model as presented by De Deugd et al. (2002a) is used. The model assumes all channels to be identical. The model consists of two

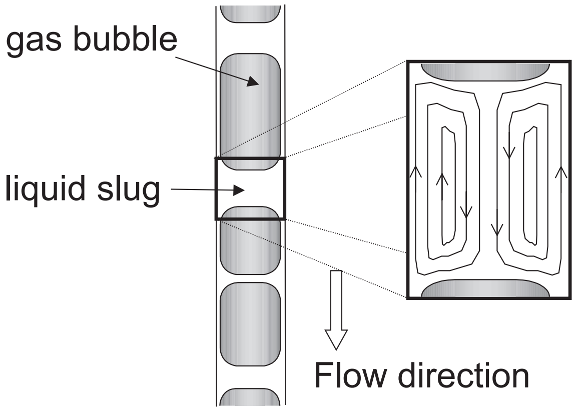

Figure 6.3: *Schematic representation of the Taylor flow regime. (Taken from Kapteijn et al., 1999)*

parts. The first part describes the hydrodynamics of the two phase stream in the reactor. The second part describes the diffusion and reaction between reactants and products inside the catalyst layer.

The hydrodynamics are distributed in axial direction only (z-direction), such that $z = 0$ corresponds with the feed location. Both the liquid and vapour phase are described as pure plug flows. The gas phase component balances are given by:

$$\epsilon_g \frac{\partial c_{i,g}}{\partial t} = -\frac{\partial u_g c_{i,g}}{\partial z} - k_{gl} a_{gl} (c_{i,g} \frac{1}{m_i} - c_{i,l}) - k_{gs} a_{gs} (c_{i,g} \frac{1}{m_i} - c_{i,s}) \tag{6.3}$$

with boundary conditions:

$$c_{i,g}(t,0) = c_{i,g,0} \tag{6.4}$$

where ϵ_g is the volumetric gas fraction, $c_{i,g}$ is the gas phase concentration of component i, u_g is the superficial gas velocity, k_{gl} is the gas/liquid mass transfer coefficient, a_{gl} is the transfer area per unit length, k_{gs} is the gas/solid mass transfer coefficient, a_{gs} the corresponding transfer area, m_i are the distribution coefficients and $c_{i,g}(t,0)$ are the gas phase concentrations at $z = 0$.

The mass transfer was modelled with the relations presented by Kreutzer et al. (2002).

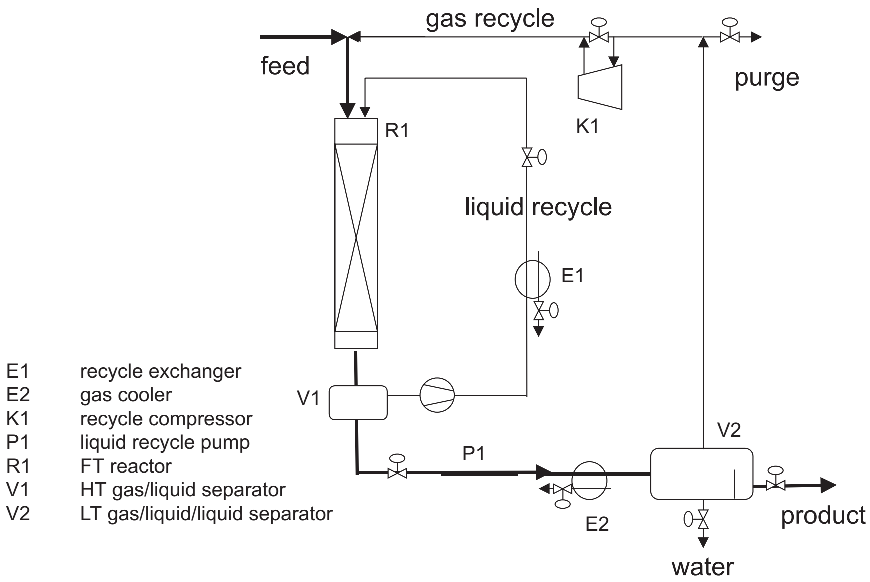
gas recycle
feed
purge
K1
R1
liquid recycle
E1
E1 recycle exchanger
E2 gas cooler
K1 recycle compressor
P1 liquid recycle pump
R1 FT reactor
V1 HT gas/liquid separator
V2 LT gas/liquid/liquid separator
V1
V2
P1
E2
product
water

Figure 6.4: *Basic concept of the reaction section for Fischer Tropsch synthesis*

The liquid phase component balances are given by:

$$(1-\epsilon_g)\frac{\partial c_{i,l}}{\partial t} = -u_l\frac{\partial c_{i,l}}{\partial z} + k_{gl}a_{gl}(c_{i,g}\frac{1}{m_i} - c_{i,l}) - k_{ls}a_{ls}(c_{i,l} - c_{i,s}) \tag{6.5}$$

with boundary conditions:

$$c_{i,l}(t,0) = c_{i,l,0} \tag{6.6}$$

The heat balance is set-up with the assumption that the heat capacity of the liquid phase is much larger then the heat capacity of the gas phase. No heat transfer limitations are assumed to exist between the various phases:

$$(1-\epsilon_g)\frac{\partial T}{\partial t} = -u_l\frac{\partial T}{\partial z} + \frac{\Delta H_{reaction}}{\rho_l cp_l} r_{syngas} \tag{6.7}$$

with boundary conditions:

$$T(t,0) = T_0 \tag{6.8}$$

where T is the temperature, $\Delta H_{reaction}$ is the heat of reaction, ρ_l is the liquid density and cp_l is the liquid phase heat capacity. The momentum balance is modelled static:

$$\frac{dp}{dz} = \frac{-4F\frac{1}{2}u_{tp}^2\rho_l}{d_h} + (1-\epsilon_g)\rho_l g - 2(1-\epsilon_g)\rho_l u_{tp}\frac{du_{tp}}{dz} \tag{6.9}$$

where u_{tp} is the sum of the superficial liquid velocity and the superficial gas velocity. The superficial liquid velocity is assumed to be constant over the monolith, leading to the following boundary condition:

$$u_{tp}(t,0) = u_l(T) + u_g(t,0) \tag{6.10}$$

The diffusion inside the catalyst is modelled in the radial direction (y-direction), such that $y = 0$ corresponds with the inside of the catalyst and $y = L_c$ with the catalyst-liquid interface. The transport of reactants and products through the catalyst is described using Fickian diffusion. Diffusion coefficients have been estimated from the method defined by Wilke and Change (1955). The relation to correct the diffusion coefficients in the catalyst layer for the restriction of the pores is taken from De Jong et al. (1998). The catalyst layer thickness is about $100\mu m$. With diffusion coefficients in the order of 10^{-8}m^2/s, the dynamics of this diffusion can be neglected compared to the dynamics of the hydrodynamics. This part of the system is hence modelled with steady-state balances. The component balances are given by:

$$\frac{D_i}{\mathcal{L}_c^2}\frac{d^2 c_{i,layer}}{dy^2} = \nu_i r_{syngas}\rho_s, \tag{6.11}$$

with the boundary condition:

$$\frac{dc_{i,layer}(0)}{dy} = 0 \tag{6.12}$$

where D is the diffusion coefficient, $\mathcal{L}_c$ is the thickness of the catalyst layer, y is the radial direction and ν_i is the stoichiometric coefficient.

At the catalyst layer-channel interface the flux of reactant and products to and from the catalyst layer is equal to the sum of gas-solid and liquid-solid mass transfer:

$$D_i \left.\frac{dc_{i,layer}}{dy}\right|_{y=\mathcal{L}_c} = k_{ls}\epsilon_g(c_{i,l} - c_{i,s}) + k_{gs}(1-\epsilon_g)(c_{i,sat} - c_{i,s}) \tag{6.13}$$

The temperature exchange between the catalyst phase and the liquid phase is assumed to be instantaneous, leading to equal temperatures in the catalyst and the liquid phase.

The kinetics are described with the relation presented by Yates and Satterfield (1991) with the temperature dependency as presented by Maretto and Krishna (1999):

$$\begin{aligned} r_{syngas} &= \frac{v p_{\mathrm{H_2}} p_{\mathrm{CO}}}{(1 + w p_{\mathrm{CO}})^2} && (6.14) \\ v &= 8.8533 * 10^{-3} exp\left(4494.41\left(\frac{1}{493.15} - \frac{1}{T}\right)\right) && (6.15) \\ w &= 2.226 exp\left(-8236\left(\frac{1}{493.15} - \frac{1}{T}\right)\right) && (6.16) \end{aligned}$$

where the reaction rate is given in $mol s^{-1} m^{-3}$.

The change in Gibbs energy of formation of the overall Fischer Tropsch synthesis reaction is calculated by:

$$\Delta G^o_{f,r} = \Sigma G^o_{f,i} \nu_i. \tag{6.17}$$

The values of the Gibbs energy of formation of the individual components under standard conditions are taken from the ASPEN Plus database. This leads to a Gibbs energy of formation at 298K of -90 KJ/mol CO. The dependence of the Gibbs energy of formation on the temperature is given by (Smith and Van Ness, 1987):

$$\frac{d(\Delta G/RT)}{dT} = \frac{-\Delta H}{RT^2} \tag{6.18}$$

Using the heat of reaction of the Fischer Tropsch synthesis the change in Gibbs energy of formation at the reaction temperature can be calculated. De Swart (1996) states that the heat of reaction for Fischer Tropsch synthesis is 170 kJ/mol at 220 °C . Application of equation 6.18 gives the change of Gibbs energy of formation at 220 °C , $\Delta G_f(220°C) = -260 kJ/mol\mathrm{CO}$.

The equilibrium constant of chemical reactions is defined by:

$$lnK = \frac{-\Delta G}{RT}, \tag{6.19}$$

where K is the equilibrium constant. So at 220 °C , $lnK = 63.4$. Hence one can conclude that the equilibrium of the Fischer Tropsch synthesis reaction is on the far right of equation 6.2.

6.3.5 Remaining design variables

The structure of the process has already been determined. The remaining design variables are the continuous design variables. The main design variables in this reaction system are the single pass conversion, the gas cooling temperature, the gas purge and the pressure. The geometric design variables reactor length and diameter are determined by the single pass conversion and the capacity respectively.

The gas cooling temperature determines the H_2 and COrecovery in the gas/ liquid/liquid separator. In order to have a high recovery, the temperature was set at the lowest temperature that can be achieved with cooling water, 35°C .

The gas purge is set at the value leading to a hydrogen loss of 2% of the fresh feed.

The pressure is set at 30 bar, corresponding to a typical value for Fischer Tropsch Synthesis.

This leaves the single pass conversion to be the key design variable. The single pass conversion is influenced by the reactor length. Six alternative designs have been made with varying reactor lengths. Table 6.1 shows the most important variables for the various designs. Typical profiles for the COconversion and the temperature over the reactor are shown in Figures 6.5 and 6.6. The calculations are based on reactor A. In the next section the TCA method, developed in

Table 6.1: *Alternative reaction section designs.*

design	**reactor length [m]**	**single pass conversion [%]**	**temperature rise [°C]**	**reactor gas capacity [kmol/s]**
A	15	36.8	9.1	59.7
B	18	49.0	11.4	45.5
C	21	61.5	14.7	35.3
D	24	73.5	17.6	28.1
E	27	82.5	19.5	24.4
F	30	88.2	20.8	22.2

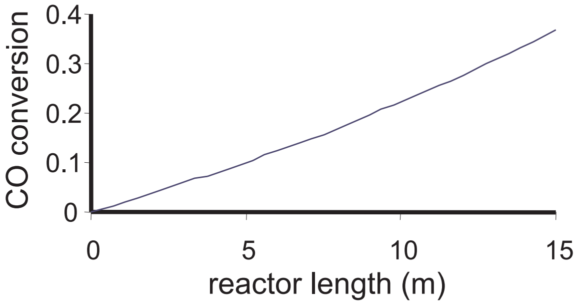

Figure 6.5: CO*Conversion as a function of the reactor length*

Chapter 4, will be applied to determine the optimal design from a controllability point of view. Then this will be validated using the closed-loop controllability index developed in Chapter 5.

6.4 Application of the TCA method

In Chapter 4 it was shown how the relation between the driving forces and flows in the system are related to controllability properties, and how this can be used in the synthesis phase to obtain better controllable processes. In order to apply this method on the Fischer Tropsch synthesis reactor, one first needs to identify all physico-chemical phenomena occurring in the reactor. Magnetic and electric phenomena are not likely to be relevant. Moreover entropy production due to friction is neglected. So the only phenomena that need to be analysed are heat transfer, mass transfer and chemical reaction.

Heat transfer The reactor is operated adiabatically. In the radial direction there is no thermal gradient. In the axial direction there is a thermal gradient. If design F of Table 6.1 is considered, the thermal gradient is $2.5 * 10^{-6} K^{-1} m^{-1}$. A typical value of the heat conductivity coefficient, κ, for liquids is $0.1 W m^{-1} K^{-1}$. The phenomenological constant for heat transfer is then given by:

$$L = \kappa T^2 = 0.1 * 518^2 = 2.7 * 10^4 W K m^{-1} \tag{6.20}$$

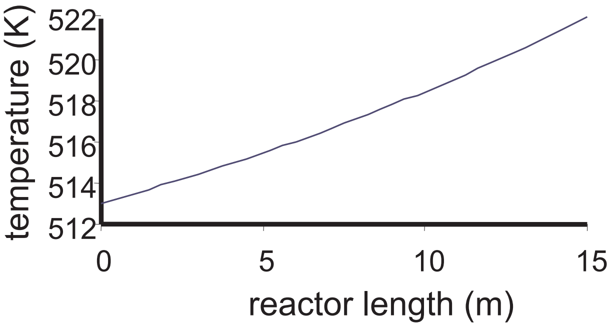

Figure 6.6: *Temperature as a function of the reactor length*

So the heat flux is $0.070 J s^{-1} m^{-2}$. Hence the entropy production due to heat transfer is extremely small. Therefore the heat transfer is neglected in our non-equilibrium analysis for control.

Mass transfer In the system there are various diffusion flows: from the gas phase to the catalyst, from the gas phase to the liquid phase, from the liquid phase to the catalyst and inside the catalyst. The Fischer Tropsch synthesis process is reaction rate limited. Therefore all gradients in chemical potential in radial direction will be very small. The diffusive flow in radial direction however cannot be neglected. The overall diffusive flow from the gas phase (via the liquid phase) to the catalyst is equal to the overall reaction rate. However because of the small driving force the contribution to the entropy production is negligible.

Just like the heat transfer, the conductive mass transfer in the axial direction can be neglected compared with the convective flow in the system.

Chemical Reaction Chemical reaction is the essential task of the reactors. Alternative reactor systems should convert the same amount of reactants to products. So the overall flow is specified. The driving force for chemical reaction is given by:

$$X = \frac{A}{T} = \frac{\sum \mu_i \nu_i}{T} \tag{6.21}$$

This driving force is in principle a locally defined property. However De Deugd et al., (2002a) have shown that the composition in the catalyst phase a rather constant. This justifies our assumption that the driving force is independent of the radial position.

Driving Force in Fischer Tropsch synthesis For an ideal component the chemical potential at an arbitrary temperature, T, and pressure, p, is given by:

$$\mu_i(p,T) = G_i + RTln(a_i) \tag{6.22}$$

where G_i is the Gibbs energy of formation of component i and a_i is the activity of component i. For an ideal gas this leads to:

$$\mu_i = G_i^{ig} + RTln(y_i) = G_i^{ig} + RTln\left(\frac{p_i}{p}\right) \tag{6.23}$$

For an ideal solution this leads to:

$$\mu_i = G_i^{il} + RTln(x_i) \tag{6.24}$$

So the driving force for chemical reaction is given by:

$$X = \frac{\Delta G^o_{f,r} + R \sum\limits_{gasphase} ln\left(y_i^{\nu_i}\right) + R \sum\limits_{liquidphase} ln\left(x_i^{\nu_i}\right)}{T} \tag{6.25}$$

In the case of Fischer Tropsch synthesis the process is a gas/liquid phase process. Part of the products will predominantly be in the liquid phase. For simplicity it will be assumed that all components up to C_{10} are only present in the gas phase, and all heavier components are only present in the liquid phase.

Under these conditions the liquid phase composition is independent of the conversion. The liquid mole fraction of component i is given by:

$$x_i = \frac{\nu_i}{1 - \sum\limits_{j=1}^{10} \nu_j} \tag{6.26}$$

Leading to:

$$R\Sigma ln\left(x_i^{\nu_i}\right) = -19.3kJ/mol \tag{6.27}$$

In contrast with the liquid mole fractions, the gas mole fraction are a function of the conversion. The partial pressures of the products are given by:

$$p_i = \frac{\nu_i}{\sum\limits_{j=1}^{10} \nu_j} \xi_{CO} p_{CO_0} \tag{6.28}$$

where ξ is the conversion, and p_{CO_0} is the initial partial pressure of CO.

Figure 6.7 shows the resulting driving force as a function of the conversion. The characters refer to the end point conditions of the designs presented in Table 6.1. From this Figure one can easily conclude that the average driving force decreases with increasing single pass conversion. In Chapter 4 it was showed that for a flow specified process a small (average) driving force is beneficial from a disturbance sensitivity point of view. Since the Fischer Tropsch synthesis reactor is flow specified, a long reactor, so a large single pass conversion, is preferred from a controllability point of view.

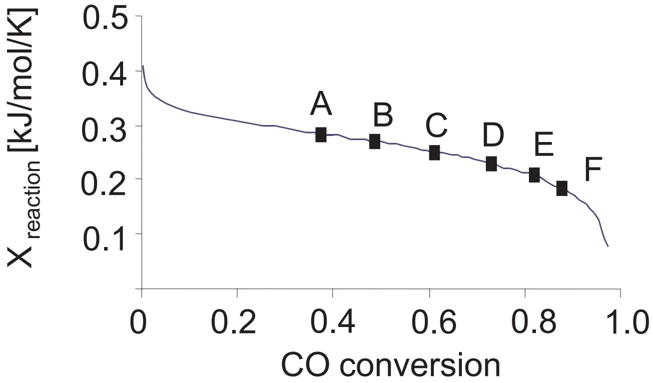

Figure 6.7: *Driving force for reaction as a function of* CO*conversion*

In the next section this result based on TCA design rules will be compared to the results of a controllability analysis method.

6.5 Controllability analysis

6.5.1 Setting up the problem

In principle the closed-loop controllability analysis can be applied on the entire reactor section. However for practical reasons it was decided to decompose the system, as shown in Figure 6.4, in the reactor (with the liquid recycle) and the gas recycle and only analyse the closed-loop controllability of the reactor, shown in Figure 6.8. This can theoretically be justified since the faster time constant of the gas recycle is much larger than the dominant time constant of the reactor.

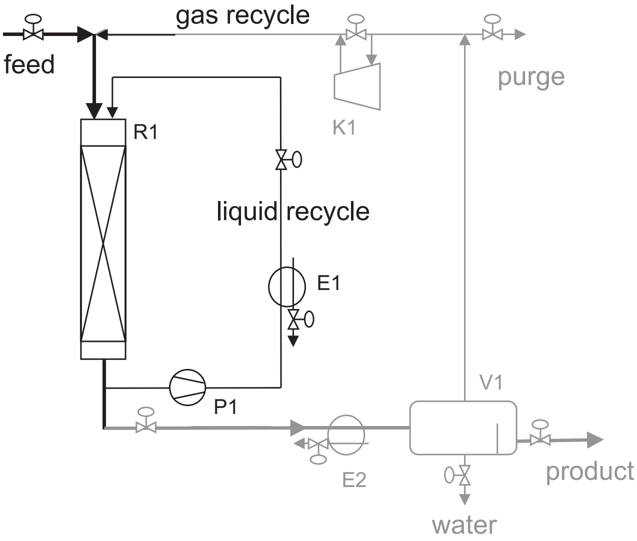

Figure 6.8: *Reactor system considered in the closed-loop controllability analysis*

Determine the Control Degrees of Freedom The control degrees of freedom can easily be determined by counting the number of control valves (Luyben et al., 1999). In this system there are two control valves: the liquid recycle flowrate and utility flowrate in the heat exchanger. The liquid recycle temperature can be controlled by the cooling medium flowrate flowing through E1. We assume that this temperature is directly available as manipulated variable. The manipulated variables are scaled such that a change in the liquid flowrate of 5% counts equally as a change of the liquid temperature of 1°C .

6.5.2 Computational Steps

All designs presented in Section 6.3 were modelled with the full non-linear DAE model presented in Section 6.3.4. This DAE model is automatically discretized in the spatial directions by gPROMS, leading to a DAE system. For the Fischer Tropsch synthesis reactor systems this leads to DAE systems with 196 differential equations and 1208 algebraic equations. For the closed-loop controllability analysis a linear(ized) model is required. This model is obtained by applying the following steps on the DAE model

step 1 The system is linearized around it's steady-state operation point. This linearization is carried out using the gPROMS build-in function LINEARIZE (gPROMS, 2002). This leads to a linear system that can be described with the standard state space description, with 196 state variables.

step 2 In order to calculate LQG controller function of reasonable dimensions, first model reduction techniques are applied on the linear models. The model reduction technique applied is Optimal Hankel norm approximation (Skogestad and Postlethwaite, 1996). The reduced order of the systems is 30. The model reduction is carried out in MATLAB.

step 3 The reduced models are augmented with Filter models, as described by equation 5.6.

step 4 The closed-loop variance is calculated according to the procedure presented in Chapter 5.

6.5.3 Results

The only somewhat arbitrary decision that needs to be made before the closed-loop variances can be calculated are the weighting matrices Q_u and Q_y used in the design of the LQG controller. In all situations we decided to use diagonal matrices where all inputs are weighted equally and all outputs are weighted equally. The weighting matrices can then be represented by:

$$Q_u = \lambda_u I, \tag{6.29}$$

$$Q_y = \lambda_y I, \tag{6.30}$$

where λ_u and λ_y are scalars and I is the identity matrix. To study the influence of the relative weight of the outputs compared to the inputs, we calculated J for

$\lambda_u = \lambda_y = 1$, $\lambda_u = 5\lambda_y = 1$ and $5\lambda_u = \lambda_y = 1$. Figure 6.9 shows the closed-loop variance as a function of the reactor length for the three different tunings. For all three tunings the results have been normalized such that the reactor with a length of 15 m has a closed-loop variance of 1. Figure 6.9 clearly shows that the closed-loop variance is better for longer reactors. This trend is independent of the tuning. So a reactor with a high single pass conversion is preferred from a closed-loop controllability point of view. This confirms the findings of the TCA method

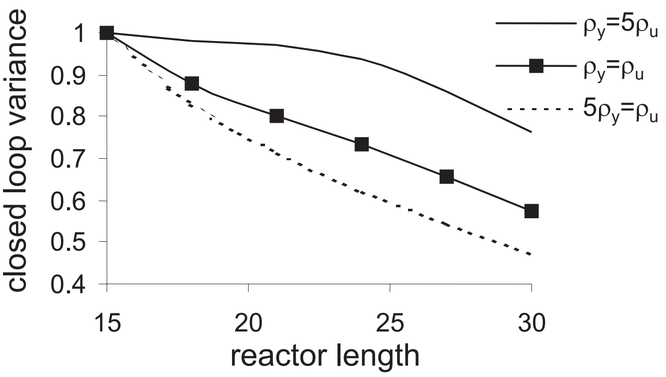

Figure 6.9: *Closed-loop variance as a function of the reactor length*

6.6 Conclusions

The non-equilibrium thermodynamic approach and the closed-loop controllability measure have been applied to the case study introduced in this section: Fischer Tropsch synthesis. With little input information available already quite a detailed non-equilibrium thermodynamic model of the process could be made. With this one can easily conclude that a long reactor, with a high single pass conversion, is desirable from a controllability point of view.

This conclusion was validated using closed-loop controllability calculations.

These calculations were based on a realistic dynamic model of the system. The conclusions of this validation fully supported the design statements based on non-equilibrium thermodynamics.

Notation

Roman symbols

A	chemical affinity
a	interfacial area
c	concentration
cp	heat capacity
d	diameter
D	diffusion coefficient
F	friction factor
G	Gibbs energy
H	enthalpy
K	equilibrium constant
k	mass transfer coefficient
L	phenomenological constant
$\mathcal{L}$	catalyst layer thickness
M	mole fraction
m	distribution coefficient
p	(partial) pressure
Q	weighting matrix
R	gas constant
r	reaction rate
T	temperature
t	time
u	velocity
v	reaction rate variable
w	reaction rate variable
X	driving force
x	mole fraction in vapour phase
y	mole fraction in liquid phase
z	spatial coordinate

Greek symbols

α	chain growth probability
ϵ	fraction
κ	heat conductivity coefficient
λ	tuning parameter
μ	chemical potential
ν	stoichiometric coefficient
ξ	conversion
ρ	density

Subscripts

g	gas phase
gl	gas-liquid
gs	gas-solid
i	component i
l	liquid phase
ls	liquid-solid
n	carbon number
u	inputs
y	outputs

7

Integrated design of a periodic operating Fischer Tropsch synthesis process[†]

A significant improvement of the performance of processes can sometimes be obtained by the integrated design of a process with its operational policy. In this Chapter an integrated design problem for a periodically operated process is presented. This problem gives rise to a dynamic optimization problem. The solution yields the optimum combination of process design (structure and sizing) with the periodic trajectories. The integrated design is carried out for a periodically operated Fischer-Tropsch synthesis reaction. The model is isothermal. The results shows that with this approach the diesel selectivity can be increased from 38 % (in optimized steady state operation) to 52 %. The robustness of this solution with respect to model uncertainties and simplifications still needs further investigation.

[†] Parts of this Chapter have been published by De Deugd et al. (2001) and Meeuse et al. (2001)

7.1 Introduction

The integrated design of a process system involves the designs of its main interacting constituents: the operational policy, the process and the control. As outlined in Chapter 3 of this thesis making the designs simultaneously is usually too demanding (with the current state-of-the-art in modelling and computing). In industrial practice the design is often decomposed in three sequential design steps with iterative passes between these designs to achieve feasible solutions. The preceding chapters in this thesis focused on methods to achieve a better integration between the process and the control designs. Controllability was explicitly addressed in the process synthesis and analysis stages of the process design as to create favourable conditions for the design of a well functioning control system. No attempt was made to include the operational policy in this design process as well. It was assumed that the plant is operating in some steady state mode and that the control system should be capable of rejecting the influences of disturbances. The potential economic gain from the joint designs of a process and the operational policy was not exploited. Yet, it is known that dynamic modes of operation for a continuous plant can bring significant benefits.

This Chapter will deal with the integrated design of continuous processes with a particular class of dynamic behaviour: periodic operation. In a periodic operated process one or more manipulated variables are forced to follow a trajectory in time. Two types of periodic processes can be distinguished. One type is of the ”action-regeneration” type, where the operation alternates between two stages. In the first stage the process is in a steady production action, but gradually deposits are being built up (with rather slow dynamics) till a saturation point. These deposits are removed in a regeneration stage of relatively short duration, in which production is suspended. The combination of an active and a regeneration stage form the period of the process (e.g. regeneration of thermal cracking furnaces). This type of periodic operation is not considered in this Chapter. The focus is on the other type of periodic operation, in which production is continuous but transient with periodic repetition of the processing conditions by external forcing. An example in this class of periodic operation is the reverse flow reactor. The incentive for this type of periodic operation is that the transient operated process can have larger time averaged product yields than possible for the optimized steady state operation. This phenomenon is called resonance (Van Neer, 1999). Silverston et.al. (1995) and Stankiewicz and Kuczynski (1994) have presented overviews of processes that benefit from periodic operation.

In contrast to steady state continuous processes, very little has been published about model based process design for periodic operated continuous processes, where both the process and the periodic operation are treated simultaneously. For a given design of a process for periodic operation, finding the optimum control reference signals leads to a so-called optimum control problem. When the process is designed simultaneously with the control reference signals to find an time averaged optimal performance, additional degrees of freedom appear relative to the design of the process. So, the integrated design of the process and the control reference signals leads to dynamic optimization problems.

The control reference signals define the optimal periodic operations. However, it should be noticed that this integrated design of process and periodic operations does not account for the presence of disturbances that might detract the process from the optimal trajectories. In the sequential design approach the second phase of design should consider whether to adapt the process design to achieve sufficient controllability for disturbance reduction along the optimal periodic trajectories. The issue of design for controllability for transient operation is not covered in this thesis. It is an increasingly relevant problem for batch, periodic and mode switch operations, but the research on this topic is still in its infancy.

The Fischer Tropsch synthesis reaction is a system that can potentially benefit from periodic operations. The process models which are presented in section 7.3, form the basis for the integrated design problem as formulated in section 7.4. Then the solution approach to and the results of the integrated design of the periodically operated Fischer Tropsch synthesis reaction will be presented and analysed.

7.2 Periodic operation of Fischer Tropsch synthesis

The Fischer Tropsch synthesis was already introduced in Chapter 6. The process converts synthesis gas into straight chain hydrocarbons. Nowadays there is substantial industrial interest in the process. The main reasons for this are:

- the products of the Fischer Tropsch synthesis are sulphur free
- the process enables one to utilize associated gas from oil fields and remote gas sources via gas to liquid technology

- it provides the possibility to use natural gas, coal and biomass for transportation fuels.

By static operation, the maximum achievable selectivity towards diesel is 38 %. Several alternative methods are available to increase this selectivity. In the Shell Middle Distillates Synthesis process (SMDS) the diesel fraction is increased by first producing predominantly heavy products that are subsequently hydro-cracked into the desired product spectrum (Sie, 1998). Figure 7.1 gives a block diagram of the resulting process.

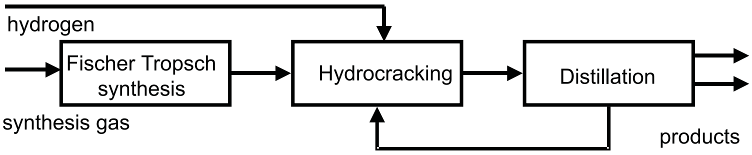

Figure 7.1: *Simplified flow-scheme of the SMDS process.*

An alternative way would be to increase the selectivity by dynamic operation. The basic idea is to periodically switch between a feed with a low hydrogen/carbon monoxide ratio and a feed with a high hydrogen/carbon monoxide ratio. During the low ratio period predominantly chain growth takes place, while the high ratio is in favour of chain termination.

In the literature some indications can be found that periodic operation indeed has an influence on the product distribution of the Fischer Tropsch process, but no work in the field of optimizing the diesel fraction, or model based studies for this process were found. Adesina et al. (1995) presents an overview of the experimental work on periodic operation of Fischer Tropsch synthesis. The recent work of Nikolopoulos et al. (2001) indicates that especially the diesel fraction (C_{10}-C_{20}) can be increased by periodic operation.

Van Neer (1999) has investigated the requirements for resonance in catalytic processes. Two phenomena for catalytic processes that are sufficient to obtain such resonance phenomena are presented:

- The sorption behaviour of the forced reactant must be at least as fast as the sorption of the other reactant involved.

- The surface of the catalyst has to be almost totally occupied at steady-state in the considered concentration range.

Since the two conditions mentioned above are satisfied in the Fischer Tropsch synthesis process it is expected that a higher selectivity can be obtained by dynamic operation. In this work the possibilities for increasing the diesel selectivity are investigated based on a model based dynamic optimization approach.

7.3 Process Model

The modelling consists of two parts: the kinetic model and the reactor model.

Kinetic model In the literature there is no general consensus about the reaction mechanism. All the reactions modelled are shown in the mechanism shown in Figure 7.2. This model consists of molar balances for paraffins and olefins up to C21. All heavier components are lumped into a heavy fraction. It is mainly

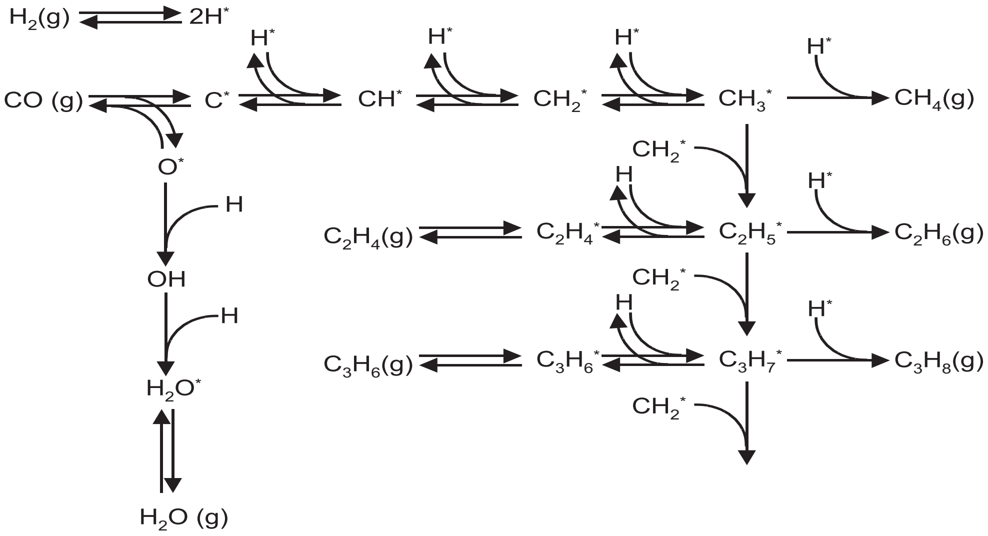

Figure 7.2: Reaction mechanism.

based on the work of Dry (1996) and Van der Laan (1999). Hydrogen and carbon monoxide adsorb dissociatively on the catalyst surface. The oxygen reacts in two steps to water. The adsorbed Carbon reacts with the adsorbed hydrogen to the carbide intermediate that serves as building block. Chain growth occurs due to the reaction of the adsorbed chain with the adsorbed carbide building block. Termination occurs either to paraffins or olefins.

Kinetic parameters For the kinetic model two types of parameters are required: rate constants and surface coverage fractions of the various components. In the literature no complete set of parameters for this model can be found. Therefore the estimation of parameters for this model is a combination of various literature sources. A detailed description of all parameters with their numerical value is presented in De Deugd et al. (2001).

Reactor network model Feinberg and Hildebrandt (1997) showed that the only reactor types required to access all possible compositions for a given reaction mechanism are the plug flow reactor, the CSTR reactor and differential side stream reactors. For simple reaction mechanisms heuristics exists that guide the designer to the optimal reactor from a conversion or selectivity point of view. For more complex reactions, the reactor configuration can be found by superstructure optimization.

In this work we modelled both the plug flow reactor and the differential side stream reactors by a number of CSTR reactors in series. In order to get the real plug flow or cross flow reactor behaviour, the number of CSTR reactors should be infinite. However a couple of reactors already give quite realistic approximations. In line with Floudas (1995) we use five reactors. Figure 7.3 shows the reactor network superstructure; in line with Floudas (1995) the superstructure contains 5 reactors in series that can represent a plug-flow or differential side-stream reactors, and one CSTR reactor in parallel. The binary variables pertain to the existence of the reactors R2 t/m R6 ($\sigma_{d,R2} - \sigma_{d,R6}$), and the existence of side feeding ($\sigma_{d,F2} - \sigma_{d,F5}$) and product removal ($\sigma_{d,P1} - \sigma_{d,P4}$). They can only have the values 0 and 1. The continuous design variables are the volumes of the reactors R1 t/m R6, the side feeding flows, the product removal flows, and the feed profile. An example of the integer modelling is the following relation for the flow into reactor 2:

$$F_{R2,in} = \sigma_{d,R2} * (F_{R1,out} + \sigma_{d,F2} * F_{F2} - \sigma_{d,P1} * F_{P1}) \tag{7.1}$$

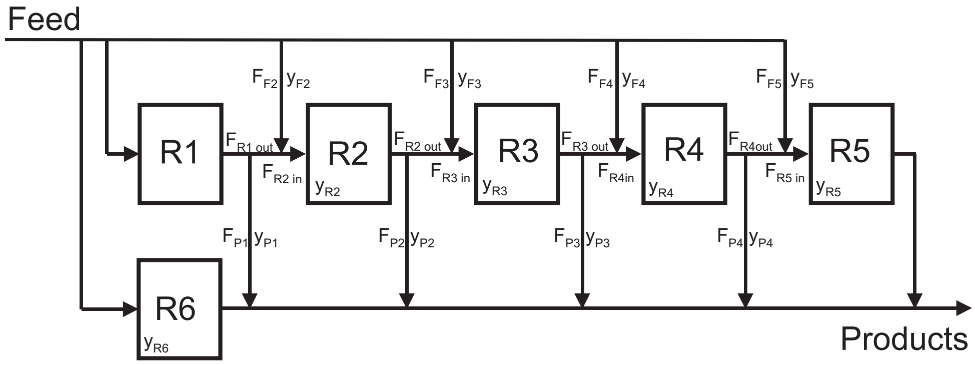
Feed
R1
R2
R3
R4
R5
R6
F_{F2} y_{F2}
F_{F3} y_{F3}
F_{F4} y_{F4}
F_{F5} y_{F5}
F_{R1 out}
F_{R2 in}
y_{R2}
F_{R2 out}
F_{R3 in}
y_{R3}
F_{R3 out}
F_{R4in}
y_{R4}
F_{R4out}
F_{R5 in}
y_{R5}
F_{P1} y_{P1}
F_{P2} y_{P2}
F_{P3} y_{P3}
F_{P4} y_{P4}
y_{R6}
Products

Figure 7.3: Reactor network superstructure.

with the integer constraints:

$$\sigma_{d,F2} \leq \sigma_{d,R2} \tag{7.2}$$

$$\sigma_{d,P1} \leq \sigma_{d,R2} \tag{7.3}$$

This describes how the inlet flowrate of reactor two is a function of the existence of reactor two ($\sigma_{d,R2}$), the existence of the side feed ($\sigma_{d,F2}$) and the product removal after reactor 1 ($\sigma_{d,P1}$).

In the whole superstructure the pressure and the outlet flowrate are maintained constant by adapting the inlet flowrate.

Although the Fischer Tropsch process is highly exothermal, the reactor is assumed to be isothermal. It is assumed that all the heat can be transferred to a cooling medium, e.g. boiling feed water that is flowing through cooling tubes.

7.4 Problem formulation

The objective is to maximize the diesel selectivity over a full cycle. The diesel weight fraction is defined as the sum of the weight fractions of the paraffins and olefins from C10 till C20. The time average diesel fraction is given by:

$$J_{diesel} = \frac{\int\limits_{cycle} \phi_{m,diesel} dt}{\int\limits_{cycle} \phi_{m,hydrocarbons} dt}, \tag{7.4}$$

where J_{diesel} is the weight fraction diesel, $\phi_{m,diesel}$ is the mass flow diesel and $\phi_{m,hydrocarbons}$ is the total hydrocarbon mass-flow.

The optimization variables are the discrete design variables defining the reactor network, and continuous variables describing the flows in the system, the reactor volumes and the feed profile.

The model can mathematically be described as:

$$\begin{aligned} 0 &= f(\dot{x}_d(t), x_d(t), x_a(t), u(t), \sigma_c, \sigma_d), \\ 0 &= g(x_d(t), x_a(t), u(t), \sigma_c, \sigma_d), \end{aligned} \tag{7.5}$$

where x are the differential states, z are the algebraic states, u are the time varying control parameters, σ_c are the time invariant continuous design variables, σ_d are the time invariant binary design variable, f are the differential equations, g are the algebraic equations

This leads to the following mathematical problem formulation for the integrated design problem:

$$\begin{array}{lll} \min\limits_{u(t),\sigma_c,\sigma_d,T} & J(x(T), z(T), u(T), \sigma_c, \sigma_d, T) & \\ s.t. & \dot{x}(t) = f(x(t), z(t), u(t), \sigma_c, \sigma_d), & \forall\, t \in [0, T], \\ & 0 = g(x(t), z(t), u(t), \sigma_c, \sigma_d), & \forall\, t \in [0, T], \\ & 0 \leq h(x(T), z(T), u(T), \sigma_c, \sigma_d), & \\ & 0 = p(\sigma_c, \sigma_d), & \\ & 0 \leq q(\sigma_c, \sigma_d), & \\ & 0 = x(0) - x(T), & \\ & 0 = u(0) - u(T). & \end{array} \tag{7.6}$$

where J is the objective function, h are the end-point constraints, p and q are the time-invariant equality and inequality constraints. The last two relations are the conditions for periodicity (Ding and LeVan, 2001).

The periodic operation was implemented using a block profile for the feed composition. Figure 7.4 gives such a typical profile. This profile is described by four parameters: cycle time, pulse time, base ratio and peak ratio. The total inlet

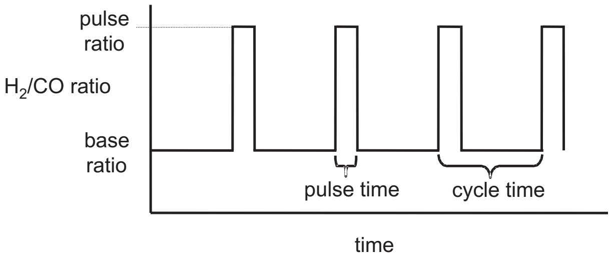

Figure 7.4: Feed profile.

flow-rate is adapted such that the pressure in the reactor and the outlet flow-rate are maintained constant. The feedprofile is modelled as follows:

$$ratio = L_1 + (L_2 - L_1) * \left[0.5 * \tanh\left(\sin\left(\frac{t * 2\pi}{T} - \pi\right) - \beta\right) + 0.5\right], \qquad (7.7)$$

where $ratio$ is the feed ratio, L_1 is the base ratio, L_2 is the pulse ratio, t is the time, T is the period length and β is a variable used for setting the pulse length.

7.5 Solution approach

A dynamic model of the system was implemented in gPROMS (gPROMS user guide, 2002). The problem is a mixed integer dynamic optimization (MIDO) problem (Bansal, 2000). The basic solution approach is to iterate between a primal problem where all continuous variables are allowed to vary and the integer variables are fixed, and a master problem, where the integer variables are varied. The primal problem will give a lower bound to the solution whereas the master problem will give an upper bound. Convergence is obtained when the upper and lower bounds cross. In Appendix B a more detailed description is given.

The time varying control parameter in this system is the inlet feed composition. We applied control vector parameterization to discretize this time varying parameter.

Periodicity conditions A periodic state in a system can be described by the condition that all state variables at the beginning of the period have the same value as they have at the end of the period:

$$0 = x(0) - x(T), \tag{7.8}$$

and

$$0 = u(0) - u(T). \tag{7.9}$$

The constraint on the inputs can be imposed on the system. We can define the error in the state variables, e, simply as:

$$e = x(T_n) - x(T_{n+1}) \tag{7.10}$$

We applied two different types of techniques to solve the system:

1. Direct substitution
2. Shooting techniques

The basic idea of direct substitution is to start the next period with as initial conditions the state at the end of the previous period. When a complete cycle of the process is expressed mathematically as a function $\mathbf{F}$:

$$x(T_{n+1}) = \mathbf{F}(x(T_n)), \tag{7.11}$$

the direct substitution method can be seen as applying the function $\mathbf{F}$ as many times as required to make the error e small enough. The main benefit of this method is that it is easy to implement. The main disadvantage is that the number of periods required to obtain periodicity can be very large.

In the shooting techniques (Ding and LeVan, 2001) the initial state conditions are treated as optimization variables that vary until the periodicity condition is satisfied. Different techniques could be used to update the initial conditions. Compared to the direct substitution approach the main advantage is that convergence could be achieved much faster. However when the number of states in the system becomes very large, this method may not work properly since it relies on matrix inversion and requires the satisfaction of a large number of constraints in multicomponent reactor systems.

For the shooting method we added the initial conditions of the systems to the optimization variables in the gOPT file. The periodicity condition was added as an additional constraint. So the optimization problem was solved simultaneously with the periodicity problem. However this lead to an optimization problem with over 600 design variables and over 600 end point constraints. This is beyond the capabilities of the software used. Moreover, for a smaller system (a single reactor with a little over 100 design variables end point constraints) the computation times were considerable higher then when applying the direct substitution. For the direct substitution we applied the following method: In the optimization runs the system is initialized in a feasible point. Then the block profile is applied to the system. After N cycles we assume that the system is in a forced limit cycle. At the optimum, the periodicity condition is checked. If this condition is not satisfied, the number N is increased and the optimization is done again.

7.6 Results

The system was initialized with the single CSTR reactor. Table 7.1 shows the values of the primal and master problem. After two iterations, convergence was achieved since the master problem solution crossed the primal solution. The selectivity in the optimum solution is 51.9%. This is a very significant increase compared with the 38% optimum selectivity under static operation. Figure 7.5 shows the optimal reactor network, together with the residence times in the reactors. The corresponding optimum feed profile has a total period of $1.05 * 10^4 s$, with a pulse time of $9.510^2 s$. This shows that the optimum reactor configuration is a CSTR reactor, followed by a relatively small plug-flow reactor. Side-feeding and product removal do not contribute to the selectivity in this system.

Table 7.1: Results of MIDO calculations

	1st iteration	2nd iteration
Structure		
reactors	R1	R1, R2, R3, R4,R5
feed to	R1	R1
product removed from	R1	R5
primal solution	49.4	51.9
master solution	54.2	51.7

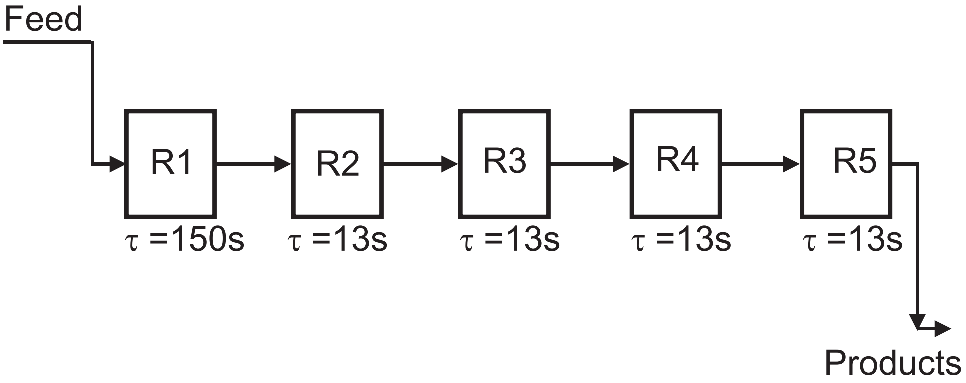

Figure 7.5: Optimum reactor superstructure.

7.7 Conclusions

In this work the integrated design of a reactor network for Fisher - Tropsch synthesis is achieved using an optimization-based methodology. The system operates under transient periodic conditions due to forced feed component ratio variations. The objective is to increase the diesel production. Therein, a dynamic optimization framework is employed for identifying not only the optimum feed ratio time profile but also the appropriate reactor type and reactor unit configuration that maximize the diesel selectivity. A set of binary variables are thus introduced, for representing the discrete decisions about the unit topology, thereby, resulting a mixed integer dynamic optimization (MIDO) formulation. The solution of this problem is accomplished with recently developed optimization techniques. The results are extremely encouraging since a 37% increase in the diesel selectivity is achieved.

Several aspects of the model require further investigations. The major assumptions are:

- mass transfer is ignored
- the energy balance is ignored
- assumptions on the kinetic parameters

It is generally known that the Fischer Tropsch process is reaction rate limited, rather then mass transfer limited. Therefore this mass transfer assumptions seems to be not very restrictive.

As already indicated in Chapter 6, the Fischer Tropsch process is rather exothermal. In the model heat effects are ignored. The effect of considering these heat effects on the model should be investigated. When thermal effects are considered, optimization of the temperature profiles could also be investigated.

In this work the integrated design is done for the nominal system only. The robustness of the solution with respect to disturbances is not investigated. It is not unlikely that adaptation of the economic driven design could be better suited to attenuate disturbances along the periodic trajectories, just like it is for the steady-state continuous processes. However the standard available methods for steady-state continuous processes cannot be applied on this system. Therefore it is recommended to study the controllability along the dynamic trajectories in the future.

8

Outlook

In Chapter 1 the general problem definition that initiated this thesis was presented, with a division into three dimensions. In this Chapter the results obtained in this thesis will be put into perspective according to these three dimensions. Recommendations for future developments are also presented.

The control performance of a chemical process is determined by a combination of the operational policy, the process and the control system. In Chapter 1 we defined the following problem definition:

> *How do process design decisions influence the achievable control performance of the system in the conceptual phase of the design?*

Then the problem is explored in three dimensions:

- What improvements in the design process itself are needed?
- Are improvements applicable to realistic situations; i.e. to a novel process with high economic impact?
- Can dynamic modes of operation be included?

The Chapters 2 - 7 give a partial answer to this central research question by exploring these three dimensions. Now the accomplishments and some remaining issues will be presented for arranged according to these dimensions.

Improvements in the design process itself

In Chapter 3, two main directions were identified related to this main problem; anticipating sequential design and simultaneous design. This work is mainly focussed on the anticipating sequential design.

In Chapter 2 the basic cycle of design was introduced. This cycle describes four steps occurring in actually all design tasks: formulation, synthesis, analysis and evaluation. These four steps will now be discussed.

Formulation In the formulation step the problem is defined. In this thesis the formulation step is only touched upon implicitly. Aspects that should be included in the formulation step are: selection of the disturbance scenario's, selection of controllability indices to be used and, discission making criteria. In the examples of the distillation column and the Fischer Tropsch synthesis all these issues are discussed.

The seemingly conflicting results on the optimal controllability of distillation systems by Govtsmark and Skogestad (2002) with the results presented in this thesis are also mainly due to a different problem formulation.

Synthesis In Chapter 4 a first attempt is made to consider controllability already in the synthesis phase. The TCA approach combines the concept of passivity with non-equilibrium thermodynamics. This leads to design guidelines to find processes with optimal controllability. The development of the design guidelines was based on systems with one dominant flow and force only. The case studies on which this method has been applied were limited to simple units, rather then entire processes. For this method there are several recommendations. The theory has to be further investigated in order to be able to consider more complex systems with more than one dominant driving force and flow. Then the method can be tested on more complex systems, integrated units like reactive separations and complete processes. Moreover it is recommended to integrate the method in an algorithmic framework. When entropy balances are included in the models this would allow a direct evaluation of the entropy production rates and hence of the controllability of the system.

Analysis The controllability analysis tools described in Chapter 5 have some significant benefits compared to the previously available indices. Both the closed-loop controllability indicator and the dynamic relative gain array do not rely on unrealistic assumptions with regard to the type of control to be applied. A possible further extension of the closed-loop controllability indicator would be to use a full model predictive controller (MPC) to determine the controllability. Advantages of this would be that constraints can be handled effectively and that the controllability analysis is done using similar criteria as will be done during operation. (Linear) MPC is nowadays a mature area. Obviously the calculational expenses will be significantly higher than by the use of the RGA or the condition number. However because of the continuous increase in computer speed this does not seem to be prohibitive.

The design of a distillation column served as a case study for both the TCA approach and the closed-loop controllability. The results of both methods are consisted: a decreasing number of trays of a distillation column leads to a better disturbance sensitivity.

Evaluation In the evaluation step the designer needs to make a decision about which alternative to select. A rational choice of a designer would be to select the alternative that has the best economic performance over the entire life-cycle, while satisfying environmental and safety constraints. The controllability of the process certainly contributes to the economic life-cycle performance. In the simultaneous approach for process and control system design the effect of disturbances and control on the economics is directly taken into account. In the sequential approaches a trade-off needs to be made between the value of the controllability indices and the steady-state economics. This pre-assumes that a better controllable plant has an economic benefit. In Chapter 5 we have shown how the, newly introduced, closed-loop controllability index can be related to the economics. For other indices the relation with the economics seems to be lacking.

All these contributions are basically contributions aimed at the anticipating sequential approach towards process design and control system design. However they are also helpful for the simultaneous approach since they can reduce the number of alternative options to be embedded within the superstructure.

Application to a novel process

Fischer Tropsch synthesis is a process of (renewed) significant industrial importance. A novel reactor type for this process is a monolithic reactor. The main benefits of this reactor is the short diffusion length combined with a small pressure drop. This has lead to the development of a monolithic reactor for Fischer Tropsch synthesis at Delft University of Technology. This was a superb opportunity to consider controllability issues from the earliest design stages on. In Chapter 6 it was shown how the newly developed tools are applied on the design of a monolithic reactor for Fischer Tropsch synthesis. The design guidelines based on TCA and the closed-loop controllability analysis consistently point into the same direction for this reactor design.

It is recommended to make such a controllability study a standard aspect in the development of novel units and processes.

Wider sets of operating modes

The majority of chemical processes are steady-state continuous processes. However sometimes different operational policies can contribute significantly to the performance of the system. Therefore the operational policy should be considered explicitly simultaneously with the process design and ideally combined with the control system design. In this work a first step in this direction is made by making an integrated design of the operational policy and the process for the periodically operated Fischer Tropsch synthesis process. It was shown that for the Fischer Tropsch process periodic operation offers significant increase in the achievable selectivity towards diesel; from 38% by static operation to 52% by periodic operation.

In this work the integrated design is done for the nominal system only. The effects of disturbances acting on the system along the periodic trajectories are not investigated. Design for good controllability for this type of dynamic operation modes would be a very interesting future development.

A

Mixed Integer Dynamic Optimization

A.1 Problem formulation

Mathematically the Mixed Integer Dynamic Optimization (MIDO) problem can be formulated as (Bansal, 2000):

$$\begin{aligned}
\min_{u(t),\sigma_c,\sigma_d,T} \quad & J(x(T), z(T), u(T), \sigma_c, \sigma_d, T) \\
s.t. \quad & \dot{x}(t) = f(x(t), z(t), u(t), \sigma_c, \sigma_d), \quad \forall\, t \in [0, T], \\
& 0 = g(x(t), z(t), u(t), \sigma_c, \sigma_d), \quad \forall\, t \in [0, T], \\
& 0 \leq h(x(T), z(T), u(T), \sigma_c, \sigma_d), \\
& 0 = p(\sigma_c, \sigma_d), \\
& 0 \leq q(\sigma_c, \sigma_d), \\
& 0 = x_0 - x(0), \\
& 0 = u_0 - u(0).
\end{aligned} \tag{A.1}$$

where $x(t)$ are the state variables, $z(t)$ are the output variables, $u(t)$ are the input variables, σ_c are the continuous design variables, σ_d are the discrete design variables, J is the objective function, f are the differential equations, g are the algebraic equations, h are the end-point constraints, p and q are the time-invariant equality and inequality constraints, x_0 are the initial conditions and u_0 are the initial values of the input variables. Note that the input variables include both the manipulated variables and the disturbance scenarios.

For periodic operation, the problem formulation is almost the same as for the standard mixed integer dynamic optimization problem. The only difference is that the initial conditions are now used to guarantee periodicity:

$$\begin{array}{lll} \min\limits_{u(t),\sigma_c,\sigma_d,T} & J(x(T),z(T),u(T),\sigma_c,\sigma_d,T) & \\ s.t. & \dot{x}(t) = f(x(t),z(t),u(t),\sigma_c,\sigma_d), & \forall\, t \in [0,T], \\ & 0 = g(x(t),z(t),u(t),\sigma_c,\sigma_d), & \forall\, t \in [0,T], \\ & 0 \le h(x(T),z(T),u(T),\sigma_c,\sigma_d), & \\ & 0 = p(\sigma_c,\sigma_d), & \\ & 0 \le q(\sigma_c,\sigma_d), & \\ & 0 = x(0) - x(t_f), & \\ & 0 = u(0) - u(t_f). & \end{array} \tag{A.2}$$

A.2 MIDO solution algorithm

An overview of Mixed Integer Non Linear Programming (MINLP) algorithms is presented by Floudas (1995). The algorithm that is central to the MIDO algorithm used in this work is the Generalized Benders Decomposition (GBD). The basic idea of GBD is to determine two sequences of updated upper and lower bounds where the upper bounds are non-increasing and the lower bounds are non-decreasing. The solution is achieved when the upper and lower bounds have converged within ϵ. The upper bound are determined by solving smaller problems where only the continuous variables are allowed to vary. This is called the primal problem. The lower bounds are based on duality theory (Floudas, 1995) and called the master problem.

Bansal (2000) has presented the following procedure for Mixed Integer Dynamic Optimization:

1. Set the termination tolerance, ϵ. Initialize the iteration counter, $k = 1$; lower bound, $LB = -\infty$; and upper bound, $UB = \infty$.

2. For fixed values of the integer variables, $y = y^k$, solve the kth primal problem to obtain a solution, J^k. Omit the search variables and constraints that are superfluous due to the current choice of integer variables. Set $UB = min(UB, J^k)$ and store the continuous and integer variables corresponding to the best primal solution so far.

3. Solve the primal problem at the solution found in step 2 with the full set of search variables and constraints included. Convergence will be achieved in one iteration. Obtain the Lagrange multipliers needed to construct the kth master problem.

4. Solve the kth master problem to obtain a solution η^k. Update the lower bound, $LB = \eta^k$.

5. If $UB - LB \leq \epsilon$, or the master problem is infeasible, then stop. The optimal solution corresponds to the values stored in step 2. Otherwise set $k = k + 1$, y^{k+1} equal to the integer solution of the kth master problem and return to step 2.

B

Design of the Internal Model Controller

The IMC design consists of two steps:

1. Decomposition of the plant model, $\hat{\mathcal{P}}$ into an invertible part and a part that cannot be inverted.
2. Design of a filter $\mathcal{F}$ such that the controller becomes proper.

The plant model is first decomposed according to (11):

$$\hat{\mathcal{P}} = \hat{\mathcal{P}}_{+1}\hat{\mathcal{P}}_{+2}\hat{\mathcal{P}}_{-} \tag{B.1}$$

where $\hat{\mathcal{P}}_{+1}$ is selected to make $\hat{\mathcal{P}}^{-1}\hat{\mathcal{P}}_{+}$ realizable and $\hat{\mathcal{P}}_{+2}$ is selected to make $\hat{\mathcal{P}}^{-1}\hat{\mathcal{P}}_{+1}\hat{\mathcal{P}}_{+2}$ stable. The following two steps are now required:

- The transfer matrix $\hat{\mathcal{P}}_{+1}$ is selected to be diagonal, as described by Morari (1983) and Garcia and Morari (1985).
- For the matrix $\hat{\mathcal{P}}_{+2}$, an inner/outer factorization (Morari and Zafiriou, 1989) is applied.

The filter is required to make the system proper. The typical filter used in IMC is given by:

$$\mathcal{F} = \frac{1}{(es+1)^r} \tag{B.2}$$

where r is selected large enough to make $\mathcal{F}\hat{\mathcal{P}}_{-}^{-1}$ proper. The parameter e is a tuning parameter. This parameter can be used to trade-off performance vs. robustness. The transfer matrix $\mathcal{Q}$ now becomes $\mathcal{F}\hat{\mathcal{P}}_{-}^{-1}$.

References

Adesina, A.A., Huidgins, R.R. and Silveston, P.L. (1995) Fischer-Tropsch synthesis under periodic operation, *Catalysis Today*, 25, 127 - 144

Anderson, J.S. (1966) A practical problem in dynamic heat transfer, *Chem Engineer*, may, 97 - 103

Applequist, G.E., Pekny, J.F., Reklaitis, G.V. (2000) Risk and uncertainty in managing chemical manufacturing supply chains, *Computers & Chemical Engineering* 24, 2211 - 2222

Åström, K.J. and Hägglund, T. (1984) Automatic Tuning of Simple Regulators with Specifications on Phase and Amplitude Margins. *Automatica*, 20, 645.

Asperen, V. van, Berends, R.H., Buhre, I. J. M., Jap A Joe, K. E., Kartal, G., Meeuse, F. M. and Posthuma de Boer, J. (1999) Synfuel process, Final Report. The production of 500.000 t/a synthetic oil products from natural gas with Fischer-Tropsch synthesis, Report TU Delft, Delft, The Netherlands

Azapagic, A. Clift, R. (1999) The application of life cycle assessment to process optimisation, *Computers & Chemical Engineering*, 23, 1509 - 1526

Backx, A.C.P.M., Bosgra, O.H. and Marquardt, W. (1998) Towards Intentional

Dynamics in Supply Chain Conscious Process Operations, presented at FOCAPO 1998.

Balas, G.J., Doyle, J.C., Glover, K., Packard, A. and Smith, R. (1998) *μ-Analysis and Synthesis Toolbox*, The Mathworks Inc.

Bansal, V. (2000) *Analysis, design and control optimisation of process systems under uncertainty*, PhD Thesis, Imperial College, University of London

Biegler, L.T., Grossmann, I.E. and Westerberg, A.W. (1997) *Systematic methods of chemical process design, Prentice Hall*, Upper Saddle River

Bristol, E.H. (1966) On a new measure of interaction for multivariable process control, *IEEE Transactions on Automatic Control*, 11, 133

CBS (2001) *Samenvattend overzicht van de industrie 2000*, Centraal Bureau voor de Statistiek, Voorburg/Heerlen

Clarck, P.A. and Westerberg, A. (1983) Optimization of design problems having more than one objective, *Computers & Chemical Engineering* 7, 259 - 278

Coffey DP, Ydstie BE, Farschman CA (2000) Distillation stability using passivity and thermodynamics, *Computers & Chemical Engineering*, 24, 317 - 322

Cross, N. (1994) *Engineering design methods, second edition*, John Wiley & Sons, Chichester

Daichendt, M. M. and Grossmann, I. E. (1998) Integration of hierarchical decomposition and mathematical programming for the synthesis of process flowsheets, *Computers & Chemical Engineering*, 22, 147 - 175

Deugd, R.M. de, Ypma, S.M., Kapteijn, F., Meeuse, F.M., Moulijn, J.A. and Verheijen, P.J.T. (2001) Model-based optimization of the periodic operation of the Fischer Tropsch synthesis, *Studies in Surface Science and Catalysis*, 133, 255 - 262.

Deugd, R.M. de, Chougule, R.B., Kreutzer, M.T., Meeuse, F.M., Grievink, J., Kapteijn, F. and Moulijn, J.A. (2002a), Is a monolithic loop reactor a viable option for Fischer-tropsch synthesis?, *submitted to Chem.Eng.Sci.-ISCRE 17*.

Deugd, R.M. de, Kapteijn, F. and Moulijn, J.A. (2002b), Trends in Fischer-Tropsch Reactor Technology - Opportunities for Structured Reactors, *submitted to Topics in catalysis*.

Ding, Y. and LeVan, M.D. (2001) Periodic states of adsoption cycles III. Convergence acceleration for direct determination, *Chemical Engineering Science*, 56, 5217 - 5320

Doherty, M.F.. and Malone, M.F. (2001) *Conceptual design of distillation systems*, McGraw Hill, Boston

Doyle, J.C. (1978) Guaranteed margins for LQG regulators, *IEEE Transactions on Automatic Control*, 23, 756 - 757

Douglas, J. M. (1985), A hierarchical decision procedure for process synthesis, *AIChE Journal* 31, 353 - 362

Douglas, J. M. (1988) *Conceptual design of chemical processes*, McGraw-Hill, New York

Douglas, J. M. (1990) Synthesis of multistep reaction processes, In: Siirola, J.J. (Ed.) Foundations of computer aided process design, Elsevier, New York, 70 - 105.

Douglas, J. M. and Stephanopoulos, G. (1995) Hierarchical approaches in conceptual process design: framework and computer aided implementation, *AIChE Symp. Ser.*, 41 (304), 133 - 197.

Dry, M.E. (1996) Practical and theoretical aspects of the catalytic Fischer Tropsch process, *Applied Catalysis A*, 138, 319 - 344

Emmerich, M., Grötzner, M., Groß, B. and Schütz, M. (2000) Pixed-Integer Evolution Strategy for Chemical Plant Optimisation. In: I. C. Parmee (ed) Evolutionary Design and Manufacture (ACDM 2000), 53 - 67

Farschman, C.A., Viswanath, K.P., and Ydstie, B.E. (1998) Process systems and inventory control. *AIChE Journal*, 44, 1841 - 1857

Farschman, C.A. (1998) *On the stabilization of process systems described by the laws of thermodynamics*, PhD thesis, Carnegie Mellon University

Feinberg, M. and Hildebrant, D. (1997) Optimal reactor design from a geometric viewpoint - I, universal properties of the attainable egion, *Chemical Engineering Science*, 52, 1637 - 1635

Floudas, C.A. (1995) *Nonlinear and mixed-integer optimization*, Oxford University Press, New York

Gagnepain, J.P. and Seborg. D.E. (1982) Analysis of process interactions with applications to multiloop control system design. *Ind. Eng. Chem. Process. Des. & Dev.*, 21, 5 - 11

Garcia, C.E. and Morari, M. (1982) Internal model control - I, *Ind. Eng. Chem. Process Des. & Dev.*, 21, 308 - 323

Garcia-Flores, R., Wang, X.Z., Goltz, G.E. (2000) Agent-based information flow for process industries' supply chain modelling, *Computers & Chemical Engineering*, 24, 1135 - 1141

Gero, J.S. (1990) Design prototypes: a knowledge representation schema for design, *AI Magazine*, winter, 26 - 36

Ghotage, A.V., Mudde, R.F., Akker, H.E.A. van den, Meeuse, F.M., and Grievink, J. (2002) Design of a gaslift loop reactor for Fischer Tropsch synthesis, *submitted to Chem.Eng.Sci.-ISCRE 17*.

Govatsmark, M.S. and Skogestad, S. (2002) Optimal number of stages in distillation with respect to controllability, *Computer-Aided Chemical Engineering*, 10, 499 - 504

gPROMS (2002) *gPROMS Introductory user guide*, Process Systems Engineering Enterprize, London

Grievink, J. (2002) Delft Matrix for Conceptual Process Design, Internal report TU Delft

Groot, S.R. de, and Mazur, P. (1969) *Non-equilibrium thermodynamics*, NHPC Amsterdam

Grossmann, I. E. (1997) Mixed-integer optimisation techniques for algorithmic process synthesis, *Advances in Chemical Engineering*, 23, 171 - 286.

Gupta, A., Maranas, C.D., McDonald, C. (2000) Mid-term supply chain planning under demand uncertainty: customer demand satisfaction and inventory management, *Computers & Chemical Engineering*, 24, 2613 - 2621

Hall, J. (2000) Environmental supply chain dynamics, *Journal of Cleaner Production*, 8, 455 - 471

Herder P.M. (1999) *Process Design in a Changing Environment; Identification of Quality Demands Governing the Design Process*, PhD Thesis, Delft University of Technology

Holt, B.R. and Morari, M. (1985a) Design of resilient processing plants VI The effect of right half plane zeros on dynamic resilience. *Chemical Engineering Science*, 40, 59 - 74.

Holt, B.R. and Morari, M. (1985b) Design of resilient processing plants V The effect of deadtime on dynamic resilience. *Chemical Engineering Science*, 40, 1229 - 1237.

Huang, H.P., Ohshima, M. and Hashimoto, I. (1994) Dynamic interaction and multiloop control system design. *Journal of Process Control*, 4, 15 - 27

Ishii, N. (1997) Life Cycle Oriented Process Synthesis at Conceptual Planning Phase, *Computers & Chemical Engineering* 21, S953 - S958

Jadhav, N.Y., Stappen, M.L.M. vander, Boom, R., Bierman, G. and Grievink, J. (2002) Mass balance and capacity optimisation in the conceptual design of processes for structured products, *Computer-Aided Chemical Engineering*, 10, 85 - 90

Jong, K.P. de, Post, M.F.M., and Knoester, A. (1998) Deposition of iron from iron-carbonyl onto working Co-based Fischer Tropsch catalyst: The serendipitous discovery of a direct probe for diffusion limitation, *Studies in Surface Science and Catalysis*, 119, 119 - 125

Kapteijn, F., Heiszwolf, J.J., Nijhuis, T.A. and Moulijn, J.A. (1999) Monoliths in multiphase catalytic processes, *CATTECH*, 3, 24 - 41

Kleineidam U.(2000) *Modelling and Control of Product Life-Cycles*, PhD Thesis, Eindhoven University of Technology

Knott, D. (1997) Gas to liquid projects gaining momentum as process list grows, *Oil & Gas Journal*, june 23, 16 - 21

Koeijer, G.M. de, Kjelstrup, S., Kooi, H.J. van der, Groß, B., Knoche, K.F. and Andresen, T.R. (1999) Positioning heat exchangers in binary tray distillation using isoforce operation, presented at ECOS'99, Tokyo, Japan

Konz, W. and Thillart, C. van den (2002) *Industrile symbiose op bedrijventerreinen* (Industrial Symbiosis in business areas), PhD Thesis, Eindhoven University of Technology

Kreutzer, M.T., Du, P., Heiszwolf, J.J., Kapteijn, F. and Moulijn, J.A. (2002) Mass transfer characteristics of three-phase monolith reactors, *Chemical Engineering Science*, 56, 6015 - 6023

Krishna, R. and Sie, S.T. (2000). Design and Scale-up of the Fischer Tropsch Bubble Column Slurry Reactor, *Fuel Processing Technology*, 64, 73 - 105.

Kroes, P. (2000) Engineering Design and the Empirical Turn in the Philosophy of Technology, In: Mitcham, C., Kroes, P. and Meijers, A. (Eds.) *The Empirical Turn in the Philosophy of Technology*, JAI Press, Stamford

Kwakernaak, H. and Sivan, R. (1972) *Linear optimal control systems*, Wiley New-York.

Laan, G.P. van der (1999) *Kinetics, selectivity and scale-up of the Fischer Tropsch synthesis*, PhD Thesis University of Groningen

Lewin, D. L. (1999) Interaction of design and control, presented at the 7th IEEE Mediterranean conference on control and automation, Haifa

Luyben. M.L. and Floudas, C.A. (1994) Analysing the interaction of design and control -1. A multiobjective framework and application to binary distillation synthesis. *Computers & Chemical Engineering*, 18, 933 - 969

Luyben, W.L., Tyreus, B.D., and Luyben, M.L. (1999) *Plantwide process control*, McGraw-Hill

Marino-Galarraga, M., McAvoy, T.J. and Marlin, T.E. (1987) Short-cut operability analysis . 3. Short-cut methodology for the assessment of process control designs. *Ind. Eng. Chem. Res.* 26, 521 - 531.

Malone, M. F. and McKenna, T. F. (1990) Process design for polymer production, In: Siirola, J.J. (Ed.) Foundations of computer aided process design (FOCAPD), Elsevier, New York, 467 - 483

Maretto, C. and Krishna, R. (1999) Modelling of a bubble column slurry reactor for Fischer Tropsch synthesis, *Catalysis Today*, 52, 279 - 289

McFarlane, D.C. and Glover, K. (1989) *Robust controller design using normalized coprime factor plant descriptions*, Springer-Verlag, Berlin

McKenna, T. F. and Malone, M. F. (1990) Polymer process design - I: continuous production of chain growth homopolymers, *Computers & Chemical Engineering*, 14, 1127 - 1149

Meeuse, F.M., Grievink, J., Verheijen, P.J.T. and Vander Stappen, M.L.M. (2000) Conceptual design of processes for structured products, in: Malone, Trainham and Carnahan (Eds) *Fifth international conference on Foundations of Computer Aided Process Design*, 324 - 328

Meeuse, F.M., Deugd, R.M. de, Kapteijn, F., Verheijen, P.J.T. and Ypma, S.M. (2001) Increasing the selectivity of the Fischer Tropsch process by periodic operation, *Computer Aided Chemical Engineering*, 9, 699 - 704

Meeuse, F.M., Samyudia, Y. and Grievink, J. (2002) Closed loop indicators for controllability analysis, *Computer-Aided Chemical Engineering*, 10, 529 - 534

Meeuse, F.M. and Toussain, R.L. (2002) Closed-loop controllability analysis of process designs: application to distillation column design, *Computers & Chemical Engineering*, 26, 641 - 647

Meeuse, F.M. and Huesman, A.E.M. (2002) Analyzing dynamic interaction in control loops in the time domain, *Ind. Eng. Chem. Res.* 41, 4585-4590

Mohideen, M.J., Perkins, J.D., and Pistikopoulos, E.N. (1996) Optimal design of dynamic systems under uncertainty. *AIChE Journal*, 42, 2251 - 2272

Morari, M. (1983) Design of resilient processing plants III A general framework for the assessment of dynamic resilience. *Chemical Engineering Science*, 38, 1881 - 1891.

Morari, M. and Perkins (1995) Design for operations, 4th Int. Confer. on Foundations of computer-aided process design, AIChE Symp. Ser., 91 (306) 105 - 114

Neer, F. van (1999) *Forced oscillations in heterogeneous catalysis*, PhD Thesis, University of Amsterdam

Nikolopoulos, A.A., Gangwal, S.K., and Spivey, J.J. (2001) Effect of periodic pulsed operation on product selectivity in Fischer Tropsch synthesis on $\mathrm{Co\text{-}ZrO_2 \backslash SiO_2}$, *Studies in Surface Science and Catalysis*, 136, 351 - 356

Ogunnaike, B.A. (1996) A contemporary industrial perspective on process control theory and practice, *Annual Reviews in Control*, 20, 1 - 8

Onsager, L. (1931) Reciprocal relations in irreversible processes. *I. Phys. Rev.*, 37, 405 - 426

Papalexandri, K.P. and Pistikopoulos, E.N. (1996) Generalized modular representation framework for process synthesis, *AIChE Journal* 42, 1010 - 1029

Perkins, J. (1998) Integration of Design and Control: The Holy Grail of Process Systems Engineering, presented at the AIChE Annual meeting, Miami Beach, November 16

Rajagopal, S., Ng, K. M. and Douglas, J. M. (1992) A hierarchical procedure for the conceptual design of solids processes, *Computers & Chemical Engineering* 13, 675 - 689

Roozenburg, N.F.M. and Eekels J. (1995) *Produkt ontwerpen, structuur en methoden*, Lemma, Utrecht

Ross, P.J. (1988) *Taguchi techniques for quality engineering*, McGraw-Hill New-York.

Rudd, D.F., Powers, G.J. and Siirola, J.J. (1973) *Process Synthesis*, Prentice-Hall, Englewood Cliffs (NJ)

Schijndel, J. van and Pistikopoulos, E.N. (2000) Towards the integration of process design, process control, and process operability: current status and future trends, In: Malone, M.F., Trainham, J.A. and Carnahan, B. (Eds) Fifth international conference on Foundations of Computer-Aided Process Design, 99 - 112

Schweiger, C.A. and C.A. Floudas (1997), Interaction of Design and Control: Optimization with Dynamic Models, In: W.W. Hager and P.M. Paradolos (Eds), *Optimal Control: Theory, Algorithms, and Applications*, 388 - 435

Seferlis, P. and Grievink, J. (1999) Process control structure screening by steady-state multiple disturbance sensitivity analysis, *Computers & Chemical Engineering*, 23, S309 - S312

Seider, W.D., Seader, J.D. and Lewin, D.R. (1999) *Process design principles*, Wiley, New York

Sepulchre, R., Jankovic M., and Kokotovic P.V. (1997) *Constructive nonlinear control*, Springer, Berlin

Sie, S.T. (1998) Process development and scale-up: IV The history of the development of a Fischer Tropsch synthesis, *Reviews in Chemical Engineering*, 14, 109 - 157

Siirola, J. J. (1995) An industrial perspective on process synthesis, 4th Int. Confer. on Foundations of computer-aided process design, AIChE Symp. Ser., 91 (306), 222 - 233

Siirola, J. J. (1996) Industrial applications of chemical process synthesis, *Advances in Chemical Engineering*, 23, 1 - 92

Siirola, J.J. (1997) Foreword in: Biegler, L.T., Grossmann, I.E. and Westerberg, A.W. (1997) *Systematic methods of chemical process design*, Prentice Hall, Upper Saddle River

Silveston, P., Hudgins, R.R., and Renken, A. (1995) Peridoic operation of catalytic reactors - introduction and overview, *Catalysis Today*, 25, 91 - 112

Sinnott, R.K. (1993) *Coulson & Richardson's Chemical Engineering volume 6*, Pergamon Press, Oxford

Skogestad, S. (1997) Dynamics and control of distillation columns. A tutorial introduction, *Chem. Eng. Res. Des.*, 75, 539 - 562

Skogestad, S. and Postelthwaite, I. (1996) *Multivariable feedback control, analysis and design*, Wiley, Chichester

Smith, J.M., and Van Ness, H.C. (1987) *Introduction to chemical engineering thermodynamics*, 4th edition, McGraw-Hill, New-York

Stankiewicz, A. and Kuczynski, M. (1995) An industrial view on the dynamic operation of chemical converters, *Chem Eng Process*, Vol 34, 367 - 377

Stephanopoulos, G. (1984) *Chemical process control, an introduction to theory and practice*, Prentice/Hall, London

Stephanopoulos, G., Ali, S., Linniger, A. and Salomone, E. (2000) Batch process developments: challenging traditional approaches, in: Malone, Trainham and Carnahan (Eds) *Fifth international conference on Foundations of Computer Aided Process Design*,46 - 57

Swart, J.W.A. de (1996). *Scale up of a Fischer Tropsch slurry reactor*, Ph.D. Thesis, University of Amsterdam

Tyreus, B.D. and Luyben, W.L. (1992) Tuning PI Controllers for Integrator-Deadtime Processes. *Ind. & Eng. Chem. Res.*, 31, 2625 - 2628

Tyrus, B.D. (1999) Dominant Variables for Partial Control. 1. A Thermodynamic Method for Their Identification, *Ind. & Eng. Chem. Res.*, 38, 1432 - 1443

Tousain R.L., Hol, C.W.J. and Bosgra, O.H. (2000) Measured variable selection and nonlinear state estimation for MPC, with application to a high-density poly-ethylene reactor, Proceedings of PCI 2000 conference, Glasgow, Scotland.

Tung, L. S. and Edgar, T. F. (1981) Analysis of control-output interactions in dynamic systems, *AIChE Journal*, 27, 690 - 693

Verwijs, J. (2001) New Challenges and opportunities for process modeling, presented at ESCAPE 11, 27 - 30 May 2001, Kolding, Denmark

Wilke, C.R. and Chang, P. (1955) Correlation of diffusion coefficient in dilute solutions, *AIChE Journal*, 1, 264 - 270

Willems, J.C. (1974) Dissipative dynamical systems. Part I, General Theory. *Arch. Rational Mech. Anal.*, 45, 321 - 351

Witcher, M.F. and McAvoy, T.J. (1977) Interacting control systems: steady-state and dynamic measurement of interaction, *ISA Transactions*, 16, 35 - 41

Yates, I.C., and Satterfield, C.N. (1991) Intrinsic kinetics of the Fischer Tropsch synthesis on a Cobalt catalyst, *Energy & Fuels*, 5, 168 - 173

Ydstie, B.E. and Viswanath, K.P. (1994) From thermodynamics to a macroscopic theory for process control. Proceedings of PSE'94 781 - 787

Ydstie, B.E. and Alonso, A.A. (1997) Process systems and passivity via the Clausius-Planck inequality. *Systems & control letters* 30, 253 - 264

Ziegler, J.G. and Nichols, N.B. (1943) Process lags in automatic-control circuits, *Transactions of the A.S.M.E.*, 65, 433 - 444

Zhou Z., Cheng, S., Hua, B. (2000) Supply chain optimization of continuous process industries with sustainability considerations, *Computers & Chemical Engineering* 24, 1151 - 1158

Summary

Traditionally, process design and control system design are carried out sequentially. The premise underlying this sequential approach is that the decisions made in the process design phase do not limit the control design. However, it is generally known that incongruent designs can occur quite easily. In the literature two different classes of approaches are being described that consider the control performance of the design alternatives from the earliest design stages: (i) *Anticipating sequential approaches* where process design and control system design are still carried out sequentially, but in anticipation of the control design the controllability properties of the process are taken into account during the process design phase. (ii) *Simultaneous approaches*. In the simultaneous approach the process design and the control system design are carried out simultaneously.

This work is focused on the first approach. Tools and methods are presented that can assist the process designer in designing processes that are well controllable. The control system design still needs to be carried out afterwards, but the process designer has already anticipated on it. The methods and tools presented in this thesis are aimed at the different stages of the conceptual process design phase: formulation, synthesis, analysis and evaluation. Primarily the synthesis and the analysis phases will be addressed to overcome some of the limitation of

the anticipating sequential approaches. Since most industrially scale processes operate in a steady state this mode of operation has been the reference for this research. However as dynamic modes of operation are becoming more important, an exploration was made of the potential of periodic operation of Fischer Tropsch synthesis. This has led to the following methods and tools for steady-state operation.

Thermodynamic Controllability Assessment A novel method is presented that enables the designer to consider controllability issues in the *synthesis* stage of the conceptual process design phase. The method, called Thermodynamic Controllability Assessment (TCA), is based on non-equilibrium thermodynamics. The basic idea is that processes can be described by fundamental driving forces and flows using non-equilibrium thermodynamics. The essence of conceptual process design then becomes establishing the relations between the various driving forces and flows. The entropy production in a system is also a function of the flows and driving forces. In this thesis we have shown how the disturbance sensitivity of processes is related with the sensitivity of the entropy production with respect to the disturbances. Based on this guidelines were formulated about how to establish the relation between flows and forces such that the disturbance sensitivity is minimized. These guidelines for flows or forces translate into clear choices for design parameters such as areas, volumes and number of trays. The effectiveness of this TCA method was tested by means of conventional unit operations, with positive results.

Controllability analysis methods Two novel controllability analysis methods were developed. The first method is closed-loop controllability analysis. This method compares the optimal closed-loop performance of processes exposed to stochastic disturbances scenarios. The main benefit of this method is that it compares alternative designs based on the *closed-loop* performance without unrealistic assumptions with respect to the type of control to be applied. Moreover this method has a clear physical interpretation.

The second controllability analysis method is a time-domain dynamic interaction analysis method. This is an extension of the Relative Gain Array (RGA). The open-loop and closed-loop time responses of a system, due to a step change in a manipulated variable are compared. The closed-loop response is determined based on the optimal achievable behaviour using an Internal Model Controller.

Of each potential control pairing, the open-loop and closed-loop responses are graphically represented. This can then guide to find the optimal pairing. The main benefits over existing methods are that the analysis can be done in the time-domain and without unrealistic assumptions on the controller.

Monolithic reactor for Fischer Tropsch synthesis To apply the newly developed methods and a process with significant potential was chosen: Fischer Tropsch synthesis. Fischer Tropsch synthesis is a process to convert synthesis gas, a mixture of H_2 and CO,converted in straight-chain hydrocarbons. A novel reactor type that is promising for Fischer Tropsch synthesis is a monolithic reactor. The most important design degree of freedom for this reactor is the single pass conversion, related to the reactor length. Both the TCA method and the closed-loop controllability indicator have been applied on the monolithic reactor. Both methods show that, from a controllability point of view, it is desirable to operate with a high single pass conversion. So a long reactor with a rather small syngas gas recycle is preferred.

Periodic operating processes All methods that were presented above are developed for steady-state continuous processes. Also different operational modes are industrially used, e.g. periodic operation of a continuous processes. The time averaged selectivity or yield can sometimes be increased over the maximum achievable value by steady-state operation. An integrated design is made of the periodic operated Fischer Tropsch synthesis process, under some idealized conditions (isothermal model, no mass transfer limitations). The maximum selectivity towards diesel can be increased from 38% by static operation to 52% by periodic operation.

Samenvatting

Traditioneel worden procesontwerp en regelsysteemontwerp sequentieel uitgevoerd. Deze aanpak veronderstelt dat het procesontwerp onafhankelijk van het regelsysteemontwerp kan worden gemaakt. Het is echter algemeen bekend dat ontwerpbeslissingen gemaakt in de procesontwerpfase, het uiteindelijk haalbare regelgedrag weldegelijk beïnvloeden. In de literatuur worden twee verschillende klassen van methodes beschreven voor de integratie van procesontwerp en regelsysteemontwerp: (i) *anticiperende sequentiële* methoden waarbij procesontwerp en regelsysteemontwerp nog steeds sequentieel worden uitgevoerd, maar dat regelbaarheidseigenschappen van het proces wel meegenomen worden tijdens het procesontwerp, (ii) *simultane methoden*. Bij de simultane methoden worden procesontwerp en het regelsysteemontwerp tegelijkertijd gedaan.

Dit werk is gericht op de eerste aanpak. Tools en methoden worden gepresenteerd die procesontwerpers helpen bij het ontwerpen van processen die goed regelbaar zijn. Het regelsysteem moet nog steeds achteraf ontworpen worden, maar de procesontwerper heeft er al op geanticipeerd. De methoden en tools gepresenteerd in dit proefschrift zijn gericht op de verschillende fasen van het conceptuele procesontwerp: formulering, synthese, analyse en evaluatie. Vooral de synthese en analyse fase zijn onderzocht om beperkingen van de huidige methoden te overkomen. Aangezien de meeste industriële processen in een steady state opereren is steady state operatie de basis van dit onderzoek. Dynamisch opereren wordt echter steeds belangrijker, daarom is er ook een verkenning uitgevoerd naar het potentieel van periodiek opereren bij Fischer Tropsch synthese. Dit alles heeft geleid tot de volgende tools en methoden voor steady state processen.

Thermodynamische Regelbaarheidsanalyse

Een nieuwe methode is gepresenteerd die de ontwerper de mogelijkheid geeft om regelbaarheideigenschappen al in de synthese fase van het conceptuele procesontwerp toe te passen. Deze methode, genaamd Thermodynamic Controllability Assessment (TCA), is gebaseerd op niet-evenwicht thermodynamica. Het basis idee is dat processen met niet evenwicht thermodynamica beschreven kunnen worden door fundamentele drijvende krachten en stromen. De essentie van procesontwerp is dan het bepalen van de relaties tussen de stromen en de krachten. De entropie productie in een systeem is ook een functie van de stromen en drijvende krachten. In dit onderzoek laten we zien hoe de verstoringsgevoeligheid van processen gerelateerd is aan de gevoeligheid van de entropie productie als gevolg van verstoringen. Aan de hand hiervan zijn richtlijnen geformuleerd over wat de optimale relatie is tussen krachten en stromen uit het oogpunt van verstoringsgevoeligheid. Deze richtlijnen vertalen zich in duidelijke keuzes voor ontwerpvariabelen zoals oppervlakten, volumes en schotel aantalen. The effectiviteit van de TCA methode is met succes getest op een aantal conventionele unit operations.

Regelbaarheidsanalyse methoden

Twee nieuwe regelbaarheids analyse methoden zijn ontwikkeld. De eerste methode is gesloten lus regelbaarheid. Deze methode vergelijkt het optimale gesloten lus gedrag in aanwezigheid van stochastische verstoringen van alternatieve procesontwerpen. Het belangrijkste voordeel van deze methode is dat verschillende ontwerpalternativen vergelijken kunnen worden op basis van het gesloten lus gedrag zonder onrealistische aannames over het soort van regelsysteem dat wordt toegepast. Ook is deze methode eenvoudig fysisch te interpreteren. De tweede regelbaarheids analyse methode is de dynamische interactieanalyse in het tijdsdomein. Dit is een uitbreiding van de RGA. De open lus en gesloten lus tijd responsies als gevolg van een stap van een gemanipuleerde variabel worden vergeleken. De gesloten lus responsie wordt bepaald gebaseerd op het best mogelijke regel gedrag met een Internal Model Controller. Van elke paring worden de open lus en gesloten lus responsies grafisch tegen elkaar uitgezet. Aan de hand hiervan kan eenvoudig de optimale paring worden bepaald. Het belangrijkste voordeel boven bestaande methoden is dat de analyse gedaan kan worden in het tijdsdomein zonder onrealistische aannames over de regelaar.

Monolietreactor voor Fischer Tropsch synthese

De ontwikkelde methoden zijn toegepast op een nieuw ontwerp voor een proces met significant potentieel: Fischer Tropsch synthese. Fischer Tropsch synthese is een proces dat synthese gas, een mengsel van H_2 en CO, omgezet in rechte koolwaterstofketens. Een nieuwe reactor die veel belovend lijkt voor Fischer Tropsch is de monoliet reactor. De belangrijkste ontwerpvrijheid voor deze reactor is de single pass conversie, gerelateerd aan de reactorlengte. Zowel de TCA methode als de gesloten lus regelbaarheidsanalyse laten zien dat het gewenst is om te opereren met een hoge single pass conversie. Dus met een lange reactor en een redelijk kleine gas recycle.

Periodieke processen

Alle hierboven beschreven methoden zijn ontwikkeld voor steady-state continue processen. Andere operatiemodes worden ook industrieel gebruikt, bijvoorbeeld periodieke continue processen. De tijdsgemiddeld selectiviteit of opbrengst kan bij deze processen hoger zijn dan de maximaal haalbare waarde bij steady-state operatie. Een geïntegreerd ontwerp van een periodiek bedreven Fischer Tropsch synthese proces is beschreven. De maximale diesel selectiviteit blijkt door periodiek opereren verhoogt te kunnen worden van 38% bij steady-state operatie, tot 52% bij periodieke operatie.

Dankwoord

De afgelopen jaren ben ik regelmatig mensen tegen gekomen die dachten dat een promotie erop neer komt dat je je opsluit in een kamer, zonder contact met de buitenwereld. Na vier jaar gaat de deur van het slot en kom je eruit, hopelijk met een proefschrift. Als dat de werkelijkheid was, zou ik alleen mijzelf hoeven te bedanken voor de fijne tijd die ik met mijzelf heb doorgebracht. Gelukkig klopt die gedachte niet helemaal. Ik wil dan ook met dit dankwoord de kans aangrijpen om de mensen die mij de afgelopen vier jaar, op welke manier dan ook, hebben geholpen te bedanken.

Ten eerste wil ik Johan Grievink bedanken. De vrijheid die je mij gegeven hebt tijdens mijn onderzoek, gecombineerd met je altijd aanwezige kritische blik en aandacht voor de details waar ik minder aandacht voor had, hebben dit werk gemaakt tot wat het is.

Mijn vakgroep genoten, Carolien, Cristhian, Gijsbert, Michiel, Panos, Peter, Pieter, Pieter, Sachin, Sean, Sorin en Yudi en semi vakgroep genoten Andreas en Wouter wil ik bedanken voor vier fantastische jaren.

Stratos Pistikopoulos, I would like to thank you for giving me the opportunity to spend a month in your research group at Imperial College. Myrian Schenk and Vassilis Sakislis, thanks for your contribution to the success of this visit, both from a professional and a social point of view. Without the three of you, the MIDO concepts would not have been penetrated so much in this thesis.

Adrie Huesman en Rob Tousain, onder andere op control gebied heb ik veel van jullie kunnen leren. Thanks! Ronald de Deugd wil ik bedanken voor de samenwerking op het gebeid van Fischer Tropsch synthese.

Een aantal studenten heeft het aangedurfd om bij mij af te studeren. Judith, Lilian, Sjoerd en Ricko bedankt voor jullie bijdragen en de nuttige discussies.

Martijn en Kitty, bedankt voor jullie ideeën en hulp bij het ontwerp van de kaft van dit proefschrift.

Paps en mams, bedankt voor jullie continue steun en aanmoediging.

Ten slotte wil ik al mijn vrienden, huisgenoten en vooral Katalijn bedanken. Niet alleen kon ik bij jullie mijn promotie sorres kwijt, maar mede dankzij jullie kon ik altijd gerust de deur van mijn kamer op slot doen... en het hele promoveren af en toe achter me laten.

Curriculum Vitae

Frederik Michiel Meeuse was born July 21, 1973

1986 - 1992 MAVO, HAVO & VWO at the Oranje Nassau College in Zoetermeer
1992 - 1998 Study Chemical Engineering at Delft University of Technology
1998 - 2002 PhD student in the section Process Systems Engineering at
Delft University of Technology